Crystalline Silicon Interfaces with Adhesive Polymer Semiconducting Glue and Thiazolothiazole Redox Active Organic Small Molecules

Daniel Clark Cohen

A dissertation submitted to the faculty of
The University of North Carolina at Charlotte
in partial fulfillment of the requirements
for the degree of Doctor of Philosophy in
Nanoscale Science

Charlotte

2020

Approved by:

_____
Dr. Michael Walter

_____
Dr. Christopher Bejger

_____
Dr. HaiTao Zhang

_____
Dr. Tom Schmedake

_____
Dr. Jordan Poler

ABSTRACT

Daniel Clark Cohen. Crystalline Silicon Interfaces with Adhesive Polymer Semiconducting Glue and Thiazolothiazole Redox Active Organic Small Molecules (Under the direction of Michael Walter)

Crystalline silicon is an extremely versatile semiconductor material used for electronics and photovoltaic devices. An organic conductive glue based on a blend of poly(3,4-ethylenedioxythiophene):poly(styrene sulfonate) (PEDOT:PSS) and d-sorbitol was examined for laminating conductors to crystalline silicon. PEDOT:PSS functions as a high-work-function solution processable conductor and exhibits an ohmic contact on p-type silicon. On n-type silicon it forms a rectifying contact, which behaves as a solar cell. D-sorbitol has adhesive properties and enhances the conductivity of the PEDOT:PSS polymer blend. D-sorbitol blended with PEDOT:PSS (s-PEDOT:PSS) was brought into contact with n-Si to form a rectifying contact that could be laminated to any sort of conductor. Conductive glue could prove especially useful for laminating to textured silicon or novel micro- or nanostructured silicon materials. However, when the d-sorbitol is added to the PEDOT:PSS and brought into contact with silicon, current–voltage characteristics suggest minority carrier trap states are formed, leading to charge recombination at the silicon/polymer interface.

To avoid creating electron trap states where recombination occurred, the surface of the silicon was modified by covalently bonding organic molecules to the silicon. The silicon surface was covered completely with methyl groups in a two-step chemical reaction,

which reduced trap state formation and charge recombination by protecting the silicon surface from oxidation. This created hybrid Si/polymer solar cells with no photogenerated current loss and enabled photovoltaic devices to be produced using s-PEDOT:PSS contacts to n-Si.

Further extending the concept of bonding organic molecules to the silicon crystal, a redox active small molecule was attached to the silicon surface. This molecule was chosen and synthesized for a number of reasons. Its reactivity with the silicon surface was essential, so an alkene moiety was used. Its ability to accept and donate electrons was also key, so a viologen was chosen. Thiazolo[4,5-d]thiazole bridged extended-viologens have a lower redox potential relative to the silicon conduction band, and can be reduced more easily than traditional viologens. Diallylpyridinium-thiazolo[4,5-d]thiazole dibromide ($(Allyl_2TTz)^{2+}(Br^-)_2$) was therefore synthesized and was used for all experiments involving silicon surface-bound redox active molecules. This compound was studied in solution to determine its properties as an electron shuttle with a silicon electrode. Bare silicon is a poor catalyst, however it did reduce $(Allyl_2TTz)^{2+}(Br^-)_2$ in solution with a dramatic increase in current vs electrolyte solution in cyclic voltammetry experiments. Next $(Allyl_2TTz)^{2+}(Br^-)_2$ was covalently bonded to the silicon surface to see whether it would retain the properties of a solution containing $(Allyl_2TTz)^{2+}(Br^-)_2$ and whether it would be catalytic for related reactions. The chemically modified silicon surface was found to pass more current to an acidic solution than methylated silicon on the first sweep of CV, but after that did not outperform Me-Si surfaces. This suggests that the molecule was reduced on the surface but did not reduce protons in solution.

DEDICATION

This thesis is dedicated to my wife Amber, who supported me throughout the time I was writing this, to my parents, who wanted me to get an education, to my step-son Miles who sometimes says he wants to be a scientist, and to my dogs Oscar and Daisy who seem pleased to see me every time I walk through the door.

ACKNOWLEDGMENT

I'd like to thank my advisor, Dr. Michael Walter for putting up with my molasses-like pace. I'd like to thank everyone in the Walter lab, especially Meesha Kaushal and Margaret Kocherga for their help taking apart the glove box and putting it back together. Thanks also go to Dr. Bernadette Donovan-Merkert, for helping me navigate the PhD requirements process as well as her skillful leadership of the Chemistry department. External to UNCC I would like to thank Miguel Caban-Acavedo at Caltech who acquired and analyzed XPS data of silicon surfaces.

Table of Contents

List of Figures

List of Tables

List of Abbreviations

$(Allyl_2TTz)^{2+}$
Diallylpyridiniumthiazolo[4,5-d]thiazole^{2+}

AMU
Atomic mass unit

AM 1.5
Air Mass 1.5 is a standard measure of power per unit wavelength per square meter approximating the power of sunlight that has passed through 1.5 earth atmospheres.

CV
Cyclic Voltammetry

DMSO
Dimethylsulfoxide

DSC
Differential Scanning Calorimetry

FF
Fill Factor

FTO
Fluorine Tin Oxide

HOMO
Highest Occupied Molecular Orbital

IR
Infrared

ITO
Indium Tin Oxide

Jsc
Short-circuit current density

MALDI-TOF MS/MALDI MS
Matrix Assisted Laser Desorption Ionization-Time of Flight Mass Spectroscopy

MeCN
Acetonitrile

NMR
Nuclear Magnetic Resonance Spectroscopy

n-Si
Negatively doped silicon

oDCB
Ortho-dichlorobenzene

OLED
Organic Light Emitting Device

PCl_5
Phosphorus pentachloride

PEDOT:PSS
poly(3,4-ethylenedioxythiophene):poly(styrene sulfonate)

p-Si
Positively doped silicon

SCE
Saturated Calomel Electrode

s-PEDOT:PSS
d-sorbitol blended with poly(3,4-ethylenedioxythiophene):poly(styrene sulfonate)

$TBAPF_6$
Tetrabutylammonium hexafluorophosphate

TFA
Trifluoroacetic acid

THF
Tetrahydrofuran

TTz
Any Dialkylpyridinium-thiazolo[4,5-d]thiazole^{2+} dication

TTz Core
The thiazolo[4,5-d]thiazole moiety at the center of a TTz^{2+} dication

UV
Ultraviolet

UV-Vis
Ultraviolet wavelengths through visible light wavelengths

Voc
Open-circuit voltage

XPS
X-ray Photoelectron Spectroscopy

Chapter 1 – Introduction

1.1 Silicon Diode Devices

The simplest and most efficient single junction solar cells are made using monocrystalline silicon. These are fabricated by taking a doped wafer of silicon and making a thin, oppositely doped layer on one side by diffusing dopants into the crystal at high temperatures. This forms a p-n junction, and a driving force for moving photogenerated charge carriers to opposite faces of the silicon. Finishing the cell for a high efficiency device also requires such steps as degenerate doping at the back side of the cell, surface etching for maximum light trapping, surface passivation, and optimal cathode and anode interdigitated contacts on the back side of the device.[1, 2]

Another way to create diodes is a to bring a metal with an appropriate work function into contact with a semiconductor such as silicon. These are referred to as Schottky diodes.[3] A high work function metal, most commonly gold,[4] but also the polymer blend PEDOT:PSS,[5] can be brought into contact with n-type silicon, resulting in band bending and the formation of a diode (**Figure 1**). The conduction and valence bands bend up close to the silicon surface, causing holes to diffuse up along the bent valence band into the high work function metal and electrons to diffuse away from the surface. These can serve as solar cells just like p-n junction diodes, with the semiconductor absorbing light and photogenerated charge carriers diffusing to the interface.[6]

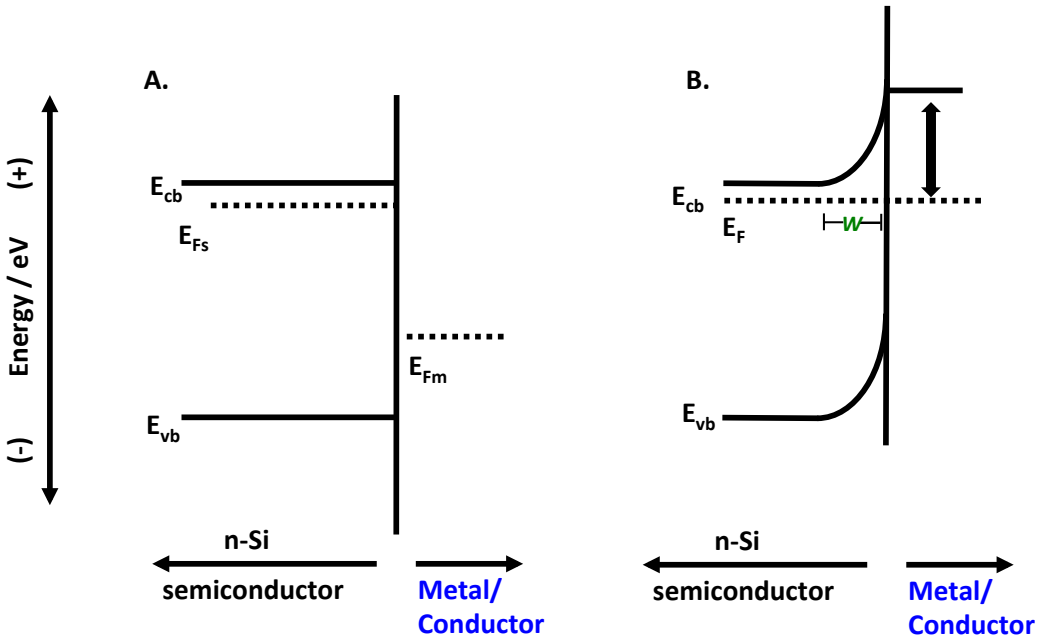

Figure 1. Band alignment of silicon before (A) and after (B) it is brought into contact with a high work function conductor.

1.2 Silicon Organic Hybrid Devices

A variety of hybrid c-Si:organic solar cells using a solution-processable p-type conductive polymer such as PEDOT:PSS in place of a high work function metal have been fabricated.[7, 8] This reduces the processing necessary on the silicon to a single dopant type, as the junction is formed between the conductive polymer and the crystalline silicon rather than in the bulk of the silicon crystal. The hybrid device eliminates the need for at least one costly processing step diffusing dopants into the crystalline silicon lattice. The diffusion step is the costliest step in the production of solar panels because these steps on the silicon take place at high temperature and under highly controlled chemical environments.[9] Conducting polymers can be solution-processed and cast onto the surface of the silicon to form stable, rectifying device contacts.

Hybrid devices also offer an attractive platform for eliminating the use of metal on the front face of a solar cell. Transparent conductors, such as indium tin oxide (ITO), can be laminated to silicon surfaces, decreasing the length charges must migrate to conductive contacts.[7] In addition, the surface of silicon solar cells is often textured for light trapping. PEDOT:PSS based adhesive can make contact between an entire non-planar silicon surface and planar transparent conductors. It can also create junctions at the end of silicon wires or nanoparticles.[10]

PEDOT:PSS blended with the sugar alcohol d-sorbitol (s-PEDOT:PSS) has already been successfully used to make entirely organic electronic devices. This method has been successfully used to mate flexible conductive oxides to organic photovoltaic devices and organic light emitting diodes.[11, 12] The interactions of s-PEDOT:PSS with an inorganic semiconductor have not been investigated, and the surface chemistry of silicon is very different from that of organic molecular devices. We set out to investigate how this conductive adhesive would interact with the chemically active surface of a silicon crystal.

We found that s-PEDOT:PSS made ohmic contacts with p-type silicon the same way neat PEDOT:PSS does, and it makes a rectifying contact with n-type silicon. However, the rectifying contact was poorly suited for solar cells, as the addition of the d-sorbitol into the polymer blend created trap sites at the interface, impeding the flow of photogenerated charges.[13] Suspecting that this was due to a chemical reaction between the silicon-hydrogen bond at the surface and the alcohol groups, we modified the silicon surface by replacing the hydrogen atoms with methyl groups to prevent chemical reactions.[14] This modification had the desired effect of eliminating trap states at the surface. Methyl-modified surfaces

have a slightly larger surface dipole than hydrogen terminated surfaces, and have been shown to perform better with a higher V_{oc}, so this was additionally desirable in devices.[5]

Modern silicon solar cells are approaching the thermodynamic limits to their efficiency.[15, 16] However, this is accomplished through feats of engineering that add considerably to the cost of the solar panels.[17] As commercial silicon solar cells approach this limit, the future of silicon solar power innovation will be primarily in sphere of cost reductions in fabricating the devices rather than increasing the efficiency of each individual cell.[18]

1.3 Silicon Surface Chemistry

Fabricating devices with crystalline silicon wafers requires an understanding of the chemistry that occurs at the surface of the silicon crystal. Crystalline silicon has surface atoms that must be bonded to a terminal atom of some other element or leave dangling bonds. In atmospheric conditions, or in the presence of water and oxygen, silicon will slowly oxidize, forming a disordered silicon oxide.[19] This oxide layer is undesirable in device applications, as it tends to contain many trap states and is somewhat electrically insulating. Trap states are vacant electronic states that will allow mobile charge carriers to become stuck in one place and prevent these carriers from freely moving through the crystal. Most commonly in processing silicon, a chemical etchant such as hydrofluoric acid is used to remove this oxide, replacing it with hydrogen atoms.

If an oxide is desired for optical purposes or for creating a small insulating layer for a tunnel junction, a thermal oxide formed from hydrogen-terminated silicon using high temperature steam or high temperature oxygen gas is formed. This oxide layer is free from

trap states that exist in oxide that forms spontaneously at low temperatures.[20] Other crystalline or inorganic materials are commonly deposited on hydrogen terminated silicon by physical processes such as sputtering, thermal vapor deposition, or e-beam deposition.

There are a variety of chemical reactions that covalently link silicon to organic compounds. Two methods are commonly used (**Figure 2**), both of which have been made use of in this work.[21] This process makes the surface band edges more stable against local chemical environments,[22] and can also add desired functionality to a surface. The first method, the chlorination/Grignard route, is to first replace the surface hydrogen atoms with chlorine atoms.[21] This is done using a radical initiator and phosphorous pentachloride in solution. The result is a silicon surface coated in chlorine rather than hydrogen atoms. This much alone is not sufficient to protect the silicon surface from oxidation or other reactions. The second step is to react the chlorinated silicon surface with a Grignard reagent or organolithium reagents. The final result is a surface that has silicon atoms bonded directly to the carbon atoms from the Grignard reagent. Best coverage is achieved using the (111) crystal plane of the silicon, where a single silicon hydrogen bond is present at each surface atom and is normal to the crystal plane. For well-polished silicon and methyl Grignard reagents, close to 100% surface site functionalization has been achieved.[14] Other silicon crystal planes result in some surface atoms that have multiple hydrogen atoms bonded, and stearic hindrance prevents attaching a carbon-bearing molecule at every possible surface atom. Organic molecules with low steric bulk, particularly methyl groups and to some extent ethynyl or propynyl groups achieve the best coverage of the silicon surface because they do not hinder other molecules from reacting with nearby chlorine atom surface sites.[23]

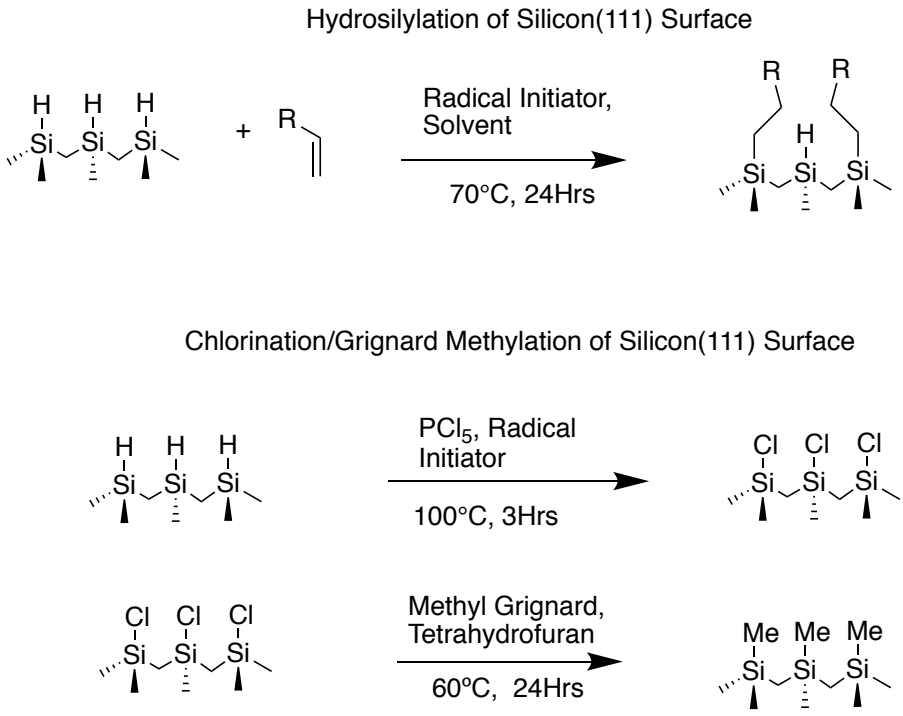

Figure 2. Hydrosilylation vs Chlorination/Grignard modification of a silicon(111) surface.

We used chlorination/methylation to create a silicon surface that is similar to hydrogen terminated silicon surfaces, but would not be reactive with the s-PEDOT:PSS polymer adhesive. The simplest and most effective version of this reaction, using methyl groups, has routinely achieved extremely well passivated silicon surfaces.[14, 21] This was used in testing how a silicon surface interacts chemically with s-PEDOT:PSS. It was also useful for solution phase electrochemical testing, as it allowed silicon electrodes to be prepared that would not react with water or oxygen.

The second method is through a process called hydrosilylation.[24] This method reacts a terminal alkene functional group directly with the hydrogen-silicon bond. This, like the chlorination from the first process, proceeds through a radical mechanism. The reaction can be done using a radical initiator or through ultraviolet light. For a UV-

mediated reaction, the wavelength must be short enough to provide enough energy to cleave a silicon-hydrogen bond. The result is an attachment between the terminal carbon of the alkene and a silicon surface atom. This method leaves an sp^3 hybridized carbon attached to the silicon atom, so it is not possible to create straight attachments to the silicon surface. The result is that there is always some hindrance preventing other alkenes attaching to the silicon surface, and full surface coverage is impossible. The alkene is also converted into an alkane.

We used this method to covalently bond small molecules we synthesized to a silicon surface. It does not achieve as high a degree of coverage as the first method, but it was more versatile and easier to synthesize chemicals with an alkene functional group. This would allow us to test how well electrons moving out of the silicon surface into electron accepting molecules would allow solution phase catalysis by a modified silicon electrode.

1.4 Viologens and TTzs

Beyond simply passivating silicon surfaces against oxidation, chemical modification can attach molecules of particular interest. Silicon is chiefly of interest due its properties as a semiconductor and light absorber. Molecules that are capable of accepting and donating electrons can be attached to the surface of semiconductors in order to facilitate moving charges in and out of inorganic crystals. This has been done with oxidative compounds such as vinylferrocene.[25] This may be necessary if the surface of the semiconductor has different behavior than the bulk or has unfavorable interactions when in contact with other materials.

We performed experiments with silicon and a class of compounds known as thaziolo[4,5-d]thiazole viologens (TTzs). These compounds, generally found as dication salts, are known to accept two electrons and are used in many applications for this reason. The monocation salt is a colored compound similar to ordinary viologens used in electrochromic applications. The neutral compound can be used to hold electrons in redox flow battery systems.[26] Adding the thiazolothiazole bridge to a viologen creates compounds that are highly fluorescent, and electrochromic.[27] Viologens, either chemically or electrically reduced, are also useful as mediators for hydrogen evolution catalysts, as they readily accept and donate electrons to catalytic species that then reduce protons.[28, 29]

The interaction of silicon electrodes with these species is especially interesting for two reasons. First, silicon is a poor catalyst for reduction, so if crystalline silicon can donate two electrons to a TTz more easily than to other species, the TTz will serve as an electron shuttle using a silicon electrode. Secondly, TTzs can be synthesized easily with any side chain desired, as they are synthesized through a simple SN2 reaction with an alkyl halide. This includes allyl halides, which have a terminal alkene, making synthesis of $(Allyl_2TTz)^{2+}$ that can be chemically attached to silicon as easily as synthesizing any other TTz. $(Allyl_2TTz)^{2+}$ was the compound studied both in the solution phase catalyst for silicon electrode hydrogen evolution, and as a chemical modifier on silicon surfaces as a permanent reducing catalyst or electron shuttle to other catalysts. We found that the silicon surface could function as an electrode for reducing this TTz but that the TTz itself was not suitable as an electron shuttle or catalyst for H^+/H_2 reduction.

Chapter 2 – s-PEDOT:PSS Silicon Hybrid Devices

2.1 Introduction

Poly(3,4-ethylenedioxytheiophene):Poly(styrenesulfonate) (PEDOT:PSS) (**Figure 3**) is a widely used conductive polymer with a high work function. In thin films it is mostly transparent and is often used as a hole specific contact for optoelectronic devices.[30] It is easy to process, needing only to be dispersed in water and spin-coated onto substrates and requiring only a low temperature (~100 °C) anneal. By adding solvents or by post-processing its conductivity can be increased by up to three orders of magnitude.[31] This reduces the resistance of a thin PEDOT:PSS layer enough that it does not substantially impact the performance of optoelectronic devices such as organic solar cells and organic light emitting diodes.

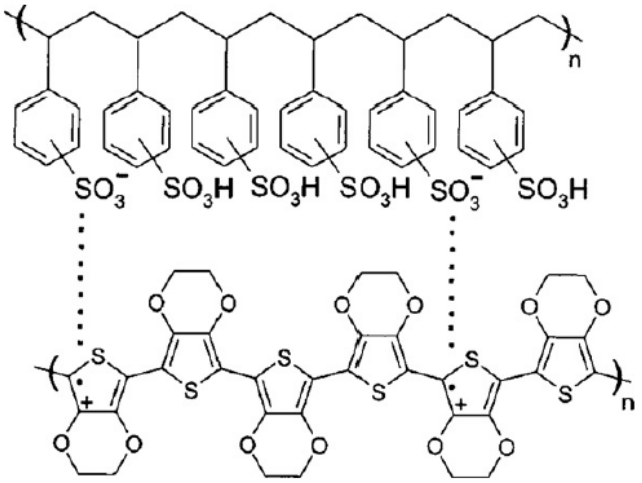

Figure 3. PEDOT:PSS chemical structure. Image from *Conductivity, work function, and environmental stability of PEDOT:PSS thin films treated with sorbitol.*[32]

Different polar solvents, such as DMSO, Ethylene Glycol, and d-sorbitol,[32, 33] change the morphology of the PEDOT:PSS layer, reducing the thickness of solid PSS phases.[34] This allows charges to more easily jump between the PEDOT phases, increasing

the conductivity. This is thought to be a product of high boiling solvents with strong dipoles, and one of the additives studied is d-sorbitol, a sugar alcohol.

D-sorbitol, a sugar alcohol, has been studied as an additive for increasing PEDOT:PSS conductivity. D-sorbitol also has adhesive properties when melted, which led researchers to investigate PEDOT:PSS blended with d-sorbitol as a conductive adhesive with useful applications to organic optoelectronics.[11, 12] Organic materials are attractive because they are flexible and solution processable, allowing their ease of use in reel-to-reel manufacturing methods.[35] An adhesive layer, which also served as the cathode of a device, allowed for a single step in the production of low cost solar cells and OLEDs. Both applications created efficient organic light-emitting diodes and organic solar cells with cathodes laminated to the active organic layer.[11, 12]

Hot melt hole conducting organics such as spiro-OMeTAD have been developed for use in organic, dye-sensitized, and perovskite based solar cells[36]. However, these materials are incredibly expensive and difficult to synthesize. Both PEDOT:PSS and d-sorbitol are cheap to produce. PEDOT:PSS is used as an anti-static coating on commercial packaging, and d-sorbitol is derived from sugar and present in countless consumer products such as chewing gum. A blend of these materials are likely to be cheaper than a majority of the specialty hole conducting organics on the market.

PEDOT:PSS has also been used with crystalline silicon to create Schottky diode rectifying contacts (**Figure 4**).[5, 8, 37] The diode, or rectifying contact, allows current to flow in one direction while restricting current flow in the other. The way the conduction and valence bands bend near the junction is both the reason for the rectification and the principle on which solar cells generate power. In the dark the current flow of the device is

dominated by majority charge carriers, but under illumination minority carriers are formed which diffuse out of the device and produce usable power. The efficiency with which these carriers are produced and collected and the usable energy of each carrier are the basis on which all solar cell efficiency rests.

Crystalline silicon can be easily fabricated with one type of dopant in bulk, but the creation of a p-n junction requires that additional dopants be diffused into the silicon crystal after it has been grown (**Figure 5**). This requires additional processing steps in furnaces with high temperature gasses for long periods of time. This p-n junction is the most common method for forming rectifying contacts in silicon. At the edge between the p-type and n-type silicon the Fermi levels align and the bands bend, creating the rectifying contact. This type of diode, and more complicated structures such as transistors, are often necessary in making logic circuits and other complex electronics.

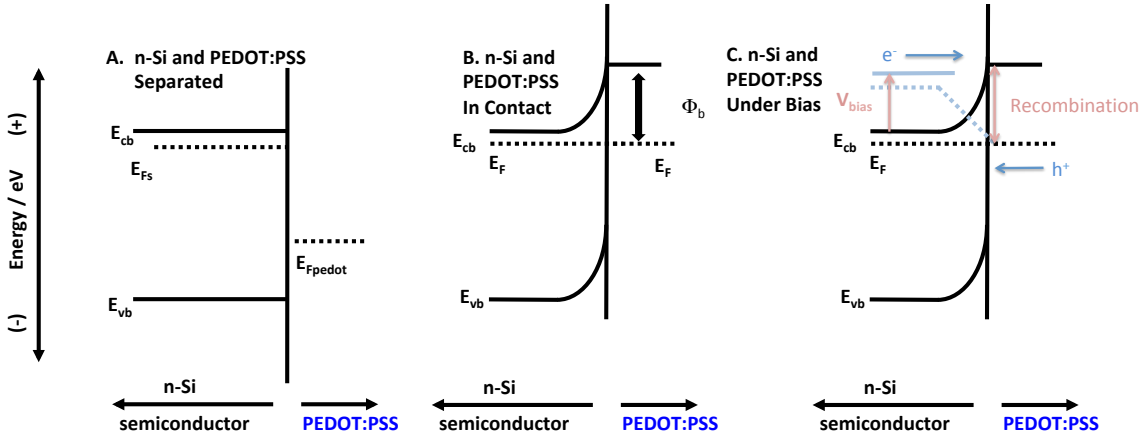

Figure 4. Schottky diode with PEDOT:PSS band diagram.

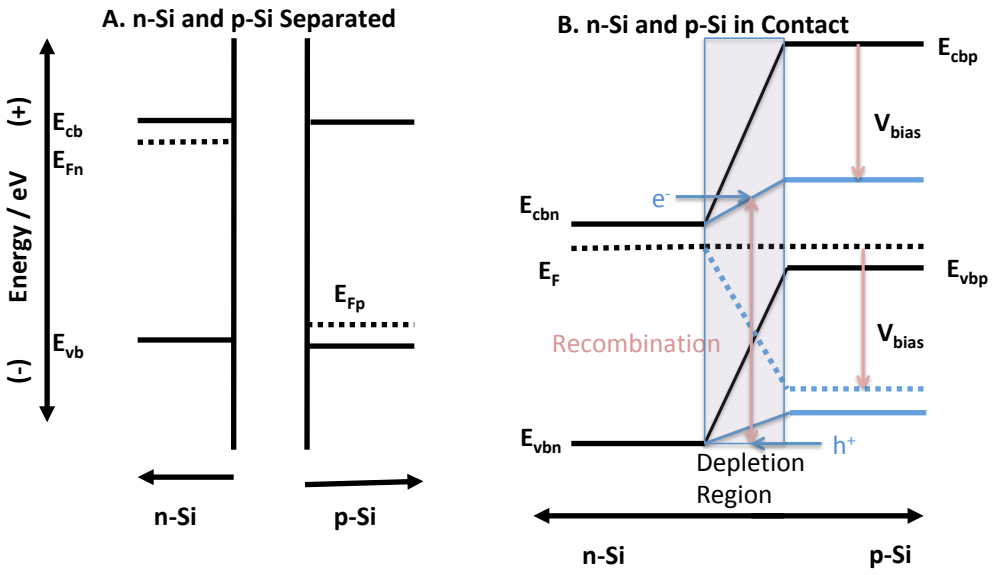

Figure 5. p-n Junction diode band diagram.

In solar cell devices, one very high-quality junction is required. Rather than forming a p-n junction, diodes can be formed by bringing a single dopant type crystal into contact with either a high or low work function conductor. This type of diode (Schottky) is often created by using n-type silicon and a high work function metal such as gold. This also eliminates the need for the additional processing steps of diffusing dopants into the crystalline semiconductor. PEDOT:PSS can function much like a high work function metal. It has a high work function (-5.0 to -5.2 eV), an intrinsic carrier concentration higher than the crystalline silicon, and when brought into contact with crystalline silicon it also forms a Schottky diode. This means that a rectifying junction can be made between the as-grown silicon and a material with a single, low temperature, solution processable polymer mixture.

Because it is a highly transparent layer, a film of PEDOT:PSS on top of silicon does not appreciably block light that is then absorbed in the silicon. Additionally, good solar

cell devices can be formed with the rectifying junction of n-Si and PEDOT:PSS.[5, 38, 39] Articles have been published detailing methods for increasing the efficiency of such devices, which have reached over 15%. Ongoing efforts to improve this efficiency are steadily increasing the efficiency through back contact fields, conductivity increases, and related methods.[37, 40]

Despite the advantages of low temperature processing and cheap materials, there are some disadvantages to using PEDOT:PSS which reduce the efficiency of the devices. Conventional p/n junction silicon solar cells often have a thin layer of degeneratively doped silicon at the front face, which is highly conductive. This layer can move charges laterally to metal fingers and bus bars for collection. This is not possible with PEDOT:PSS, as degeneratively doped n-Si makes an ohmic rather than rectifying contact with PEDOT:PSS by forming a tunnel junction.[5] n-Si:PEDOT:PSS devices replace the n+ Si with PEDOT:PSS which is less conductive laterally, trading increased device area for small increased series resistance.

Adhesives are clearly useful for reel-to-reel fabrication of organics, but are also of interest to crystalline silicon solar cells. All high efficiency cells employ textured surfaces for more efficient collection of light. This is most often done by etching nanosized features into the silicon surface that rely on optics to minimize reflection.[41] While this is an excellent method for reducing the reflected light, it poses some problems when trying to mate conductors to the surface. It is not as much an issue with deposited conductors such as sputtered, atomic layer deposited (ALD) or evaporated metal fingers, but prefabricated conductors such as transparent oxides on glass or plastic substrates, or even graphene, will not make contact to much of the patterned surface. If they are simply placed on top of the

silicon they will contact only at the highest atoms, and they will fall off if not clamped or glued down. This problem only becomes worse with other shapes, such as etched pillars, or with silicon microwire arrays.

A conductive adhesive solves these problems. It fills in the gaps in the etched silicon surface or in between the microwires or pillars, making contact to the entire available silicon surface.[7] It also holds in place the conductive contact. It is often cheaper to fabricate conductive oxides or graphene in a different process such as reel to reel, which cannot mate perfectly to any patterned silicon. The only way to get a good, low resistance contact between these materials and silicon is to have a conductive material infill the etched patterns in the silicon surface and to have adhesive properties to hold the contact to the infilled material.

One final advantage of these materials is that they are transparent conductors. Metal contacts on the front face of the silicon block the light where they make contact. Graphene and conductive oxides absorb small amounts of light, but leave the entire face of the silicon crystal available to absorb, so an increased amount of light can be absorbed in the crystal itself.

Devices fabricated using s-PEDOT:PSS on top of n-Si did produce rectifying contacts, however they exhibited unusual characteristics. Rather than a single diode type curvature, a double diode with different degrees of ideality was realized. This effect was not evidenced in the organic devices, but was pronounced in the crystalline silicon devices. One result of this is that the devices performed extremely poorly as solar cells. A significant amount of charge recombination of photogenerated carriers was likely present in the devices which did not appear in control devices using neat PEDOT:PSS.[13]

This leads to the conclusion that the d-sorbitol's interaction with the silicon surface caused recombination of charges, either through chemical reaction with the surface, natively trapping holes, or some field effect on the charges in the crystal. D-sorbitol has six polar –OH groups that could be repelling holes from the surface through the strongly charged proton.[3, 42] Most likely, oxygen atoms in the D-sorbitol are forming Si-O bonds. Disordered silicon-oxygen layers are well known for creating trap states, and the d-sorbitol, much like atmospheric water, would form a native oxide. If the Si-O bonds are trapping holes where they can recombine with electrons, surface modification is the best route to take to combat the recombination issue.

To address this issue, another possible option is to modify the surface of the silicon itself. Silicon can be alkylated at the (111) plane, which can either be acquired in polished planar configuration or is the exposed face of the inverted pyramid structure of light trapping silicon. Alkylating the silicon can be a way of protecting it from chemically interacting with the adhesive through oxidation.[43]

2.2 Materials and Methods

2.2.1 Silicon and s-PEDOT:PSS Processing

We investigated whether s-PEDOT:PSS glue laminates perform in a similar fashion to traditional processing methods, in which PEDOT:PSS is cast on the silicon surface, then contacted with a metal electrode.[8] Laminated contacts cast the film on a transparent conductor, which is then pressed to the silicon surface to make contact. For device testing purposes, it was easier to use a thick, drop-cast PEDOT:PSS or s-PEDOT:PSS layer and a mercury drop contact for silicon devices. With this method, good ohmic contact is formed

to p-Si and a rectifying contact is formed to n-Si. However, the addition of the d-sorbitol adhesive severely impacts the performance of a rectifying junction as a solar cell due to charge recombination. Under illumination the n-Si/s-PEDOT:PSS junction functions as a p-n solar cell but the photocurrent is greatly reduced by charge recombination.

Polished Si(111) wafers of n,p-type (10 Ω*cm) were cleaved into approximately 1 cm^2 pieces and sonicated for 10 min in acetone, Milli-Q H_2O and methanol with a final rinse of Milli-Q H_2O. The pieces were then dipped in piranha solution heated at 100ºC for approximately 30 min. The cleaned pieces were then rinsed multiple times with Milli-Q and dried under a stream of N_2. They were then etched with buffered HF (Transene Co.) for 1 min to remove native silicon oxides and create an H-terminated surface and brought into a glove box with <5 ppm H_2O, O_2.

Following the recipe of Shimada et al.,[12] 1 mL of PEDOT:PSS PH-1000 solution was mixed with the appropriate mass of d-sorbitol and stirred for 1 h. This mixture was sonicated for 30 min, then filtered through a 45 μm PTFE filter to remove large particles. Fluorine-doped Tin Oxide films (20 Ω/□) on glass were cut into approximately 1 cm x 1 cm pieces and sonicated in acetone, isopropanol, and milli-Q H_2O, then cleaned with a UV/Ozone etch to remove any surface contamination. 125 μL of conductive glue solution was spin-cast at 2000 rpm on top of the FTO films. The films were allowed to spin for 15 s before removal, and allowed to dry in air.

2.2.2 Device Designs

For press contact device (**Figure 6 a ,c**) testing, the s-PEDOT:PSS/FTO films were heated face up at 140˚C and then the prepared silicon wafers were placed face down on the glue surface. A glass slide was placed on top of the silicon to press the contacts together,

and they were allowed to anneal for 15 min. The films were then allowed to cool slowly to room temperature, and held together with clips. Control devices (**Figure 6d**) were prepared by spin coating PEDOT:PSS with no sorbitol on FTO glass and the same procedures were followed. The FTO was contacted with an alligator clip. The backside of the silicon was scratched with a glass cutter, and an InGa eutectic was painted on, and then brought in contact with a strip of copper foil.

A slightly different approach was used for mercury drop devices using thick PEDOT:PSS films on silicon (**Figure 6 b**). Testing the effect of sorbitol concentration on the n-Si/s-PEDOT:PSS rectifying junction were made with thick, drop-cast layers of s-PEDOT:PSS directly on clean n-Si chips of approximately 1cm^2. The silicon test chips were contacted by scratching InGa eutectic on to the back of the silicon. InGa contacts were electrically connected to a large copper block. Front side contacts were made by dropping a small bead of Hg onto the s-PEDOT:PSS film and making contact to the Hg with a platinum wire. For p-Si devices, the same procedure was used except that gold was thermally evaporated onto the backside of freshly HF etched silicon rather than an InGa eutectic. Various device architectures are illustrated in **Figure 6**.

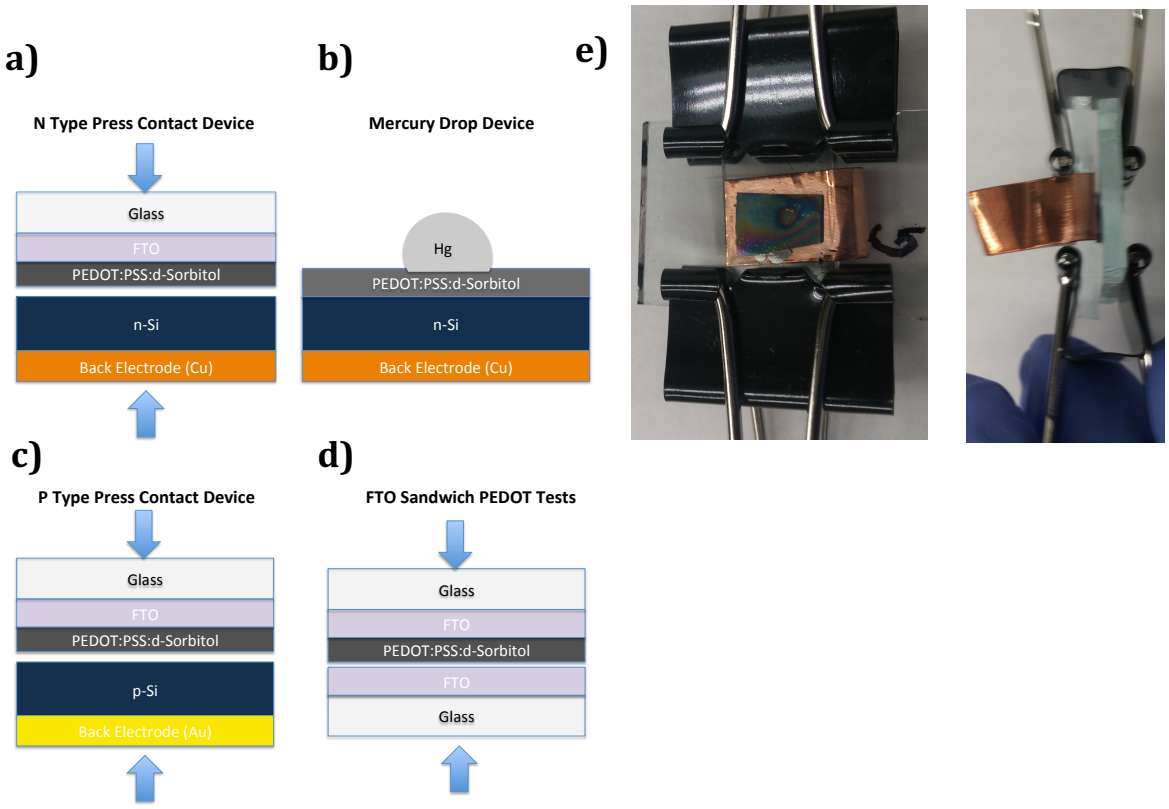

Figure 6. Device architecture for press contact p-type devices a), s-PEDOT:PSS/FTO sandwiches b), press contact n-type devices c), and mercury drop devices d). Pictures of actual press-contact devices e).

2.2.3 Measurement Techniques

Images were taken of the entire device sandwich along with a scale bar, and the contact area was calculated from the area of the silicon. *JV* curves were taken using a Keithley Source-Meter unit. Dark curve measurements were made in the dark to prevent any photocurrent from being present at the n-Si/PEDOT junction, while light curves were taken under a mercury-xenon solar simulator lamp.

Scans were run measuring the current from -2*V* to +2*V* in increments of 0.02*V* using a Keithley 2600 series source-measure unit. Due to the inconsistent film formation

thicknesses were not obtained. UV-Vis absorbance data was taken by spin-casting thin films of s-PEDOT:PSS on FTO glass and comparing the absorbance to bare FTO glass with a Cary 300 spectrometer. Differential scanning calorimetry was taken on a METTLER 800 series after drop casting s-PEDOT:PSS solution into a crucible, allowing it to dry overnight.

2.3 Results and Discussion

2.3.1 Conductivity Measurements

A study of the effects of the concentration of d-sorbitol in the PEDOT:PSS solution on the conductivity and device performance of the s-PEDOT:PSS layer was performed to determine whether a balance between conductivity enhancement, adhesion, and performance loss from recombination was possible. First, a series of PEDOT films were drop-cast onto glass slides with concentrations of sorbitol varying from 0% to 10% by solution weight. The sheet resistance of these films was evaluated using a four-point-probe. Concentrations of 5% and 10% did not give well behaved *JV* curves from which to extrapolate sheet resistance, either because the films were too conductive or because the high sorbitol concentration caused phase separation resulting in insulating regions and a high degree of measurement noise. This is likely because at high d-sorbitol concentrations the dry film is higher in d-sorbitol phases than PEDOT or PSS phases.

Layers of PEDOT:PSS with 0% d-sorbitol had a sheet resistance of 1065 Ω/□, 1% (277 Ω/□), and 2% (11 Ω/□). The conductivity enhancement is noteworthy, spanning three orders of magnitude with even small concentrations (1-2%) of sorbitol. This gain in the conductivity is important for preventing parasitic resistances that negatively impact

device efficiencies. This is important for organic conductors as they are less conductive than metals or other inorganic conductors, however the problem of loss of photocurrent due to charge recombination is equally as important. This conductivity enhancement was also seen in the *JV* curves of the devices made using these concentrations of d-sorbitol in PEDOT:PSS.

2.3.2 FTO Sandwich Devices

The *JV* curves of the FTO/s-PEDOT:PSS/FTO sandwich devices showed an ohmic contact between the transparent conductor and the organic layer (**Figure 7**). Both neat PEDOT:PSS and s-PEDOT:PSS films had good ohmic contacts when making a press contact. The straight line in the JV curves implied there was minimal barrier to consider with the s-PEDOT:PSS/FTO interface when laminating contacts. The conductivity enhancement of the s-PEDOT:PSS over the neat PEDOT:PSS was also evident with a lowered contact resistance (44 Ω•cm^2 vs. 62 Ω•cm^2).

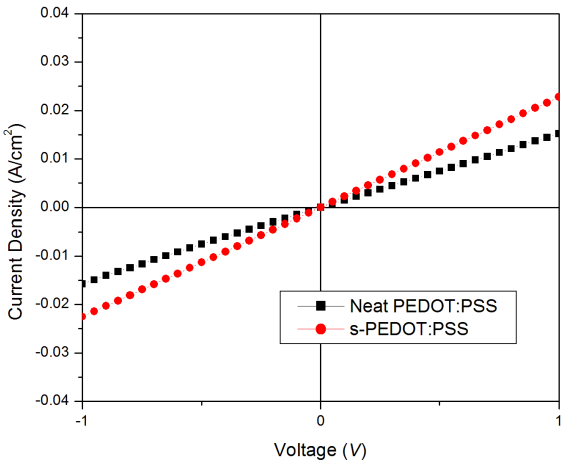

Figure 7. FTO on FTO pressed sandwich contacts with a neat PEDOT:PSS or s-PEDOT:PSS glue interlayer.

2.3.3 P-Type Silicon Ohmic Contacts

The p-type silicon also shows an ohmic contact to the s-PEDOT glue with symmetrical *JV* curves obtained from -1 to +1 *V* applied potential and enhanced conductivity up to 10% D-sorbitol concentration (**Figure 8**). It is expected that there should be no rectification to the p-Si, as the work function of PEDOT:PSS is high and the Fermi levels of p-Si and PEDOT:PSS are similar. Doping d-Sorbitol into PEDOT:PSS films lowers the HOMO level of the s-PEDOT:PSS film and is concentration dependent.[44] A small barrier generated by mismatch between the Fermi level of the p-Si and the HOMO of the s-PEDOT:PSS film would account for the non-ohmic behavior of these devices near zero applied potential, while at small applied biases this is easy to overcome.

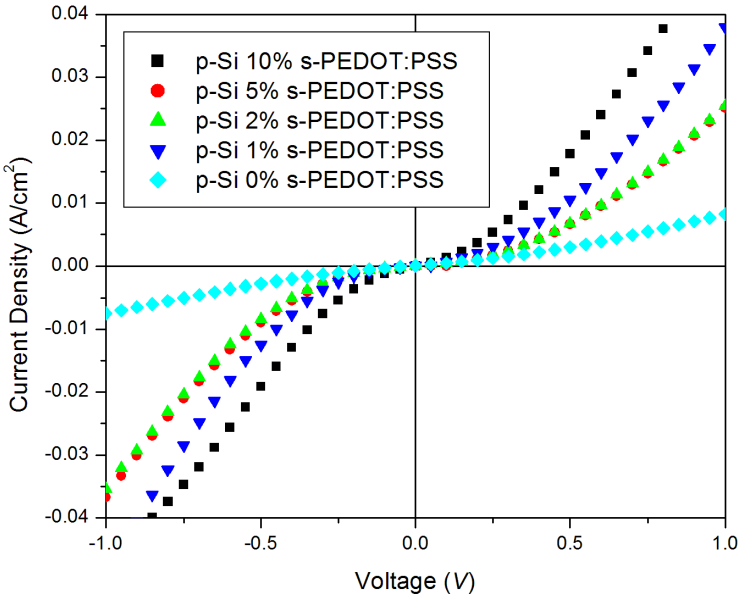

Figure 8. *JV* curve of p-Si contacts to s-PEDOT:PSS (Au/p-Si/s-PEDOT:PSS/FTO).

2.3.4 N-Type Silicon Rectifying Devices

The n-type silicon made a rectifying contact to the s-PEDOT:PSS glue, but with slightly different characteristics than with neat PEDOT:PSS. There is an additional feature in the *JV* curve introduced when the sorbitol is added to the mixture. When viewing the semilog plots it is clear that between 0.3 *V* and 1.5 *V*, different effects dominate the device current. (**Figure 9a, b**).

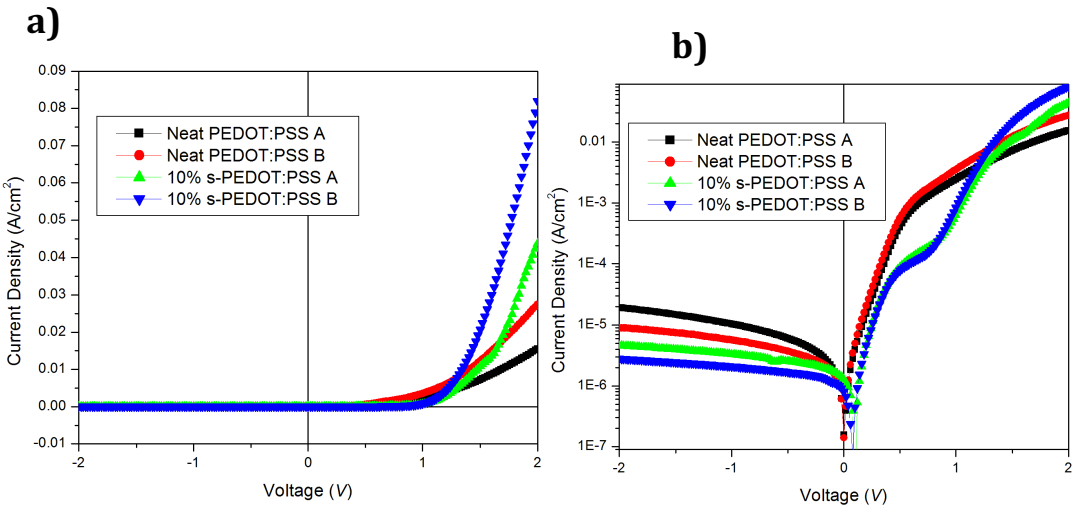

Figure 9. Linear a) and logarithmic b) neat PEDOT:PSS vs. s-PEDOT:PSS dark *JV* curves for Hg drop devices (Cu/InGa/n-Si/s-PEDOT:PSS/Hg). A and B represent two different devices fabricated the same way for s-PEDOT:PSS and neat PEDOT:PSS using thick films.

This secondary feature is commonly associated with recombination of charges in the depletion region of a diode.[45] In inorganic devices, this is most commonly associated with trap states in the depletion region. Since the silicon side of our devices is not altered in any way by the addition of d-sorbitol, this suggests that trap states are being introduced

by the d-sorbitol in the PEDOT:PSS layer which are becoming centers for charge recombination.

When exposed to light, the s-PEDOT:PSS devices show greatly enhanced conductivity and short circuit current over the neat PEDOT:PSS/n-Si devices, but performed much lower than expected due to interfacial charge recombination (**Figure 10**). Although all of the devices were illuminated with 100 mW cm-2 (AM 1.5 light), the photocurrents are limited due to the use of thick ~1-5μm PEDOT:PSS films.[5] The open circuit voltages were similar or higher than the neat PEDOS:PSS/n-Si devices, however the fill factors (*FF*) were decreased. The n-Si/s-PEDOT:PSS glue devices likely demonstrated either significant charge recombination or large series resistance. The photogenerated charge carriers could be extracted at negative voltages (approximately -150 *mV*), but the photocurrent diminished as the voltage approached zero.

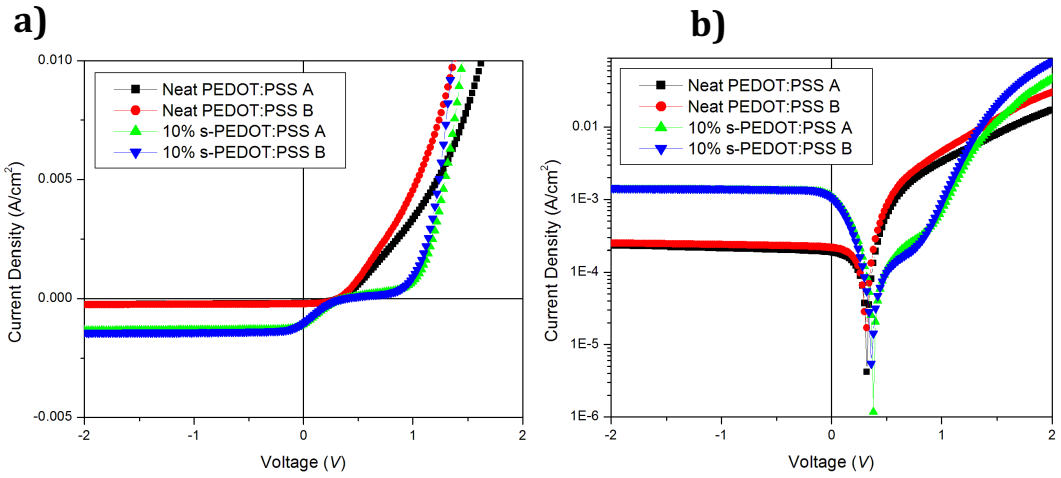

Figure 10. Linear a) and logarithmic b) neat PEDOT:PSS vs. s-PEDOT:PSS *JV* curves under illumination. The same devices from Figure 6 were exposed to AM1.5 illumination.

Since recent work has demonstrated highly efficient solar cell devices fabricated with PEDOT:PSS on silicon,[38, 39] we considered the presence of d-sorbitol at the interface a likely candidate for charge recombination. This may occur either through trapping charges on the d-sorbitol molecule or through surface energy modification by the highly polar hydroxyl groups from the d-sorbitol. In a typical solar cell, photogenerated charges are extracted at the same rate at zero or negative biases. With the addition of the d-sorbitol to the PEDOT:PSS the devices requires a negative driving force to extract all the charges. This is indicative of shallow trap states preventing charges from moving at zero voltage. A study of d-sorbitol doping of PEDOT:PSS interlayers between p-Si and Al metal based Schottky diodes has shown both a change in HOMO levels and the presence of the trap states we have seen in our devices (**Figures 11,12**).[44]

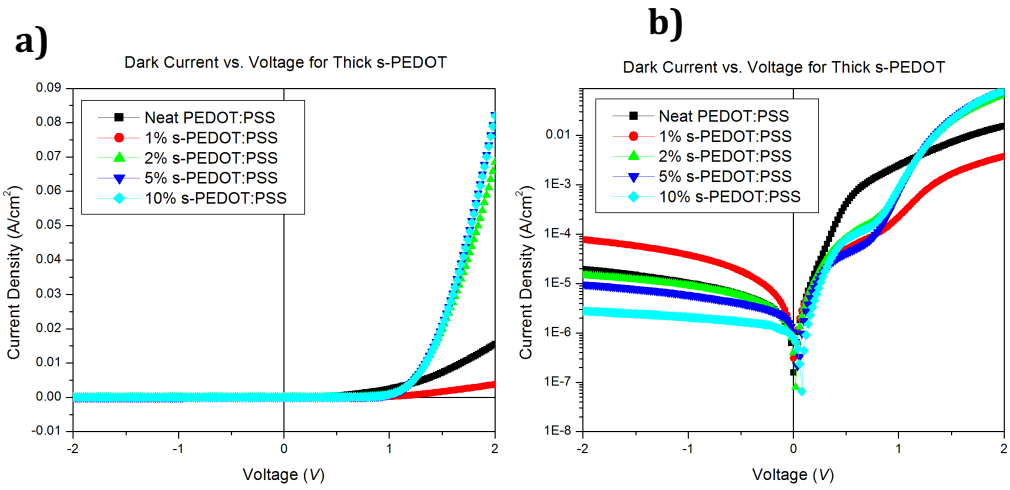

Figure 11. Linear a) and logarithmic b) dark *JV* Curves of Hg drop devices (Cu/InGa/n-Si/s-PEDOT:PSS/Hg) with varying d-sorbitol concentrations.

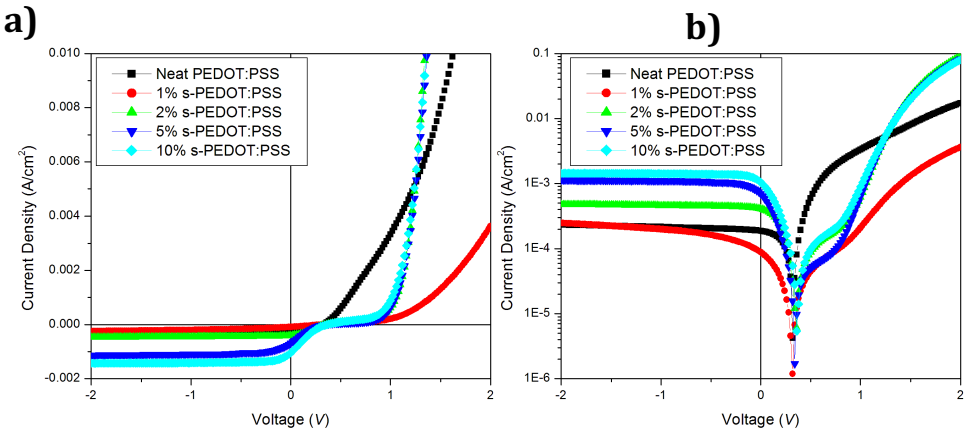

Figure 12. Linear a) and logarithmic b) *JV* Curves of Hg drop devices (Cu/InGa/n-Si/s-PEDOT:PSS/Hg) with varying d-sorbitol concentrations under AM1.5 illumination.

Table 1. Device characteristics data.

	0%d-	1%d-Sorbitol	2%d-Sorbitol	5%d-	10%d-
J_{sc}	0.188	0.0885	0.405	0.689	1.04
V_{oc}	0.35	0.32	0.35	0.35	0.37
FF (%)	41.6	26.6	30.9	17.9	18.9

2.3.5 s-PEDOT:PSS Film Characterization

The mechanical bonding strength was not quantitatively tested, however all the devices fell into two categories. At 0 or 1 wt. % d-sorbitol, the s-PEDOT:PSS layers showed poor adhesion. Inverting these devices caused the FTO to fall off the silicon wafer. At 2, 5, and 10 wt.% d-sorbitol, the Silicon and FTO layers could not be separated even after several months under ambient conditions.

The thick drop-cast films of s-PEDOT:PSS are highly absorbing, resulting in low current densities (**Table 1**) in the light curves of these devices. The transmittance of the thick films (**Figure 13**) shows that highest transmittance is only 5% of light. This only decreases for red and IR light, reducing photons absorbed by the silicon by more than 99% above 550 nm. This accounts for the low photocurrents in the Hg drop devices. In addition, in this device configuration the Hg drops cast a small shadow, further limiting the photocurrent. Thin spin-cast films (**Figure 15**) on the other hand are highly transparent (lower than 0.05 absorbance), and could be used in press-contact architectures without large parasitic absorption.

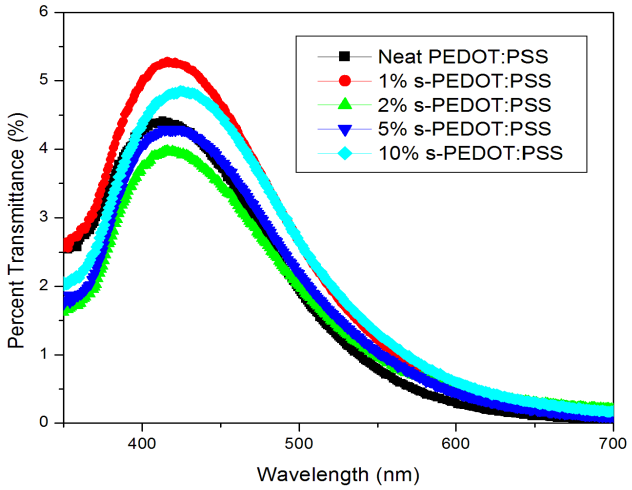

Figure 13. Percent transmittance of thick drop-cast films of s-PEDOT:PSS on glass slides with different d-sorbitol concentrations.

It is evident from the saturation region of the dark curves that the higher concentrations of sorbitol increase conductivity and thus reduce series resistance in the

devices. In the light curves, this increases the photogenerated current and allows higher extraction of charge carriers under reverse bias. The trend towards higher conductivity is clear in both devices and films. However, this conductivity enhancement comes at the cost of a more pronounced recombination in the area of interest for power production. At 1% d-sorbitol by weight, films were not tacky and devices easily fell apart. Therefore, lowering the d-sorbitol concentration to mitigate the recombination is not a viable option for the proposed device lamination strategy.

Differential scanning calorimetry (DSC) shows that there is little or no phase change in the s-PEDOT:PSS film (**Figure 14**) through the temperature range evaluated. The d-sorbitol doped PEDOT:PSS polymer films are tacky at room temperature and heating reduces the viscosity and allows improved contact during the lamination of the two layers. This increases the adhesiveness of the film and allows for better flow of charges through the device. The heat capacity of a pure polymer film is higher than that for films incorporating sorbitol, but the shape of the curves is substantially similar, showing that the addition of sorbitol does not add any phase changes. The large difference between the heat capacity of the neat PEDOT:PSS films and the d-sorbitol doped films can be accounted for by the fact that d-sorbitol is added as a weight percent of the solvent, so the dry films would have a higher weight percent of d-sorbitol than the solution. UV-Vis absorbance data shows that spin-coated films are highly transparent across the visible and nearby regions. The d-sorbitol has little effect on the light absorbing properties of the film although the absorbance is somewhat lower at higher concentrations. (**Figure 15**).

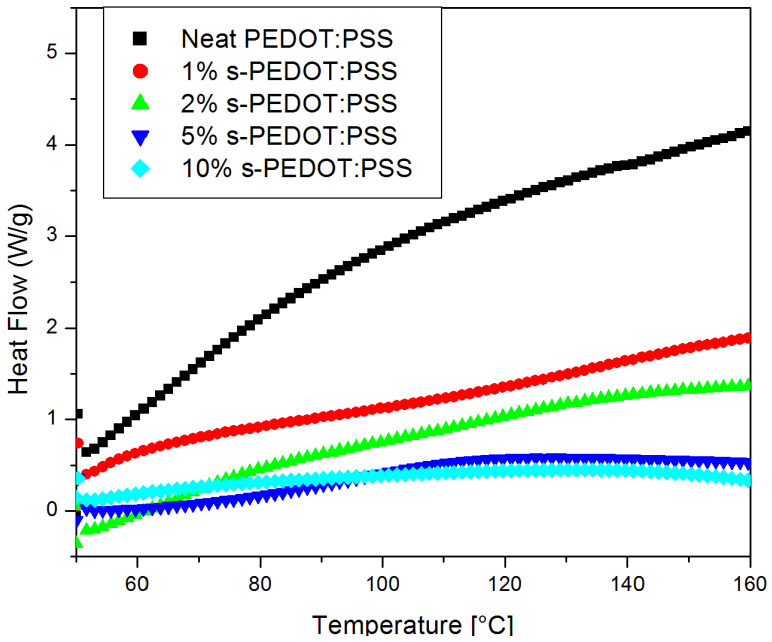

Figure 14. Differential scanning calorimetry of dried PEDOT:PSS and s-PEDOT:PSS samples.

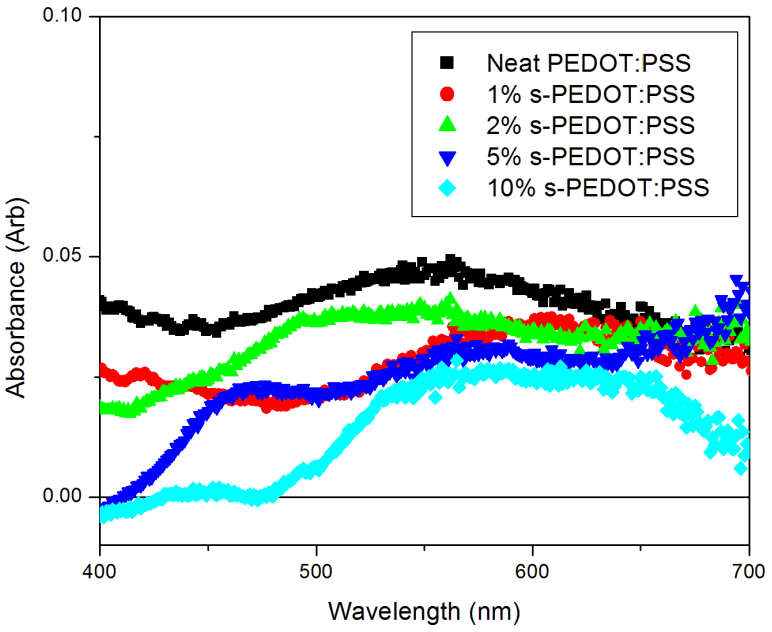

Figure 15. UV-Vis Absorbance of spin-cast thin films of PEDOT:PSS and s-PEDOT:PSS.

2.4 Conclusions

D-Sorbitol is a useful additive to aqueous suspensions of PEDOT:PSS to produce a conductive glue and electrical contact for p- and n- type silicon. The s-PEDOT:PSS forms an ohmic contact with p-Si and a rectifying, photoactive junction with n-type silicon. The conductivity, adhesion, and minority carrier trapping are all d-sorbitol concentration dependent. The highest conductivity was realized at 10% d-sorbitol by weight in both devices. For laminating to p-Si, the higher conductivity realized by higher concentrations of d-sorbitol is desirable and resulted in s-PEDOT:PSS/p-Si devices with a low contact resistance. Higher concentrations also improve the PEDOT:PSS/p-Si adhesion and lamination. On n-Si, the presence of d-sorbitol induces interfacial charge recombination that is likely due to minority carrier trapping in the d-sorbitol-doped polymer layer. At low d-sorbitol concentrations (<1% wt.) good electrical contact is observed, however insufficient adhesion fails to hold s-PEDOT:PSS/n-Si devices together. Future work in this area will require materials with both high conductivities and good lamination properties as was observed in this work, coupled with more versatile interfacial charge transfer characteristics for producing viable laminate s-PEDOT:PSS/n-Si solar cells.

Chapter 3 – Silicon Surface Modifications

3.1 Introduction

While it is possible to choose an adhesive additive with no –OH bonds, the chemistry of modifying the silicon surface is well known,[43] and is a more useful strategy to fix the charge recombination problem than choosing a new adhesive. Alkylating the surface silicon is a well-known form of surface modification, and can prevent oxidation of the surface by -OH containing materials in the s-PEDOT:PSS.[46] Longer chain alkyl groups could be used to increase adhesion to the silicon surface but methyl groups were used for simplicity.

A key component to choosing a new adhesive or surface modification is understanding the mechanism by which recombination is occurring in the devices made in chapter 2. It is very unlikely that recombination is occurring in the bulk of the s-PEDOT:PSS layer. There was no difference in FTO sandwich and p-Si devices between PEDDOT:PSS layers with and without sorbitol besides conductivity changes. However, in n-Si devices there is a qualitatively different *JV* relationship when d-sorbitol is added for both light and dark curves. Therefore we concluded that the interaction between n-Si surface and the PEDOT:PSS was responsible for recombination. Also, s-PEDOT:PSS has been used successfully in organic photovoltaics and OLEDs in previous work,[11] therefore, surface recombination was the issue addressed. Two possible modes of interaction at the surface could be distinctly identified and mitigated against. The easiest to identify is whether the d-sorbitol is chemically interacting with the silicon surface. Silicon can easily oxidize in the presence of water and alcohol groups and sorbitol has hydroxyl groups that

react in a similar way (**Figure 16**).[43] This sorbitol functionalization of the surface can be identified by washing off the s-PEDOT:PSS layer and then analyzing the surface for any remaining, bonded d-sorbitol molecules. This can be accomplished through XPS or surface enhanced Raman spectroscopy. In this case, the surface would be alkylated to prevent forming any d-sorbitol bonds to the silicon surface (Si-O-C bonds). Should there be no chemically attached d-sorbitol, then field effects from the polar –OH bonds in the d-sorbitol would most likely be to blame for the phenomenon. In this case, a thin (several nanometer) interlayer of MoO_3 could be used as a p-type spacer to remove the effect of any fields associated with the d-sorbitol. Should the method of charge recombination turn out to be in the bulk of the s-PEDOT:PSS layer, then a new adhesive molecule with different properties would be required. Due to the ease of testing, methylating the surface and testing the devices was done to see if that would fix the recombination problem.

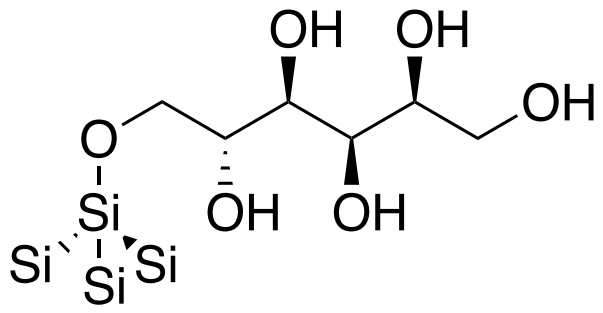

Figure 16. Silicon surface functionalized by d-sorbitol.

Multiple methods exist for chemical modification of a silicon surface by wet chemical reactions at low temperatures.[47] Of the two most common, one is through a chlorination/Grignard reagent, and the other is a radical process bonding alkenes to the surface known as hydrosilylation. Both have advantages and drawbacks. The hydrosilylation route is more versatile, since alkene groups can be synthesized on almost

any small molecule organic compound, while Grignard reagents are highly reactive with many other functional groups. The chlorination/alkylation with a Grignard reagent route is advantageous in that it can alkylate almost every surface atom in crystalline silicon.[14, 47]

Hydrosilylation is a process where a hydrogen atom on the silicon surface is abstracted from a silicon atom by a radical process and reacts with a terminal alkene.[24] The result is a hydrogen radical in solution and a silicon radical at the surface. An alkene can react with the silicon radical, leaving a carbon-silicon bond and a radical carbon on the other side of the alkene. This carbon radical can abstract the nearest hydrogen, propagating the process to the next silicon surface atom, or it can react with a hydrogen radical to end the chain reaction. A radical initiator is needed to abstract the initial hydrogen in the process, but it is a highly self-propagating reaction. However, the alkene reacts to form an alkane, and is therefore bent at an angle from the surface. This leads to stearic hindrance in at least one direction, preventing the process from attaching the alkene at every surface site. This is further compounded if the molecule attached to the alkene is bulky. Also, since the reaction often proceeds by radical abstraction from a nearest neighbor, local groups of attachment will occur, but they may run up against other groups of reacting alkenes and form patches with disordered boundaries (**Figure 17**). This process can be terminated by a silicon radical abstracting a hydrogen atom from any other chemical species in solution.

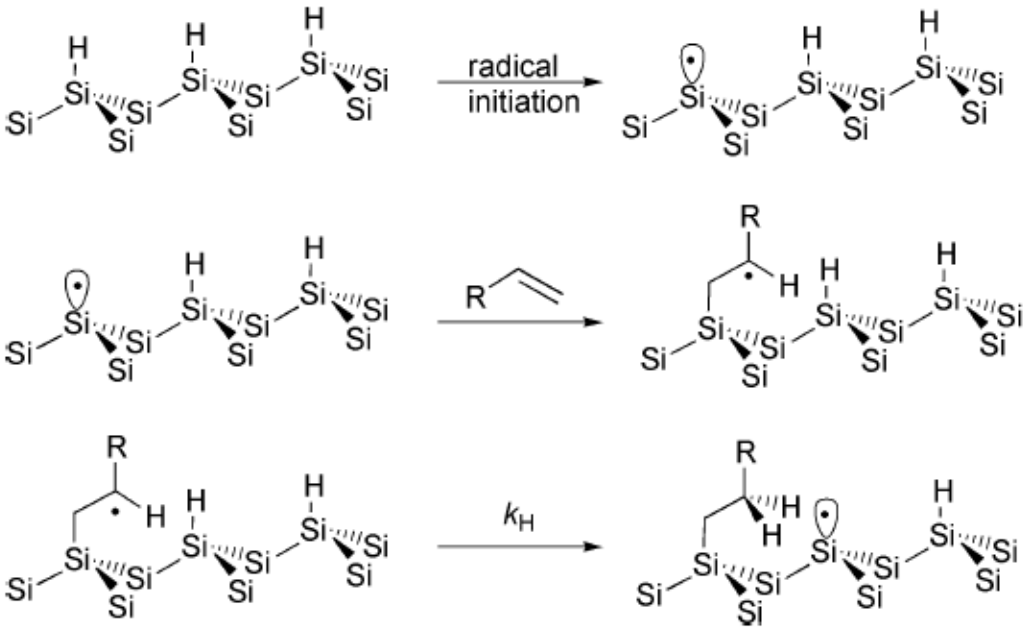

Figure 17. Radical addition of alkenes to hydrogen terminated Si(111) surfaces. Image from *Organic Modification of Hydrogen Terminated Silicon Surfaces.*[43]

This method is most useful for attaching small molecules with specific functionality but where complete surface coverage is not absolutely necessary. This method will always leave some amount of surface atoms vulnerable to oxidation, The silicon-carbon bond formed does not spontaneously oxidize in the presence of water and oxygen, but the leftover silicon-hydrogen and silicon-silicon bonds at the surface will still oxidize. Crystalline silicon surface modified by alkene hydrosililation were used and tested in a subsequent experiment. XPS analysis was used to determine whether a chemical modification had occurred as intended. Details of this experiment can be found in Chapter 5.

The second route is the chlorination/Grignard route. This reaction is carried out in two steps, first chlorinating a hydrogen terminated silicon surface and then reacting the silicon-chlorine bonds with an appropriate Grignard reagent. It is also possible to use

organolithium, but it is more common to use R-Mg-X reagents. The chlorination is a radical halogenation achieved using phosphorous pentachloride as a source of chlorine atoms and an appropriate radical initiator. Benzoyl peroxide is the most common choice. Short-chain, alkyl Grignard reagents give the best surface coverage, with methyl Grignards being the best option in terms of reaction speed and surface coverage. This results in as little stearic hindrance as possible when reacting with neighboring silicon surface atoms. Any Grignard reagent will work, but the bigger the molecule, the less likely it is to achieve full surface coverage and the longer the reaction will take. Propynyl and ethynyl Grignards have been shown to achieve close to 100 percent coverage, though the reaction times needed are much longer than methyl groups.[47] Bent or cyclic molecules will invariably hinder some surface atoms from reacting at all. The silicon (111) crystal plane provides the best surface for fabricating devices on a functionalized surface, as each silicon surface atom will have one hydrogen bonded normal to the surface. Silicon (100) planes have two hydrogen atoms attached to each surface silicon atom,[43] and not pointing normal to the surface will result in steric hindrance when attaching molecules. Mixed Grignard reagent coverage is also possible using this method.[46] A small number of longer chain alkanes or other groups can be mixed with methyl Grignard in the second step of the process to produce a number of sites where an alkyl chain or other linking group extends above the passivating layer of methyl groups.[48] This method is useful for creating surfaces with a very specific affinity for liquid or solid layers that contact it. This method is ideal for passivating a surface, and tends to generate better surface coverage than other methods for small molecules, up to complete passivation, but is more limited in the diversity of molecules and functionality that can be attached. Often, a small, conjugated linker such as a thienyl Grignard is used to

form a monolayer,[48] then that surface can be reacted further to link molecules that would not easily be bonded via a Grignard process.

Lastly, the two processes can be combined to attach alkenes but mitigate against oxidation of unreacted surface sites.[21] This is accomplished by chlorinating the surface first and running a modified reaction where an alkene can react with a silicon-chlorine bond to form a silicon-alkane linkage, and then reacting the surface with a methyl Grignard reagent to methylate any leftover surface sites. This would passivate many leftover silicon surface atoms, but has two drawbacks. One is that stearic hindrance can still prevent alkylation by the Grignard reagent due to the size of the alkene-bearing compound. Another is that the alkene containing compound must not be reactive to methyl Grignard reagents.

To produce flat, hydrogen terminated silicon, a multi-step process is necessary. A hydrofluoric acid treatment followed by a basic ammonium fluoride treatment produces the flattest possible surfaces.[43, 49] Even highly polished silicon wafers are atomically rough, and an anisotropic chemical etching method is needed. Immersion in hydrofluoric acid is sufficient to remove surface oxide and terminate all surface sites with hydrogen, but it tends to etch pits and ridges into the silicon. This was enough to remove surface oxide when making hydrogen terminated silicon devices, but is not enough to achieve good surface coverage when chemically modifying the surface. In order to maximize the number of surface atoms that have a single hydrogen atom attached, such as the top of a terrace or mesa, the silicon must be etched in such a way as to etch atomic planes sideways rather than downwards. That is, silicon with one hydrogen atom attached must react most slowly with the etchant while more than one increases the likelihood of being etched. This corresponds to the situation where the edge of a crystalline plane is more reactive than the

atoms on the inside. In an acidic solution, such as HF, the etching is very isotropic, and does not follow such a pattern. However, in a basic solution this is the case. Hydrofluoric acid does react more quickly with oxide, so it is essential to remove large scale surface oxide quickly, however in order to flatten the resulting silicon surface, a basic etchant is necessary. Aqueous ammonium fluoride works well for this purpose, but must be carefully degassed of any dissolved oxygen. Dissolved oxygen in water will start new oxide in the center of the flat terraces and result in pitting on the surface. By etching the silicon surface in degassed aqueous ammonium fluoride, flat, terraced silicon surfaces can be prepared which are ideal for surface modification.

Once prepared, the atomically flat silicon surfaces are in an optimal state for surface functionalization, through either method described above. This functionalized silicon is interesting enough on its own, but our first intent was to identify d-sorbitol interactions with hydrogen terminated silicon, and to find a way to mitigate against that. The most common surface modification that yields the best passivation is the Grignard methylation route, so we used this and compared methylated silicon devices with hydrogen terminated silicon devices using an n-Si/s-PEDOT:PSS junction. We studied the surface by removing the polymer layer and using XPS analysis, and we studied the device performance using Hg drop contacts, similar to Chapter 2.

Modifying the silicon surface will have an effect on the Schottky junction independent of any changes in the organic layer, including the presence or absence of d-sorbitol. Because the Si-Me bond has a difference electric dipole than the Si-H bond, the built in barrier height is slightly modified.[3, 50] Previous experiments have shown the surface dipole of methyl-terminated devices changes the barrier height by about 100 mV.[5] This is

due to the increase in electronic field that an electron would cross to move from the semiconductor into the PEDOT:PSS and thus results in an effective greater difference in work functions between the inside of the semiconductor and the PEDOT:PSS layer.

3.2 Materials and Methods

3.2.1 – Oxidation of Silicon by Water and Alcohol Groups

Silicon-hydrogen bonds tend to spontaneously oxidize in the presence of water. This occurs through an addition by oxygen electrons to silicon resulting in a pentacoordinate silicon atom, leaving a positive charge on the oxygen atom and an extra conduction band electron in the silicon crystal. The hydrogen from the pentacoordinate silicon atom reacts with one of the hydrogen atoms from the water molecule, leaving as hydrogen gas and generating a silicon-hydroxyl bond (**Figure 18**). This can proceed further through an energetically favorable rearrangement where the oxygen atom moves back into the crystal, leaving another surface site terminated with hydrogen, and the process will repeat until a layer of oxide is built up on the surface. This process is not extremely fast, but is increased in speed with humidity and temperature.

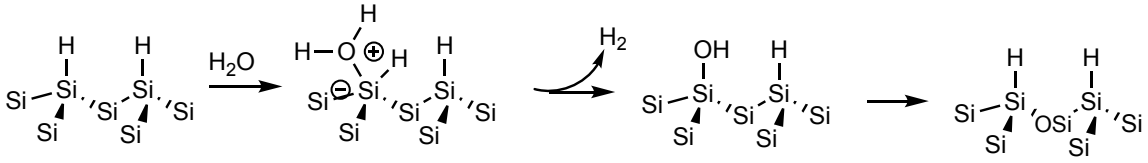

Figure 18. Oxidation of Si(111) by H_2O.[43]

Reaction by alcohol groups follows a similar mechanism. First the oxygen electrons bind to a surface silicon atom, leaving a positively charged oxygen atom and a

pentacoordinate silicon with an extra conduction band electron. Next hydrogen is lost leaving a neutral species. However, due to the oxygen-carbon bond in the alcohol, a rearrangement is no longer favorable, so the alcohol is bonded to the surface through an oxygen atom (**Figure 19**).

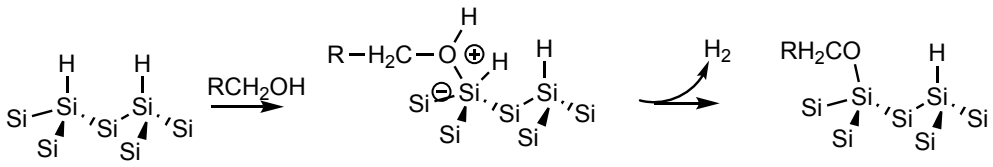

Figure 19. Oxidation of Si(111) by alcohol groups.[43]

In the presence of a bulky alcohol some surface sites will be hindered from reacting with other large molecules. Therefore, in the presence of water and a bulky alcohol, some surface sites will inevitably also react with water. This results in a layer of alcohols bonded to the surface and the formation of some amount of silicon oxide as well. D-sorbitol has not one but six alcohol groups, as well as being extremely hydrophilic. Since annealing the s-PEDOT:PSS was necessary to drive the water out of the layer, this type of reaction would have been accelerated by heat.

3.2.2 – Chlorination-Grignard Methylation

Construction of all tested devices began with the n-Si processing. In order to ensure that the silicon surfaces are clean, the wafers were diced into chips and etched in a piranha bath for 1 h. This removed any organic compounds on the surface of the silicon and generated a thick oxide layer on all surfaces. Next, we etched the silicon chips in a hydrofluoric acid bath for 10 seconds. This removed the oxide layer, and left a hydrogen terminated silicon surface, which is clean and free of any oxide or organic contamination.

Further etching was performed in degassed aqueous ammonium fluoride, resulting in flat terraces with the greatest number of (111) plane silicon atoms bonded to terminal hydrogen atoms possible.[43]

At this point, the silicon surface was modified by replacing the terminal hydrogens with methyl groups.[51] The silicon was immersed in a dry chlorobenzene bath in the glove box saturated by PCl_5 with benzoyl peroxide, a radical initiator, replacing the hydrogen atoms with chlorine. Then the chlorinated silicon was rinsed with THF, and reacted with 3M methylmagnesium chloride in THF for 24 h to form the final methyl terminated surface. (**Figure 20**)

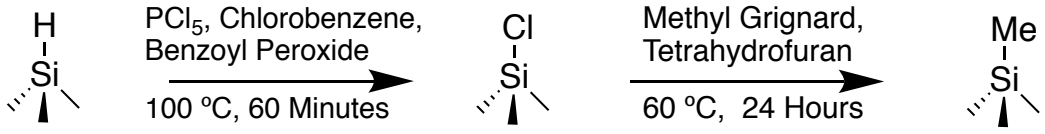

Figure 20. Scheme for methylating a silicon surface by the chlorination/Grignard route.

Hydrogen terminated and methyl terminated Si(111) surfaces were testing using a Kratos Ultra XPS system using an Al Ka x-ray source to look at species present at the surface. Carbon 1s and Silicon 2p orbitals binding energy was examined to determine the presence of Si-C bonds, Si-O bonds, or lack thereof. Freshly prepared samples of each type were tested, as well as four samples that had had polymer layers drop cast and then removed, hydrogen terminated crystals with and without d-sorbitol, and methyl terminated crystals both with and without d-sorbitol. The organic layers were removed by sonicating the samples in acetone for 1 h, peeling off the organic layer, and sonicating in MilliQ water for 1 h.

3.2.3 – Device Preparation and Testing

A highly efficient device would have used a thin film of s-PEDOT:PSS and a transparent conductive oxide such as FTO, but for comparison we used the same mercury drop architecture that was used in Chapter 2.

Double side polished 15 Ω•cm n-Si(111) wafers were diced into chips approximately 1cm^2 and then rinsed in isopropanol and MilliQ H_2O to remove any dust and dirt. These were subsequently cleaned in a piranha bath for 30 min at 100°C to remove any surface contamination and form a thick oxide layer on the surface, and then rinsed in MilliQ H_2O several times to clean the piranha off the oxide. Next, these chips were etched in buffered HF (aqueous 5% HF to 35% NH_4F) for ten seconds to remove the oxide formed by the piranha and any other contamination that may have survived the piranha bath. The chips were rinsed with MilliQ water again into an HF waste container and then transferred immediately to a nitrogen filled glove box or vacuum to prevent surface oxidation. An etchant bath was prepared with 40% weight to volume percentage aqueous ammonium fluoride for a second fluoride etch. This etch leaves a much flatter surface, with large atomically flat terraces rather than the rough etch under the acidic conditions while still leaving a hydrogen atom at every terminal site.[43] To avoid pitting the surface, there can be no oxygen present in the solution, so this solution was degassed by bubbling argon through for one hour prior to etching. After this, the silicon chips were etched for 10 min, resulting in an atomically flat, hydrogen terminated surface. At this point the chips were moved into a glove box to prevent any surface oxidation. Hydrogen terminated silicon devices used this silicon with no further processing steps.

The silicon chips were methylated according to the common process depicted in **Figure 20**. The following processes were all carried out in a nitrogen atmosphere glove box to prevent reactions between atmospheric oxygen or water and the silicon wafers or highly reactive Grignard reagents. The silicon chips were then placed in vials and covered with chlorobenzene. Enough PCl_5 was added to create a saturated solution, and a few grains of benzoyl peroxide were added as a radical initiator. The solution was heated to 100°C for 1 h, and then allowed to cool to room temperature. At this point, the silicon crystal terminal hydrogen atoms had been replaced with chlorine atoms.[51] The chips were rinsed with chlorobenzene, and then THF. Following this, the chips were submerged in a 3 M methylmagnesium chloride solution in THF and subsequently heated to 60°C for at least 24 h. This is a slow reaction, so extra time is helpful. At the end of 24 h, the extra solution was poured off, and the chips were once again rinsed with THF to remove as much methylmagnesium chloride as possible. At this point the chips were removed from the glove box and rinsed with acetone to quench any remaining Grignard reagent, and finally rinsed with MilliQ water to remove any organic bases and magnesium salts that may have been left on the surface. These chips were dried and used for tests involving methylated silicon chips.

Solution Preparation

Solutions containing dispersions of PEDOT:PSS and d-sorbitol (s-PEDO:PSS) were prepared by adding 1, 2, 5, and 10% wt.% d-sorbitol to a premade 1.5 wt.% PEDOT:PSS solution purchased from Ossila. Due to the small percentages, 10, 20, 50, and 100 mg of d-sorbitol were added to a vial, and 1 mL of neat PEDOT:PSS solution was added via a micropipette. A stir bar was used and the solutions were kept at room

temperature and used within one week. To remove any aggregates, immediately before being used, the solutions were filtered through a polysulfone membrane filter with a 40 micron pore size.

Device Fabrication

Devices were made by drop-casting thick films of either neat PEDOT:PSS as received from Ossila or prepared s-PEDOT:PSS solutions directly onto silicon chips that were either hydrogen or methyl terminated as needed for testing. These solutions were allowed to dry in a fume hood with a petri dish cover over them in order to prevent dust or dirt falling into the wet layer. Once dry, the chips were baked on a hot plate at 110°C to drive off any excess water that may still have been present in the layer. The back side of the device was contacted by painting a small amount of Indium Gallium eutectic onto the silicon and placing it on a copper plate. The front side contact was made by pipetting a small mercury droplet onto the s-PEDOT:PSS anode, and contacting this droplet with a platinum wire. In addition, devices were made using the same procedure but with higher conductivity PEDOT:PSS at 5% d-sorbitol. The s-PEDOT:PSS was made deliberately thinner by diluting the s-PEDOT:PSS suspension with milliQ water, reducing the concentration by one half and resulting in thinner layers when drop-cast. This allowed more light to reach the silicon and increase photocurrent to show how devices with significant current density were affected by hydrogen termination versus methyl termination of the crystal face. The higher conductivity PEDOT:PSS was necessary for charge transport laterally through the s-PEDOT:PSS layer to the Hg drop contact.

Device Testing

IV curves were obtained for the devices using a Keithley 2400 series source-measure unit from -2 to 2 V, both in the dark and using a solar simulator lamp to produce AM1.5 equivalent radiation (100 mW cm^{-2}). The area of the devices were also measured in order to generate *JV* curves from the acquired *IV* data. Using these measurements device parameters were calculated.

3.3 Result and Discussion

3.3.1 Methylation by Grignard – XPS

Chemically etched, hydrogen terminated n-Si (111) was methylated by the chlorination/Grignard route. This was analyzed by x-ray photoelectron spectroscopy. Silicon-carbon bonds were present, indicating a substantial degree of surface coverage (**Figure 21**). The Si-C bond shows up as a shoulder around 284 eV on the larger adventitious carbon peak.[52] This peak captures any carbon containing molecules that adsorb onto the surface from the atmosphere, usually small molecules such as alcohols, aldehydes and carboxylic acids that adhere more strongly to the surface than alkanes. Because carbon is slightly more electronegative than silicon, there is a greater amount of electron density on the carbon in the Si-C bond, slightly lowering the energy needed to free the surface C 1*s* electrons. In carbon-oxygen bonds, the polarity of the dipole is opposite and more energy is required, resulting in a peak around 287 eV.[50] Some oxidation was present in the methylated samples as seen at 102 – 103 eV in the silicon 2p spectrum (Figure 21b).

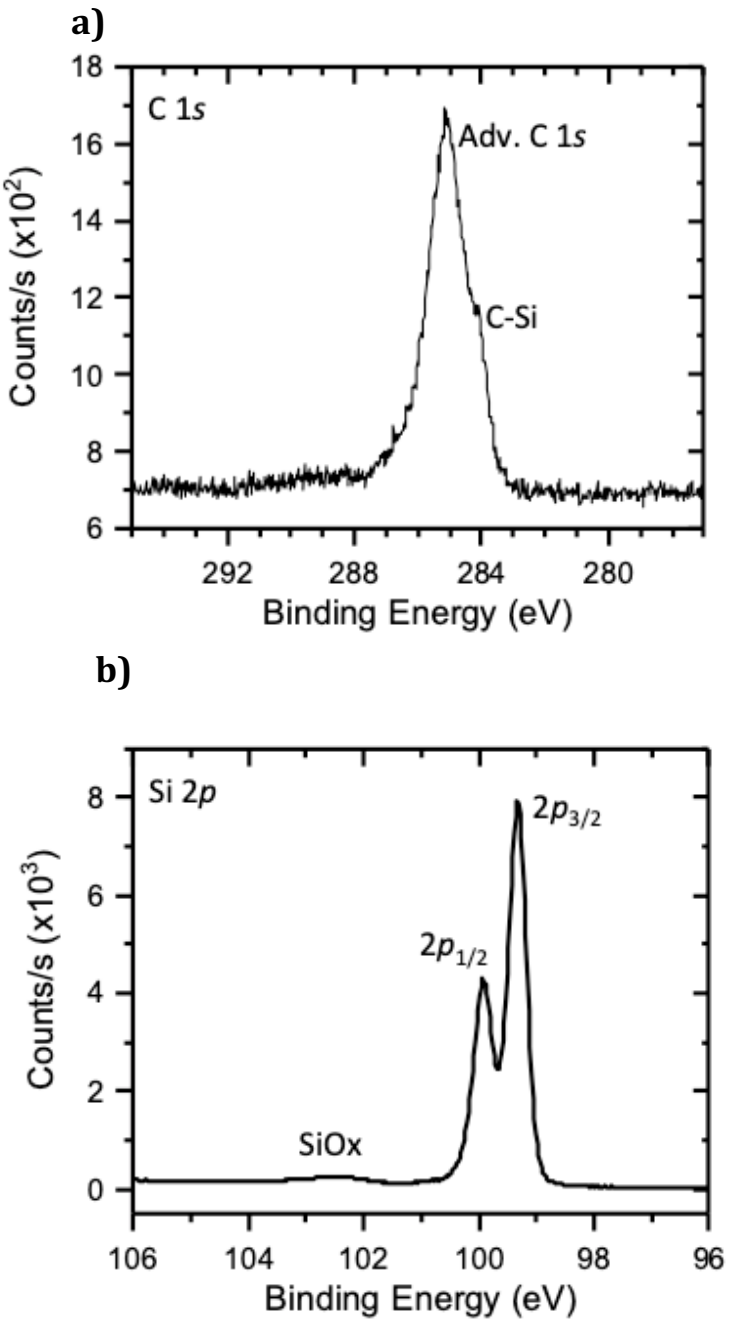

Figure 21. Methylated Si (111) surface. a) Carbon 1s electrons and C-Si Bonding. b) Silicon 2p electrons and SiOx formation.

3.3.2 Oxidation by Sorbitol of H-Si(111) and Me-Si(111) - XPS

Chemically etched, hydrogen terminated Si(111) and methyl terminated n-Si (111) prepared through chlorination/Grignard reaction were each coated in both PEDOT:PSS and

s-PEDOT:PSS layers. These samples were drop cast, annealed at 100 °C for ten min, and then left in the glove box for 1 week. The glove box was an attempt to prevent oxidation by atmospheric moisture and oxygen, although this may not have been sufficient. Four samples were prepared, H-Si(111)/PEDOT:PSS, H-Si(111)/s-PEDOT:PSS, Me-Si(111)/PEDOT:PSS, and Me-Si(111)/s-PEDOT:PSS. The polymer layers were then washed off by sonicating the samples in acetone, isopropanol, and water until no polymer layer was observed on the surface. These were sent out for XPS analysis (**Figures 22-23**).

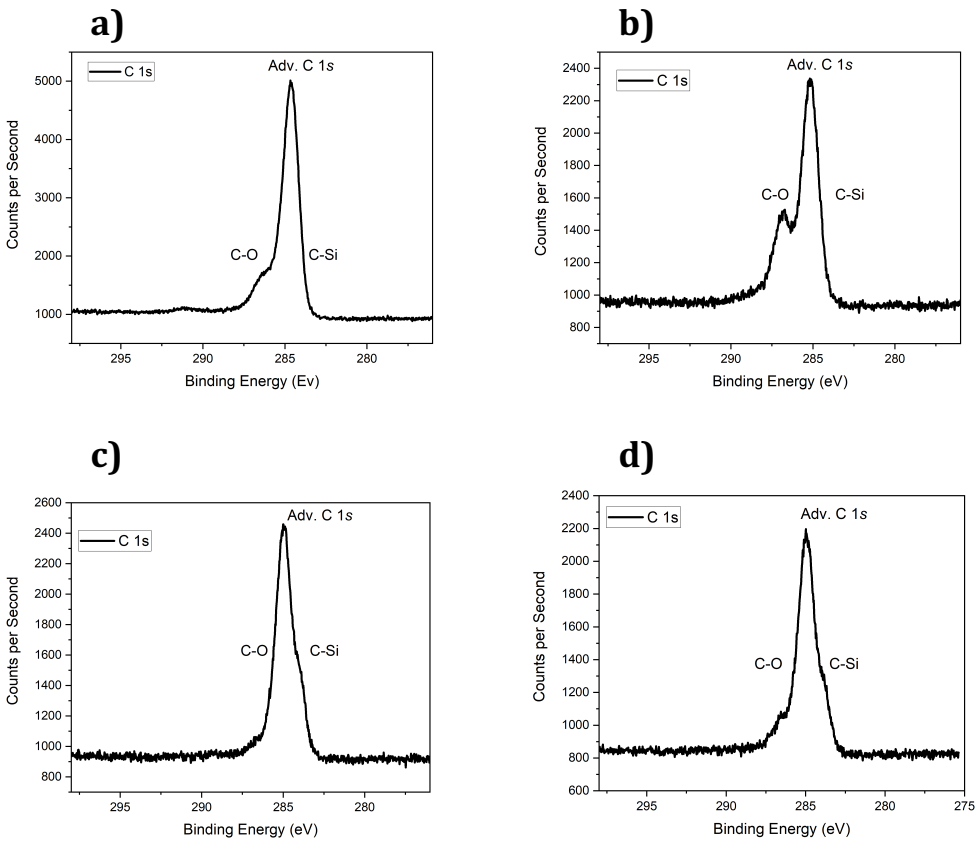

Figure 22. Carbon 1s XPS spectrum of a) H-Si(111)/PEDOT:PSS, b) H-Si(111)/s-PEDOT:PSS, c) Me-Si(111)/PEDOT:PSS, d) Me-Si(111)/s-PEDOT:PSS.

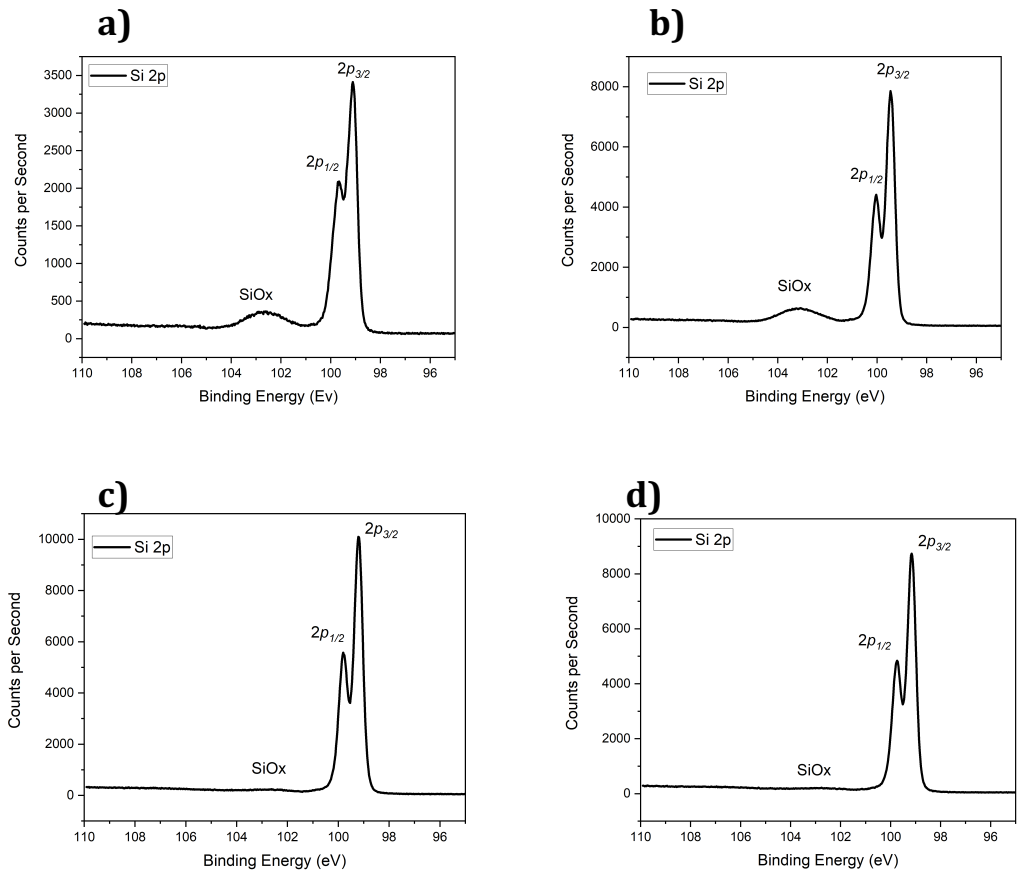

Figure 23. Silicon 2p XPS spectrum of a) H-Si(111)/PEDOT:PSS, b) H-Si(111)/s-PEDOT:PSS, c) Me-Si(111)/PEDOT:PSS, d) Me-Si(111)/s-PEDOT:PSS.

Measuring the exact percentage of coverage for methyl groups was not possible due to the large amount of adventitious carbon, but the surface was significantly more protected by the methylation process. **Figures 22c** and **22d** show the Si-C bond in the methylated devices, which appears as a shoulder in the graphs between 283 and 284 eV. The rest of the C1s signal comes from adventitious carbon on the surface from atmospheric sources. Unfortunately, it is not possible to distinguish the Si-O or the O-C bond on the surface, as they are lost in the SiOx peak for Si 2p electrons and the large adventitious carbon peak in the C 1s peak using this method. The SiOx peak in **Figure 23b** indicates

that there was oxidation on the H-terminated silicon surface while **Figure 23c** shows the methyl groups protecting the surface from oxidation. We find it likely that some of this is due to the reaction with d-sorbitol and not just water, as the mechanism is the same, and the d-sorbitol has six -OH moieties (**Figure 4**) that could be reacting. **Figure 23d** clearly shows that SiOx bonds are prevented from forming on the methylated surface, eliminating sorbitol bonding to the silicon surface.

A careful study of **Figure 22** shows a growing shoulder on the left side of the C1s electrons in different cases. This is probably correlated with C-O bonds, which show up at a binding energy of 287 eV.[5, 50, 52] This is particularly noteworthy, as it stands out from the adventitious carbon that has adsorbed on the silicon surface between processing and testing, which is similar in all of the surfaces tested. The C-O peak would be expected to be significantly larger if d-sorbitol is present on the surface, since it has 6 C-O bonds per d-sorbitol molecule. The C-O peak size correlates with surface preparation, and suggests that d-sorbitol will stick very strongly to an untreated surface. If we consider **Figure 22a** vs **22b** there is a much larger C-O shoulder in **Figure 22b**. Since **Figure 22b** had d-sorbitol in the original organic layer, this indicates that d-sorbitol in the original film preparation stays on the surface even after extensive cleaning when a hydrogen terminated surface is used. In addition, if we consider **Figure 22b** vs **Figure 22d**, we see the effect of surface methylation on the relative size of the C-O shoulder. The signal is greatly reduced in **Figure 22d**, suggesting that the surface methylation is effectively blocking or significantly reducing the amount of C-O bonds at the silicon surface, which suggests that it is blocking the formation of an adsorbed d-sorbitol layer. As expected, **Figure 22c** has the lowest C-O signal, as it had no d-sorbitol in its processing and was also methylated to prevent

oxidation by any other source. This means that neither water nor alcohol groups, which are the possible causes of trap states, are binding to the methylated silicon surface.

Although this experiment was not conclusive for functionalization by d-sorbitol, the strong oxidation suggests that the hydrogen-terminated silicon is highly prone to oxidation and it is likely that d-sorbitol would be reacting with the silicon surface.

3.3.3 Methylated N-Type Silicon Rectifying Devices

The *JV* curve relationships in the dark in **Figure 24** clearly show that a high conductivity is essential for passing high amounts of current. Increasing the sorbitol content of the solution results in a higher conductivity layer, able to pass more current when bias is applied. Also, Figure 5 shows how the methylated silicon surface results in a much more single diode structure, whereas the hydrogen terminated devices showed charge trapping or a double-diode features in their *JV* curves. The two distinct features in evident in the H-terminated devices show trap states that require almost 500 mV of extra bias to move electrons out of. This is likely due to the fact that at some surface sites there are sorbitol molecules covalently bonded to the silicon, while at others the PEDOT:PSS is in direct contact with the silicon. At the sites in direct contact with the PEDOT:PSS, the device passes current normally, while where there are trap states caused by the sorbitol-Si bonds, an extra bias is needed to move current.

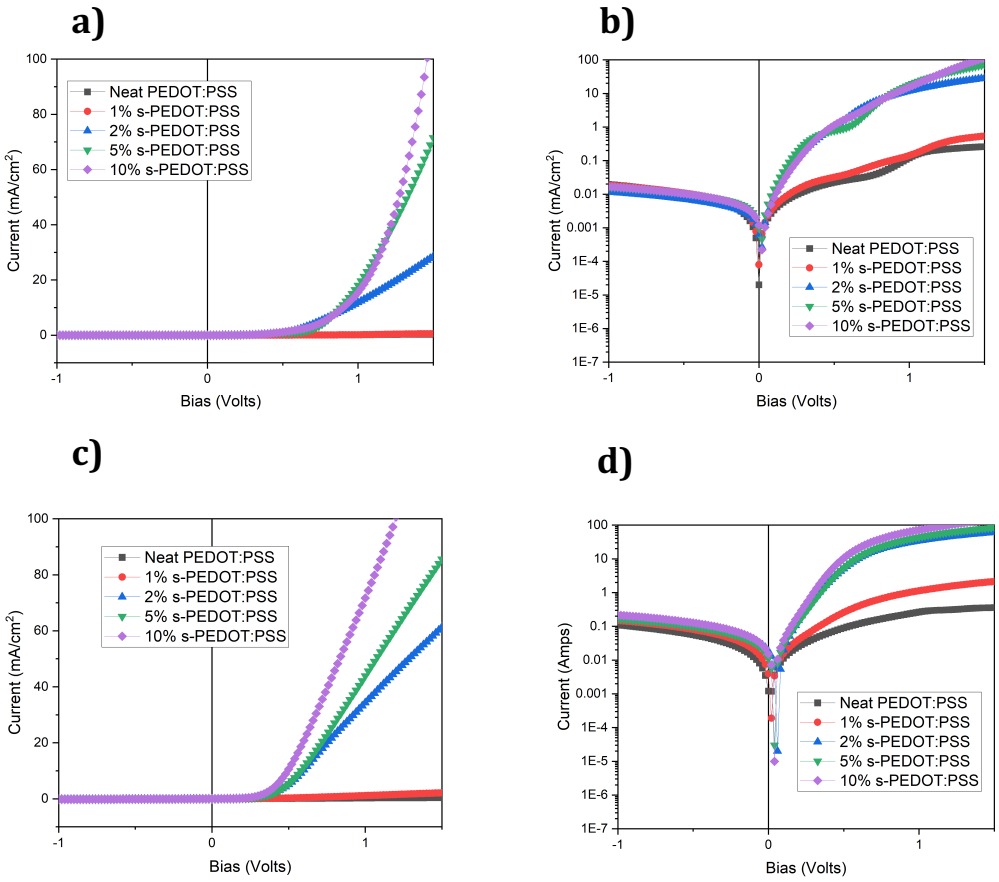

Figure 24. Hydrogen-terminated a) linear, b) logarithmic and Methyl-terminated c) linear, d) logarithmic n-Si(111)/s-PEDOT:PSS Devices *JV* Relationships in the dark.

Figure 24 demonstrates quite conclusively the effectiveness of d-sorbitol in increasing the conductivity of the PEDOT:PSS layer on its own. The difference between neat PEDOT:PSS and 1% d-sorbitol is quite clear, and the conductivity increases further with 2%. There are to be significant changes as the d-sorbitol concentration increases from 0% to 2%, while increases after 2% show less significant gains. While it is not easy to see from the linear curves, the logarithmic plots of the data show that all of these devices act as diodes and as solar cells. The charge trapping effect of the d-sorbitol reaction with the silicon surface in hydrogen terminated devices is present and can be seen in the linear and

the logarithmic plots as multiple features in the forward bias regime. To illustrate this phenomenon better, it is easier to compare methyl terminated silicon surface devices with hydrogen terminated silicon surface devices at a conductivity that allows for a reasonable current density.

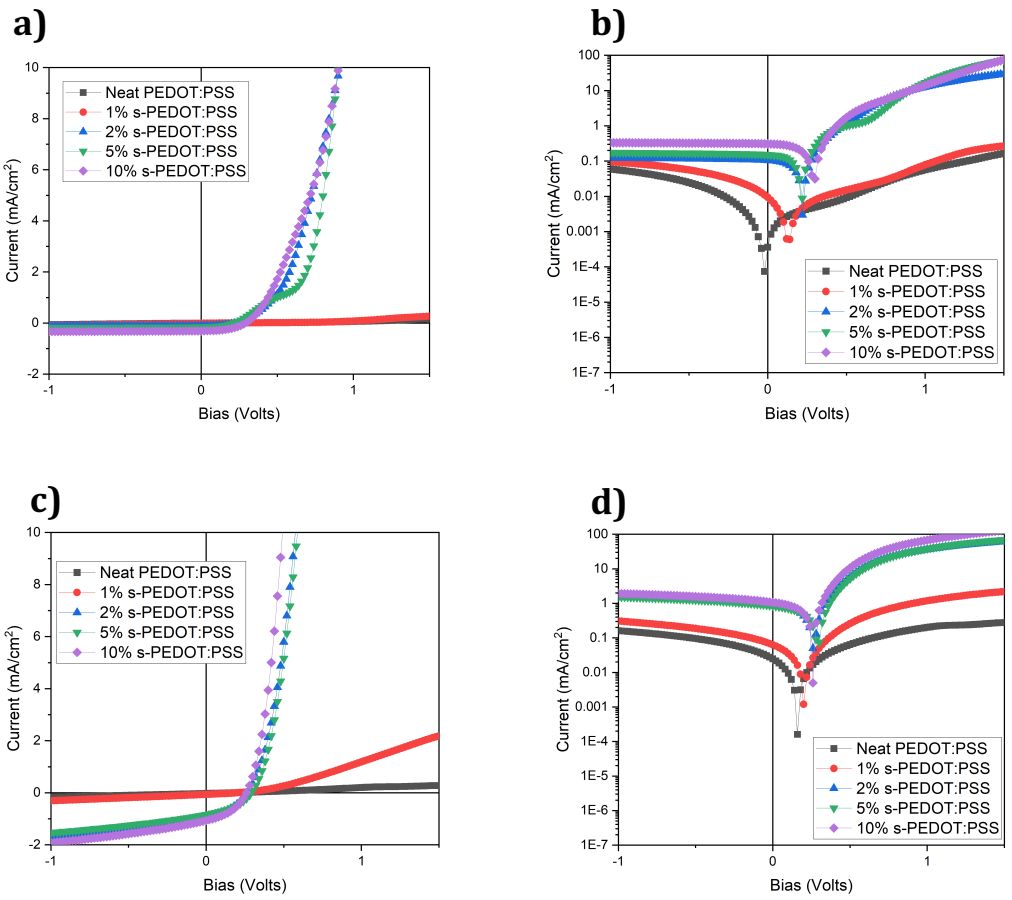

Figure 25. Hydrogen-terminated a) linear, b) logarithmic and Methyl-terminated c) linear, d) logarithmic n-Si(111)/s-PEDOT:PSS Devices *JV* Relationships under AM 1.5 Illumination.

With a the 5% s-PEDOT:PSS devices in **Figure 26** we see a double featured curve in the H-Si graphs, while the Me-Si graphs show normal solar cell behavior. What appears

to be a higher turn on voltage for the H-Si device can be seen in the logarithmic plot (**Figure 26a**, inset) to be one turn on voltage where there are no trap states at the surface plus another to overcome the potential well of these traps. This shows conclusively that trap states caused by the presence of d-sorbitol covalently bonded to the Si(111) surface result in charge trapping. This not only prevents current from flowing in the power producing region of the JV curve, but also prevents current under reverse bias (**Figure 26b**) from extracting photogenerated charge. This is evident in the loss of photogenerated current in reverse bias for the hydrogen-terminated silicon. The methyl-terminated silicon does not show this problem, indicating that the reaction of the H-Si bond with the -OH moiety on the sorbitol is creating the trap states. Because it is not present in the device with the H-Si and the neat PEDOT:PSS dispersion, which is dispersed in water, it cannot simply be the result of oxidized silicon on the surface. The XPS data shows that the H-terminated silicon does oxidize in the presence of water, meaning that there is SiO_x present at the surface in all of the H-terminated samples regardless of the presence of sorbitol, so the sorbitol-Si interaction must be the cause of the trap states.

Interestingly, the loss of current density in reverse bias between H-terminated and Me-terminated surfaces is about an order of magnitude both for light curves and dark curves. This suggests some mechanism is impeding charge flow even in the dark. While trap states would not directly impede the flow of the majority carrier electrons, the positive charge trapped near the surface could build a dipole or cause a self-assembled layer of d-sorbitol to form, increasing resistance in the H-terminated devices.

a)

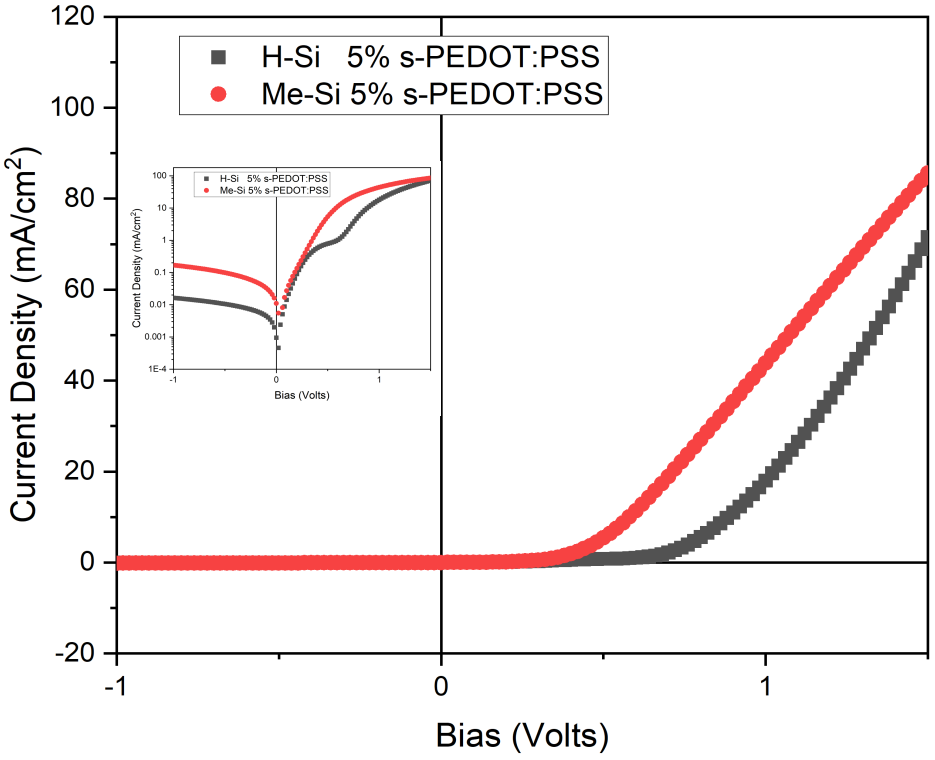
H-Si 5% s-PEDOT:PSS
Me-Si 5% s-PEDOT:PSS
Current Density (mA/cm^2)
Bias (Volts)
120
100
80
60
40
20
0
-20
-1
0
1

b)

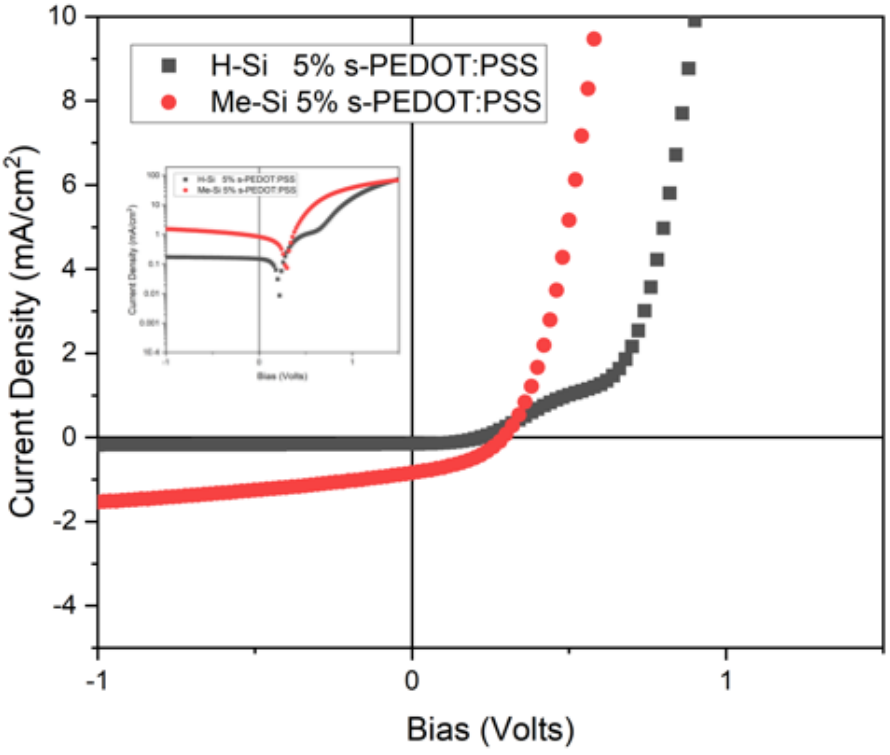
H-Si 5% s-PEDOT:PSS
Me-Si 5% s-PEDOT:PSS
Current Density (mA/cm^2)
Bias (Volts)
10
8
6
4
2
0
-2
-4
-1
0
1

c)

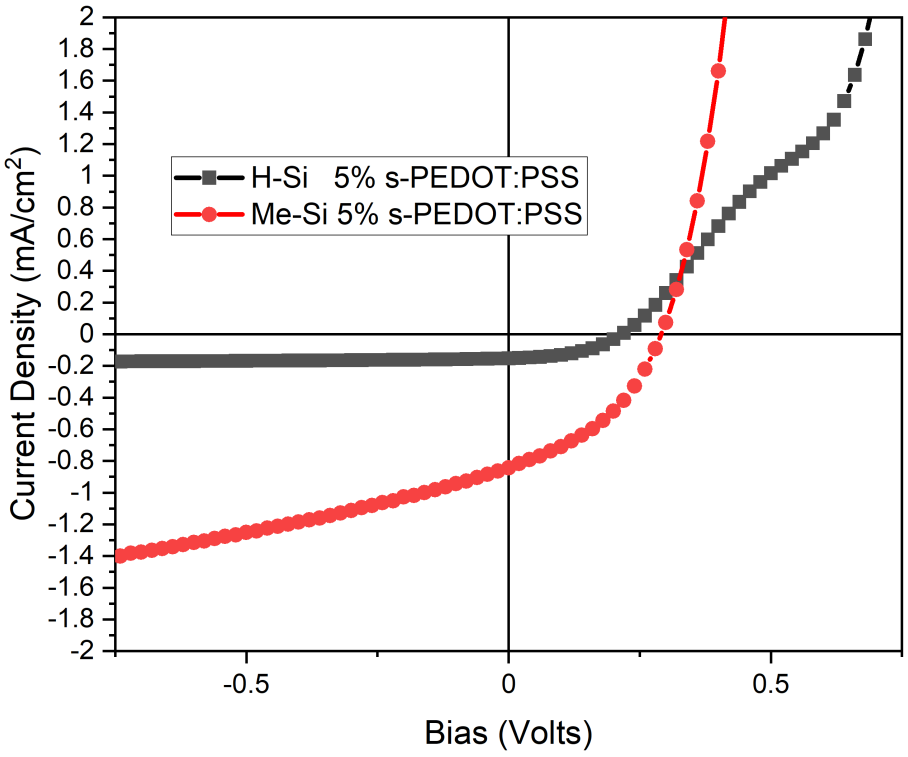

Figure 26. Methyl terminated and hydrogen silicon devices using 5% d-sorbitol wt/vol% devices in the dark a) and under illumination b) and a close up of the power producing region under illumination c).

Table 2. Methyl-terminated and Hydrogen Terminated Si(111)/s-PEDOT:PSS Devices *IV* Relationships under AM1.5 Illumination

	V_{oc} (V)	J_{sc} (mA cm^{-2})	*FF*	R_s (Ω)
H-Si Neat	000748	.0000000193	0	487
H-Si 1%	0.130	.00094	0.23	586
H-Si 2%	0.258	0.140	0.46	1.2
H-Si 5%	0.216	0.152	0.47	4.15
H-Si 10%	0.282	0.372	0.47	4.20
Me-Si Neat	0.0101	0.00121	0.25	1240
Me-Si 1%	0.203	0.0633	0.28	725
Me-Si 2%	0.261	1.03	0.38	4.78
Me-Si 5%	0.291	0.844	0.40	7.21
Me-Si 10%	0.260	1.07	0.41	10.9

Table 2 further illustrates how critical highly conductive PEDOT:PSS layer is to this experiment. With so little current density, this doesn't show much about the charge trapping issue. Hydrogen terminated devices with s-PEDOT:PSS have dramatically lower fill factors than those with methylated surfaces. While there is relatively little change in the open circuit voltage, charge trapping does reduce the short circuit current a small amount, and the fill factor by a large amount, resulting in a major loss of efficiency without the methyl groups present on the surface. The V_{oc} is not dramatically altered between hydrogen

terminated silicon and methyl terminated silicon devices. However, the drop in J_{sc} is somewhat reduced, as is evident from both the table and the graphs, due to the difficulty of extracting trapped charges even at zero bias. This experiment was repeated with a higher conductivity PEDOT:PSS using only 5% d-sorbitol in order to more clearly demonstrate the difference between methyl terminated Si surfaces and hydrogen terminated Si surfaces. The results are shown in **Figure 27** and **Table 3**.

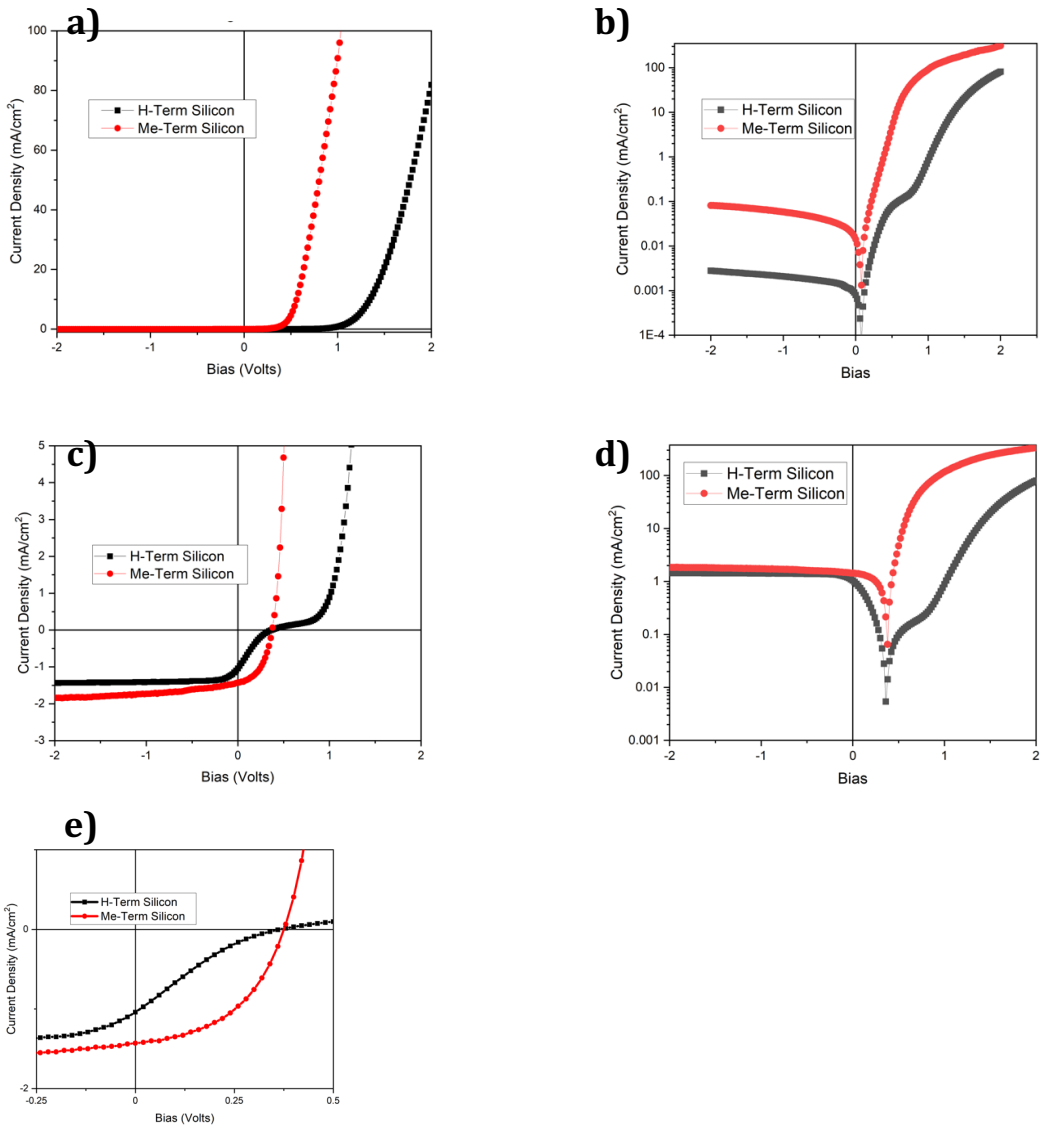

Figure 27. 5% D-sorbitol Linear a) and Logarithmic b) *JV* Curves in the Dark. Linear c) and Logarithmic d) Curves Under AM 1.5 Illumination. Close-up of c) is Shown in e).

Table 3. Device Characteristics of Methyl and Hydrogen terminated s-PEDOT:PSS devices under illumination.

	H-Si(111):s-PEDOT:PSS	Me-Si(111):s-PEDOT:PSS
J_{sc} (mA/cm^2)	1.04	1.43
V_{oc} (Volts)	0.370	0.370
FF (%)	18.9	47.7

From the curves in **Figure 27** and the data in **Table 3** it is clear that the loss in power from the devices is related to the dramatic drop in fill factor. The small drop in J_{sc} due to the slope of the curve also plays a part, since negative bias is needed to extract all the photogenerated charges trapped at the H-Si(111) S-PEDOT:PSS interface, but a much greater loss comes from the fill factor, which drops from 47.7% to 18.9%. In the dark curves, it is also clear that the H-Si(111) devices require a much higher turn on voltage ($>1V$) to overcome the charge trapping versus the Me-Si(111) devices ($0.4V$). This means that even used as simple diodes, the surface needs to be methylated to reduce power loss across the device. Prior works have identified a higher built in barrier height due to the surface dipole created by methylating the Si(111) surface, but due to bulk recombination in the silicon, V_{oc} was not affected.[5] We also showed no difference between V_{oc}s of methylated and hydrogen terminated silicon surface devices.

3.3.4 Thin Film Indium-Tin-Oxide Devices

Thin film devices were fabricated using 10% s-PEDOT:PSS spin coated onto ITO glass. Device area was also measured to find current density rather than absolute current and the *JV* relations were measured in the dark and under illumination (**Figure 28**). Power density was calculated (**Figure 29**) as well as *Jsc*, *Voc*, Fill Factor (FF).

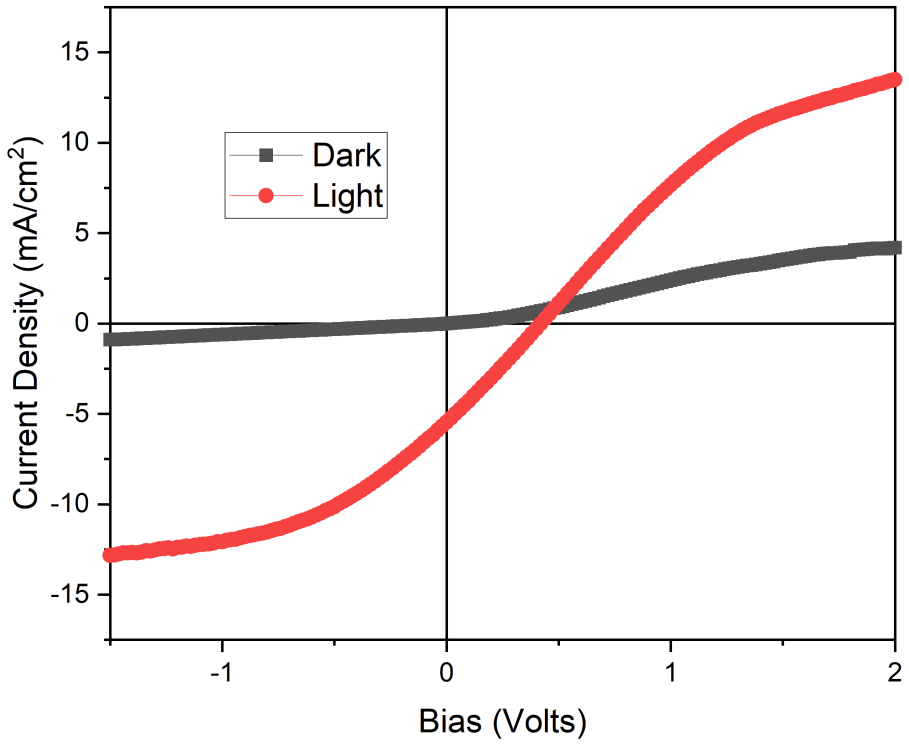

Figure 28. Light and Dark *JV* Curves of a Thin Film Device With 10% D-sorbitol.

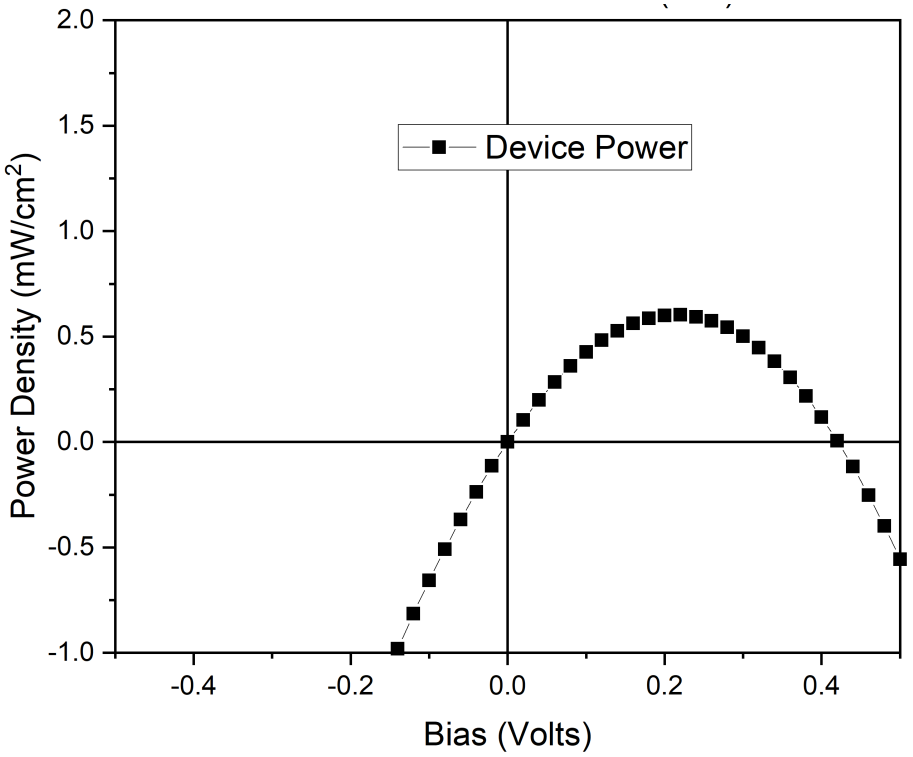

Figure 29. Power Density of a 10% D-sorbitol Thin Film Device Under AM1.5.

From the *JV* curve, it is clear that reasonable current densities can be achieved under illumination in reverse bias (13 mA/cm^2). However, even though this amount of charge is photogenerated, it was not able to be extracted. This resulted in a low *Jsc* of 5.4 mA/cm^2 using the methylated silicon surface. The measured *Voc* of 0.42 volts was comparable to the thick film devices, which may suggest poor contact. The maximum power point occurred at 3 mA cm^{-2} and 0.2 V, resulting in a total device efficiency of 0.6% assuming an illumination power of 100 mW/cm^2. As with the hydrogen-terminated devices using thick films, the resulting fill factor was incredibly low, at 26.5%. The curve shape also suggests a high series resistance which would also result from poor contact. These devices were not made by sputtering ITO on top of a thin film of s-PEDOT:PSS, so merely pressing the two together could easily form large areas of poor contact.

3.4 Conclusions

Methylating the silicon surface conclusively proved that the trap states were being formed due to the presence of oxidized silicon atoms at the surface in the presence of the d-sorbitol. The methylation of silicon surfaces solved the difficult problem of the crystalline silicon reacting with the adhesive d-sorbitol molecule, allowing for the creating of a solar cell without trap states. While this may have been possible with inorganic interstitial layers, the simple processing step of methylating the surface was easy and effective. Because these trap states were not observed in the *J-V* curves of PEDOT:PSS without the adhesive molecule, it indicates that the d-sorbitol is the compound that likely reacts with the surface silicon atoms.[13] Methylation protects them with a monolayer of unreactive methyl groups, which does not cause a significant series resistance between the silicon and the conductive polymer layer. This is consistent with methylation studies showing that the surface is rendered unreactive to oxygen and hydroxyl groups by the methylation of the surface.[51]

XPS studies confirmed the oxidation of hydrogen terminated silicon surfaces in the presence d-sorbitol molecules, while this did not happen with methyl terminated silicon surfaces. There is a high likelihood that the d-sorbitol formed the covalently linked silicon-oxygen-carbon moiety due to the amount of oxidation that took place. The multiple hydroxyl groups from the d-sorbitol can link to multiple silicon atoms, forming a disordered SiOx-like layer. Since the neat PEDOT:PSS on hydrogen terminated silicon devices from chapter 2 did not show the same charge trapping behavior but did show heavy

oxidation under XPS, it is probable that the reaction of the d-sorbitol with the silicon is responsible for the charge trapping rather than the pure SiOx layer.

Chapter 4 – Thiazolo[4,5-d]Thiazole Viologens

4.1 Introduction

Viologens are a well-studied class of molecules created by attaching side groups to the nitrogen atoms of 4,4'-bipyridine resulting in dication salts. Viologens are interesting compounds because they are easily reduced twice, resulting in a neutral compound.[53] This process makes them useful as electron transport disruptors in herbicides.[54] The singly reduced form (and many chemical derivatives) is a very strong light absorber. It becomes a dark blue color, almost black at higher concentrations. It is stable under applied voltage, so it is used in electrochromic applications (**Figure 30**).[55, 56]

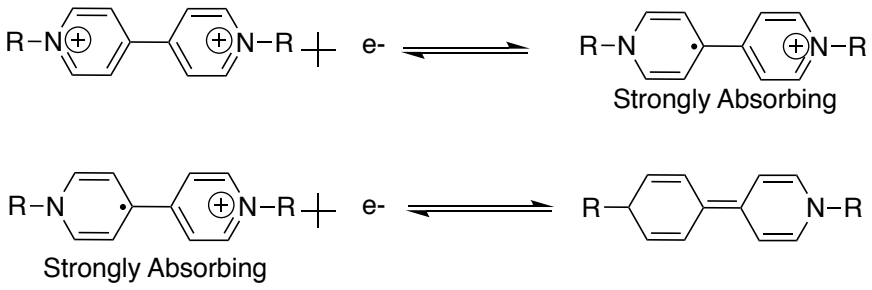

Figure 30. Viologen and its singly reduced and its quinone form.

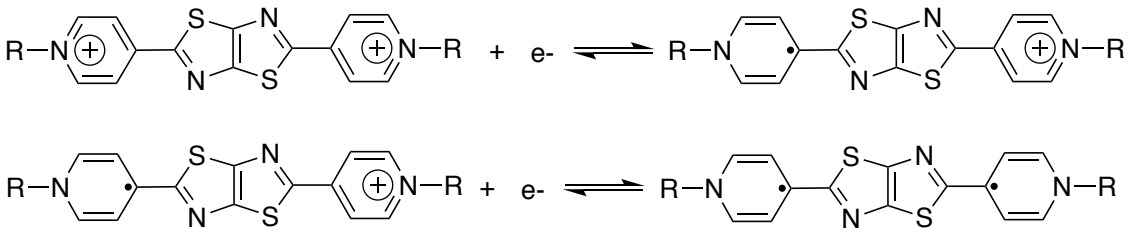

Figure 31. Thiazolo[4,5-d]thiazole-bridged viologen in its singly and doubly reduced forms.

Inserting fused thiazolothiazole rings in between the pyridine rings (**Figure 31**) creates a molecule (TTz) that is more stable in reduced form. Due to the electron accepting nature of the thiazolothiazole moiety, the redox potential of adding electrons to the TTz molecule is raised,[27, 57] and due to the separation of the pyridinium rings by the thiazolothiazole bridge, reductions are brought much closer together in potential. The two reductions are so close that they are difficult to differentiate when using a suitable catalyst, such as platinum metal. Due to the stability of the reduced form, they are also interesting as charge storage species in redox flow battery settings.[26] We have synthesized and characterized diallylpyridinium thiazolothiazole ($(Allyl_2TTz)^{2+}$) and investigated its properties through UV-vis absorbance and fluorescence and cyclic voltammetry. The alkene moiety is useful in many chemical reactions, especially due to its reaction with silicon surfaces in hydrosilylation reactions.

Crystalline silicon is useful as a semiconductor and in photovoltaic systems, but its surface is not known to be a good catalyst. This is especially true for hydrogen evolution reactions due to the high binding energy of silicon hydride, as opposed to platinum group metal hydrides.[58] It is also prone to spontaneous oxidation in the presence of oxygen or water. Viologen derivatives are useful shuttles for electrons to catalysts for hydrogen evolution reactions.[59] The reduced forms will also spontaneously react with strongly acidic protons, reducing those protons in the presence of a catalyst, resulting in the dication form of the viologen.[60] Silicon electrodes can more quickly reduce viologens or TTzs than they can acidic protons in solution. We have investigated using a solution of TTzs with silicon electrodes as solution phase catalysts for hydrogen evolution.

A system that allows a silicon surface to easily shuttle electrons to reduction reactions could be useful in various ways. Silicon is a cheap and stable light absorber, so it could be part of a solar powered or solar assisted hydrogen generation system with an appropriate solution phase hydrogen evolution catalyst. By harnessing the extra potential available to the silicon electrons by absorbing a photon, the applied external potential needed for the hydrogen evolution could be reduced or even brought to zero, allowing a fully solar powered hydrogen generation system.[25, 61] This change in potentials under illumination has been shown with n-type silicon and ferrocene oxidation.[25]

The ability of silicon to reduce this $(Allyl_2TTz)^{2+}$ was shown by using a methylated silicon electrode and a solution of $(Allyl_2TTz)^{2+}$. While it does require some overpotential to reduce the TTz using a silicon versus a platinum electrode, silicon does reduce the $(Allyl_2TTz)^{2+}$. Next, we demonstrated that the silicon electrode reduced the TTz in an acidic solution in an aprotic solvent, DMSO. We controlled for the strength of the acid as well as the presence of the TTz to prove that the silicon reduced the strong acid in the presence of a TTz, but not with a weak acid with the TTz. This showed that the silicon is not catalytic in itself for reducing strong acids, and that the TTz must interact with a strong enough acid for it to be catalytic reduction. In a solar redox battery system, a stable and reversible reduction in some chemical species could be substituted for the acid.[26]

4.2 Materials and Methods

4.2.1. Synthesis of TTzs

A condensation reaction was carried out by refluxing an excess of pyridine-4-carboxaldehyde with dithiooxamide in dimethylformamide at 140°C for 24 h (**Figure 32**).

The mixture was cooled, filtered, and washed with DI water and cold ethanol, yielding beige crystals with low solubility in most solvents. The resulting dipyridyl-thiazolo[4,5-d]thiazole was used to synthesize the diallypyridinium-thiazolo[4,5-d]thiazole dibromide ($Allyl_2TTz\text{-}VG^{2+}(Br^-)_2$) final product.

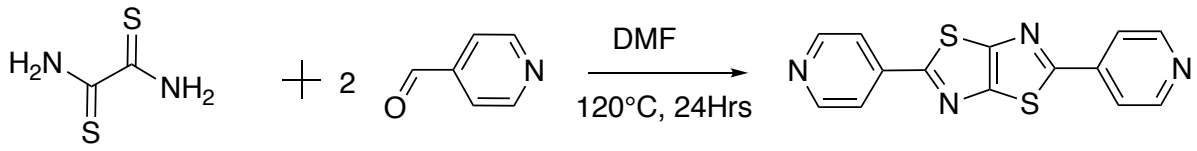

Figure 32. Synthesis of the unsubstituted, neutral bipyridyl-TTz.

The disubstituted salt was obtained through an alkylation process using the dipyridyl, neutral TTz and allyl bromide. (**Figure 33**) An excess of allyl bromide was refluxed with bipyridyl-TTz in 1:3 acetonitrile:chlorobenzene at 70°C for 48 h. The process takes a long time to complete as the TTz-pyridine is a poor nucleophile for these reactions. This is further weakened by the inductive effect of the positively charged nitrogen after the first S_N2 reaction, so a significant amount of time is needed for the reaction to go to completion. The product was dried under vacuum, and then dissolved into DI water. The disubstituted salt was water-soluble while the monosubstituted salt was not. The DI water was filtered, and then removed under vacuum, yielding the diallylpyridiniumthiazolo[4,5-d]thiazole salt or $(Allyl_2TTz)^{2+}(Br^-)_2$.

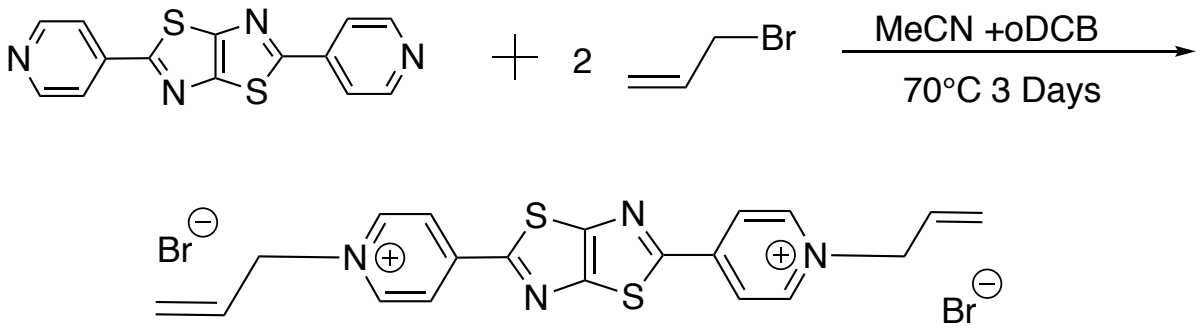

Figure 33. Synthesis of the allylpyridinium-TTz ($Allyl_2TTz\text{-}VG^{2+}(Br^-)_2$).

The dibromide salt was soluble in water and acetonitrile, but was less soluble in other solvents such as DMSO and chlorobenzene. A hexafluorophosphate salt was prepared by dissolving the dibromide salt in water and then adding ammonium hexafluorophosphate. The hexafluorophosphate salt was insoluble in water, and precipitated out. The precipitate was filtered and dried under vacuum to yield the hexafluorophosphate salt. This was more readily soluble in DMSO and chlorobenzene.

4.2.2 Cyclic Voltammetry

Cyclic voltammetry was performed on using a saturated calomel electrode as reference, and either a platinum button working electrode or a silicon working electrode and a platinum foil counter. Hydrogen or argon gas was bubbled through the solution as needed. Methylated silicon chips were then made into electrodes by scoring the back side of them with a diamond scribe and coating them with a small amount of indium gallium eutectic. A nickel wire was brought into contact with the InGa, and a waterproof epoxy was applied to hold the wire in contact. Finally, another layer of epoxy was applied to cover

any bare wire and to leave only a small area of the front surface of the silicon exposed to solution. (**Figure 34**) This formed the working electrodes for cyclic voltammetry studies.

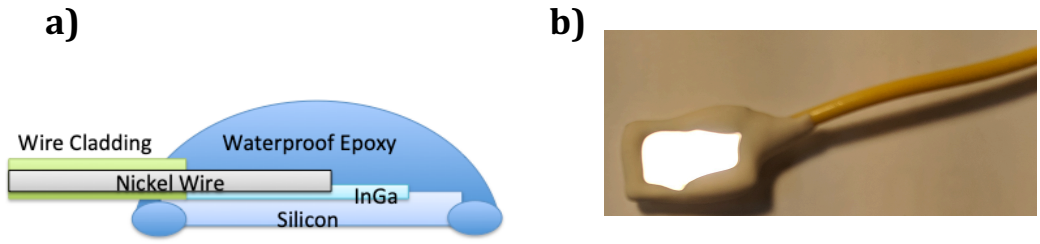

Figure 34. a) Schematic of electrode materials. b) Picture of actual electrode.

4.3 Results and Discussion

4.3.1 Analysis of $(Allyl_2TTz)^{2+}$ Synthesis

The product of the $(Allyl)_2TTz^{2+}$ synthesis was analyzed by proton NMR and MALDI-TOF ionization spectroscopy. If unsubstituted or singly substituted TTz was present in the sample, a signal from the free base pyridine ring on one or both sides of the TTz core ring would have been present in the NMR spectrum. Since no proton signals in this range (7-8 ppm) were observed, there were no singly substituted or fully unsubstituted pyridine rings in the final product. The ^1H NMR Spectrum of $(Allyl_2TTz)^{2+}$ is **Figure B1-B5** in Appendix B. (300 MHz, D_2O, δ): 9.03-9.01 (d, J=6.88, 4H), 8.70-8.68 (d, J=6.88, 4H), 6.29-6.12 (m, 2H), 5.65-5.55 (m, 4H), 5.32-5.30 (d, J=6.19, 4H).

To ensure that there was no further attachment of the allyl groups at additional points in the molecule, such as the nitrogen atoms in the thiazole rings, MALDI-TOF MS was performed to find the molecular weight of the product (See Appendix A, **Figure A1**). No peaks were present beyond the molecular weight of the finished product (378.51AMU), so no additional attachments occurred. A significant amount of the product did fragment

under the laser illumination, so the molar mass of the final product with one less allyl (337.44AMU) group was also prominent at the detector. The matrix compound (226.06AMU) also showed a significant peak in the MALDI-TOF MS spectrum.

4.3.2 Photophysical Properties of $(Allyl_2TTz)^{2+}$

The optical properties of the TTz were similar to those of other alkyl TTzs.[27] In solution, they exhibited strong absorbance in the UV and were highly fluorescent in the blue-green region with fluorescence quantum yields between 80-90% (**Figure 35**). In solid state and in DMSO, the fluorescence was quenched. Due to their similarities with uncharged TTz compounds, we concluded that most of the optical properties are due to the TTz core and not the pyridinium side groups.

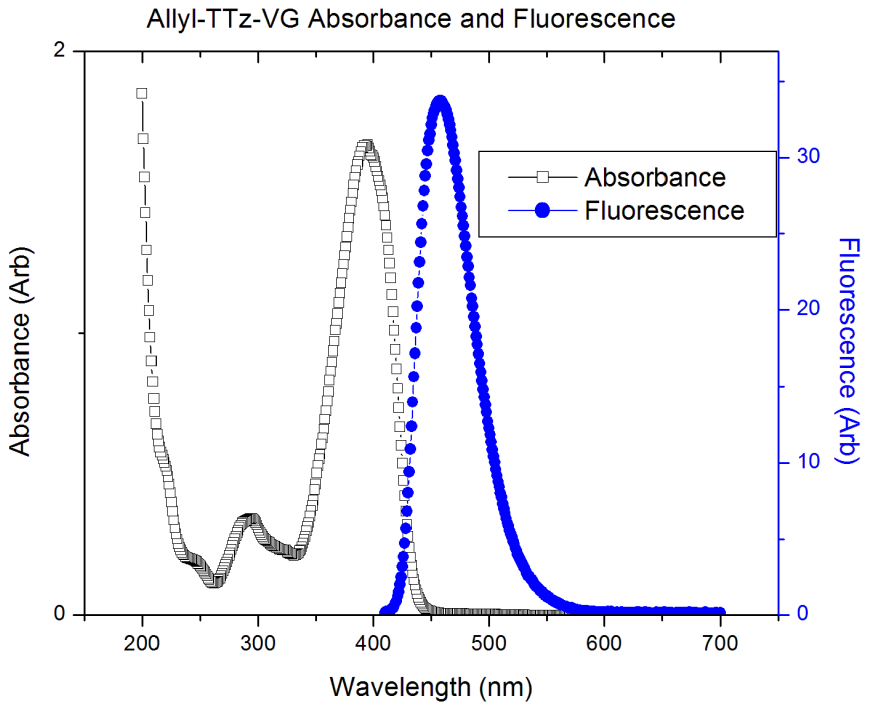

Figure 35. Absorbance and Fluorescence of $Allyl_2TTz\text{-}VG^{2+}$ in acetonitrile.

4.3.3 Cyclic Voltammetry of $(Allyl_2TTz)^{2+}$

Using a platinum button working electrode in 0.1M $TBAPF_6$ in DMSO the two reversible reduction peaks were indistinguishable (**Figure 36**). Only one highly revesible reduction could be observed. This is a similar result to other published TTzs, and is only weakly dependent on the substituents on the pyridinium nitrogen atoms.[27, 57] These two reductions occurring so close together has been reported in the literature for other TTz bridged viologens,[26] and is a useful property for energy storage applications, but is only present when using a highly catalytic electrode such as platinum and in nonaqueous solvents such as DMSO or acetonitrile.

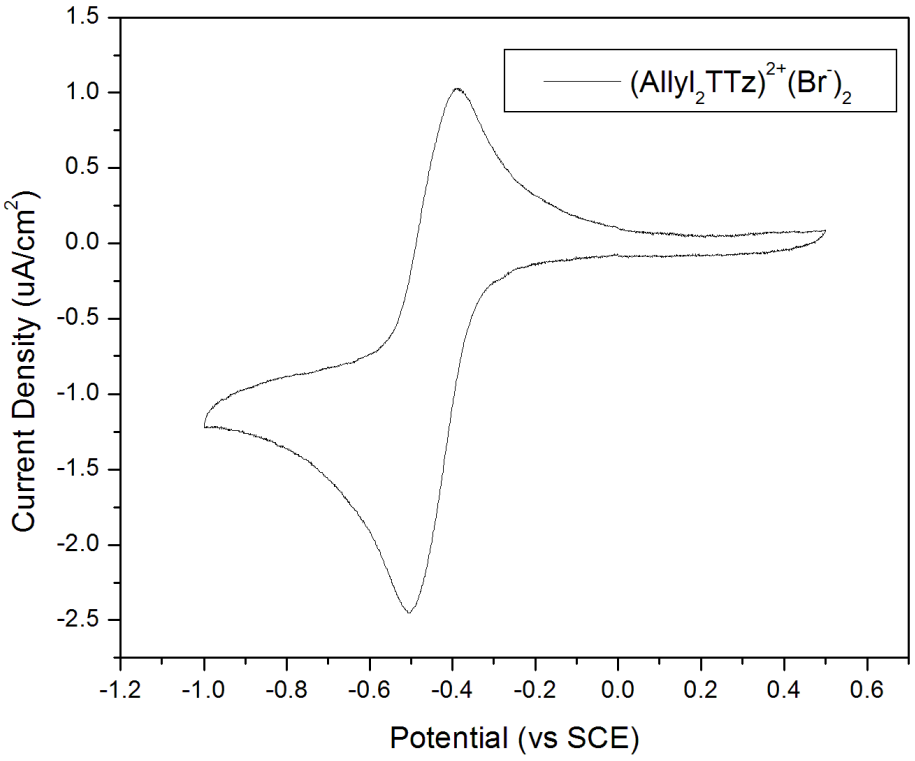

Figure 36. CV of 3 mM $(Allyl_2TTz)^{2+}(Br^-)_2$ in DMSO with Pt button working electrode.

When using a silicon working electrode and scanning out to -2 V vs. SCE, two electrochemical reductions were observed. The 1st electrochemical reduction is irreversible at -0.6 V, and gradually gets smaller with each successive CV scan (**Figure 37**). When using methyl-terminated silicon working electrode it is difficult to identify this reduction as a one or a two electron TTz reduction like the reduction seen with a Pt electrode. It is also unclear at this time whether the semi-reversible reduction observed at -1.75 V is the TTz^{1+} or another electroactive species due to the very large spacing between both reductions. It is likely that this is the reversible reduction of the TTz core, whereas the pyridinium groups are reduced at the lower voltage.

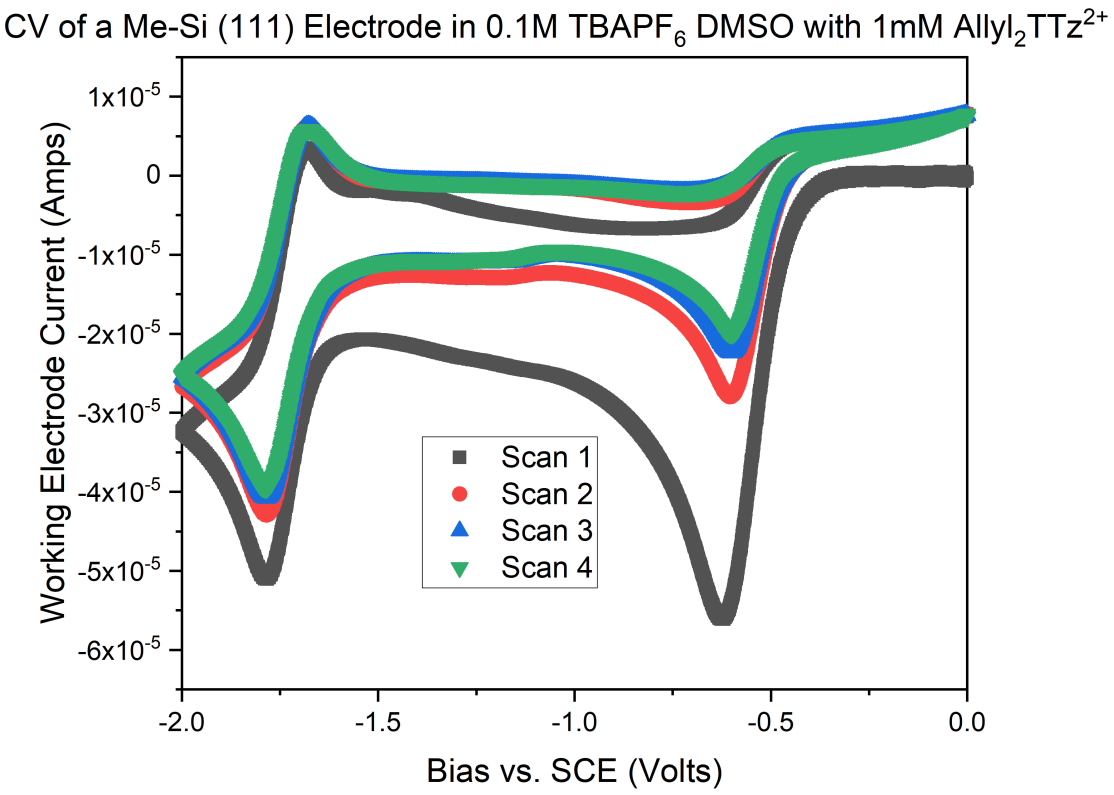

Figure 37. Me-Si(111) (Black Curve) working electrode with 3mM $(Allyl_2TTz)^{2+}(Br^-)_2$ in DMSO with 0.1M $TBAPF_6$ as supporting electrolyte.

Methyl-terminated silicon is a poor catalyst for reduction reactions, so they are usually coupled with a catalyst.[62] In 1M H_2SO_4 there was no significant reduction by the Me-Si electrode (**Figure 38)**. However, by adding $(Allyl_2TTz)^{2+}$ to the solution, two distinct irreversible peaks were observed, suggesting the first and second reduction of the TTz-VG in solution (**Figure 38**). By increasing the concentration of $(Allyl_2TTz)^{2+}$ in solution, the peak current increased, indicating that the concentration of $(Allyl_2TTz)^{2+}$ was responsible for the observed current increase through the electrodes. The change in voltage of the second reduction could be the result of the difference in reduction potential for a protonated TTz species. This suggests that the $(Allyl_2TTz)^{2+}$ was reduced twice. The $(AllyTTz)^{2+}$ can be doubly reduced to form a dark blue material, similar to traditional viologens.[27] This color change is easily visible to the naked eye using a chemical reductant or through bulk electrolysis.[27]

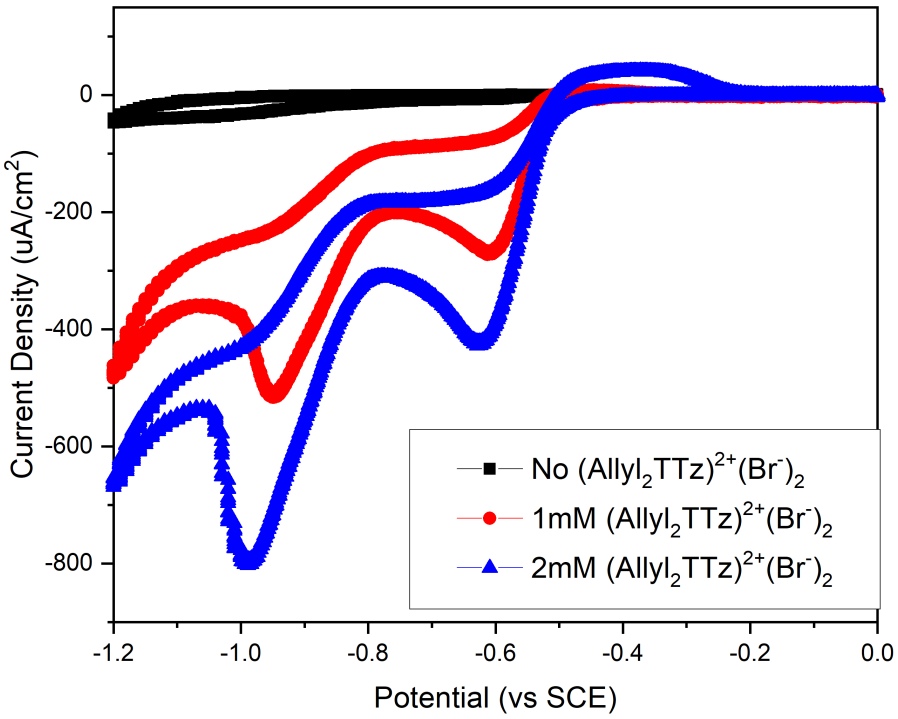

Figure 38. Cyclic voltammetry of 1M H_2SO_4 and a Me-Si (111) working electrode with no $(Allyl_2TTz)^{2+}(Br^-)_2$, 1 mM $(Allyl_2TTz)^{2+}(Br^-)_2$, and 2 mM $(Allyl_2TTz)^{2+}(Br^-)_2$ in H_2O.

Additional studies were carried out using acids of differing strength (acetic acid and trifluoroacetic acid) to determine whether protons were being reduced or whether the acid was simply making it easier to reduce the $(Allyl_2TTz)^{2+}$ by modifying energy levels or even reacting with the molecule itself. The results were not conclusive for determining what exactly was being reduced or the mechanism by which it occurred. Acid strength caused a different CV curve shape and showed different redox potentials, but the scans were not clean and exact nature of the reductions or chains of reductions could not be ascertained from the scans. Scans of these figures are presented in **Appendix C**.

4.4 Conclusions

The new thiazolothiazole compound $(Allyl_2TTz)^{2+}$ was synthesized and the final product structure was confirmed using ^1H NMR and MALDI-MS data. This TTz has similar properties to published TTzs in terms of absorbance, fluorescence, and reduction potentials. The dibromide salt was soluble in water and acetonitrile and to some extent DMSO and chlorobenzene, while the hexafluorophosphate salt was highly soluble in DMSO and chlorobenzene.

Cyclic voltammetry showed that silicon electrodes could reduce the TTz in DMSO and in water with acid present. Adding the TTz to an acidic aqueous solution allowed the Me-Si(111) electrode to pass current. The combination of TTz with an acid is necessary for Me-Si electrodes to function in an aqueous solution. Further studies in aprotic solvents showed that TTzs coupled with a strong acid were necessary for methyl terminated silicon electrodes to carry out these reductions.

Chapter 5 – Hydrosilylation of Silicon Surfaces by TTzs

5.1 Introduction

By covalently bonding a group that is easily reduced by silicon and can loosely bind protons, the catalytic ability of the silicon to reduce solution phase species is increased. This has been shown with electroactive compounds such as ferrocene.[25] If crystalline silicon is able to oxidize or reduce a compound in solution, it is also likely able to oxidize or reduce that compound covalently bound to the surface. This may also occur even though that compound is separated by a non-conjugated linkage of at least 2 carbon atoms. Thus, a solution phase catalyst should be able to perform as well by being covalently bound to the silicon surface. In an acidic solution and with a surface functionalized by an electron shuttle for reduction reactions, the overpotential needed to drive the reduction reaction is greatly diminished. This has been done with organic, hybrid, and inorganic catalysts such as Fullerene, Iron(II) Porphyrins, and Platinum nanoparticles bound by conductive linkages to silicon surfaces.[63]

The two most common forms of covalently attaching groups to a silicon surface are through a chlorination/Grignard process or through hydrosilylation of an alkene.[64] Alcohol groups can also react with the silicon surface, however the Si-O bond tends to create charge traps, as demonstrated in chapter 3, so this route was avoided. We chose to use the hydrosilylation route, as Grignard reagents will react with the TTzs, reducing them and inactivating the Grignard moiety. This explains the choice of the allyl side group when synthesizing a TTz in the previous chapter. To do this we synthesized dipyridyl thiazolo[4,5-d]thiazole and reacted this with allyl bromide to form the dipyridinium dibromide salt. Hydrogen terminated silicon was then heated in a solution of the TTz salt

with a radical initiator to form the final silicon carbon bond. Testing the TTz-functionalized silicon electrodes showed that the electrode gives a higher working electrode current and a lower turn on voltage than a methyl-terminated silicon surface.

5.2 Materials and Methods

5.2.1 Hydrosilylation Reaction of $(Allyl_2TTz)^{2+}$

Hydrogen terminated 10 ohm-cm n-type silicon with a (111) crystal face was prepared using the following procedure. The silicon surface was fully oxidized by immersing it a piranha bath (3:1 concentrated H_2SO_4:30%H_2O_2) for 30 min. It was then left to rinse in DI H_2O for an additional 30 min to remove any trace metal ions that might be left. Next it was immersed in buffered HF solution (7% HF, 30% NH_4F in H_2O) for 10 seconds to remove the surface oxide and leave a hydrogen terminated surface. Finally in order to achieve as flat a surface as possible with no defects, it was immersed in a 40% aqueous ammonium fluoride solution that was degassed with argon for 30 min. The freshly hydrogen terminated silicon was then immersed in the degassed aqueous ammonium fluoride for 10 min. Argon bubbling was kept continuous during the etching process as well to prevent any oxygen from dissolving into the water, which could lead to new surface oxides. The silicon was rinsed quickly with DI water, and dried in a vacuum. This silicon was either used immediately or kept in a nitrogen flush box for no more than 24 h prior to being functionalized.

The $(Allyl_2TTz)^{2+}$ was then attached to the surface of an n-Si (111) chip via hydrosilylation using a few grains benzoyl peroxide as a radical initiator in chlorobenzene at 70 °C for 48 hours. UV light was also tried, but did not result in significant attachment

of the alkene to the silicon surface (**Figure 39**). The silicon was then washed with chlorobenzene, acetone, and DI water to remove any unbound TTz. The coverage was tested using X-ray photoelectron spectroscopy (XPS) to detect the presence of sulfur, nitrogen, and bromine atoms on the surface.

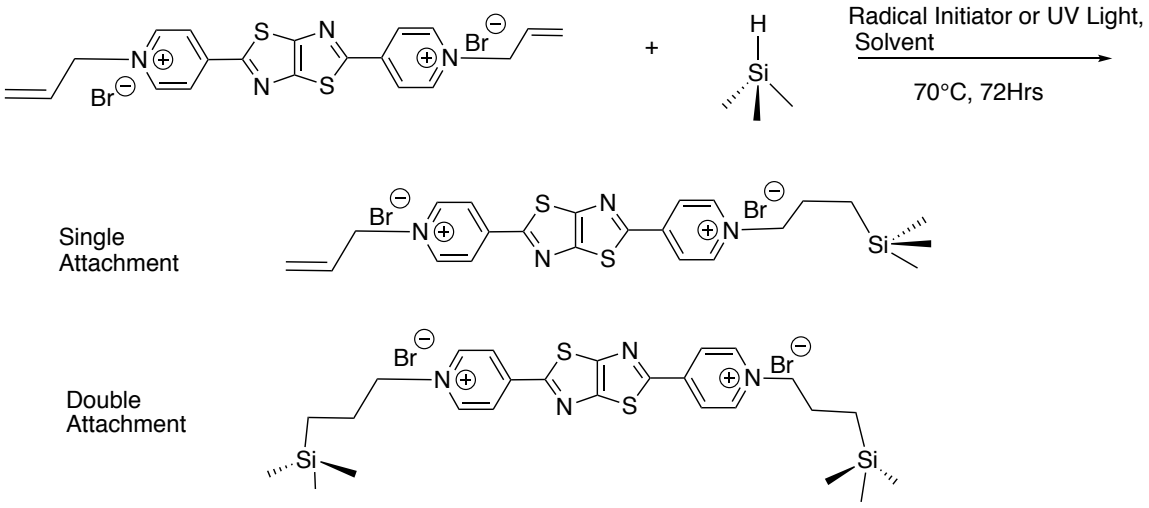

Figure 39. Attachment of $Allyl_2TTz\text{-}VG^{2+}(Br^-)_2$ to Si(111) surface atoms.

5.3 Results and Discussion

5.3.1 XPS of Me-Si(111)-TTz Surfaces

X-ray photoelectron spectroscopy was performed on silicon surfaces that had undergone hydrosilylation with the TTz using various solvents and methods. It was determined that chlorobenzene and a radical process yielded the best results, rather than any other solvent or UV-light initiated reactions. The surfaces were thoroughly washed in chlorobenzene, acetone, and water afterwards to remove any TTz or radical initiator that may have gotten stuck to the surface during the reaction, leaving only covalently bound TTz molecules on the surface.

TTz attachment was analyzed and sulfur, bromine, and nitrogen electrons were shown to be present on the surface (**Figure 40**) showing the presence of TTz. In addition, silicon and carbon atoms were analyzed. The TTz functionalized surface showed significantly more oxidation than a methyl functionalized surface, possibly because stearic hindrance prevented attachment at all surface silicon atoms. The presence of sulfur, nitrogen, and bromine atoms were conclusive, since none of those atoms were present in the solvent, on the silicon, or in the radical initiator. The presence of carbon atoms was expected, but could have been possible from the initiator (benzoyl peroxide). With molecules larger than methyl groups attached on the surface, it is almost impossible to see silicon-carbon bonding electrons in XPS, so the other elements present in the XPS data were more definitive for demonstrating TTz attachment.

a)

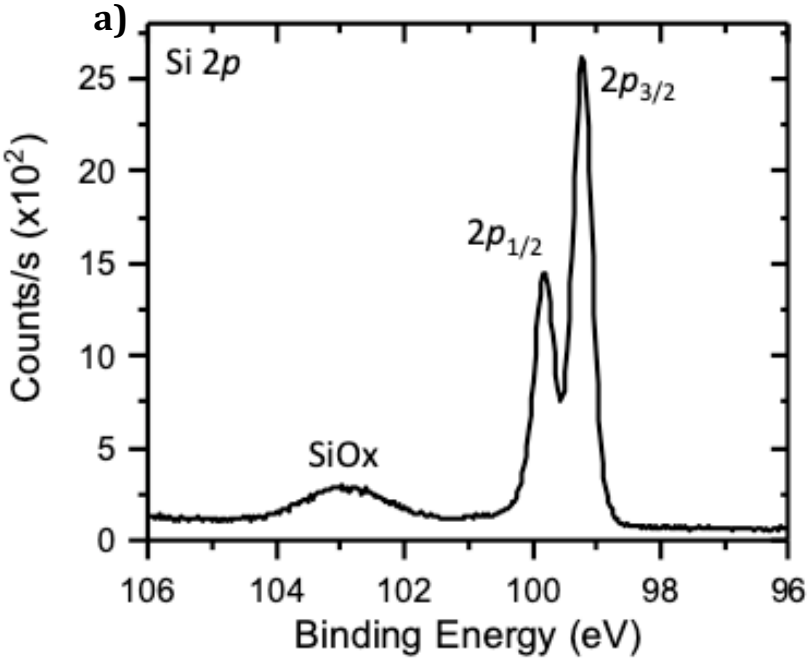
Si 2p
2p3/2
2p1/2
SiOx
Counts/s (x10^2)
Binding Energy (eV)
0
5
10
15
20
25
106
104
102
100
98
96

b)

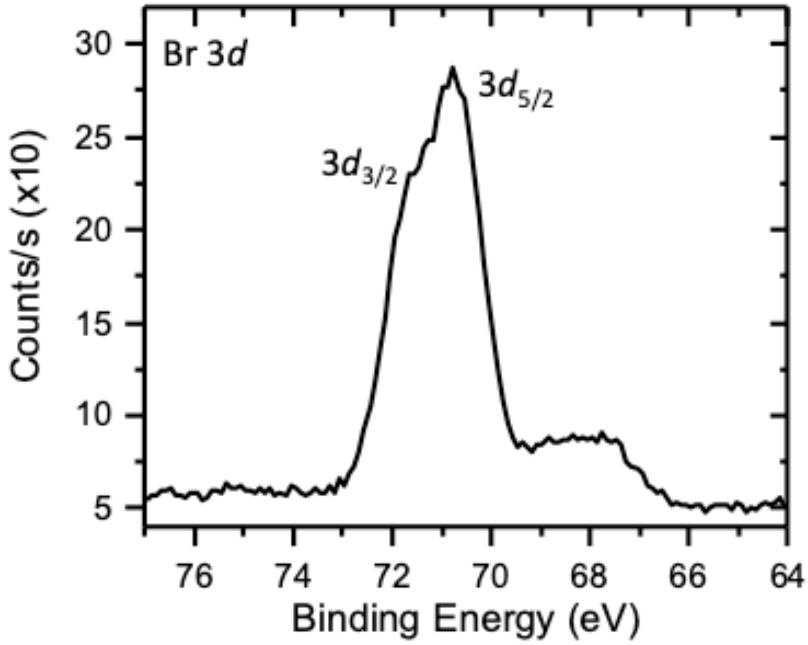
Br 3d
3d5/2
3d3/2
Counts/s (x10)
Binding Energy (eV)
5
10
15
20
25
30
76
74
72
70
68
66
64

c)

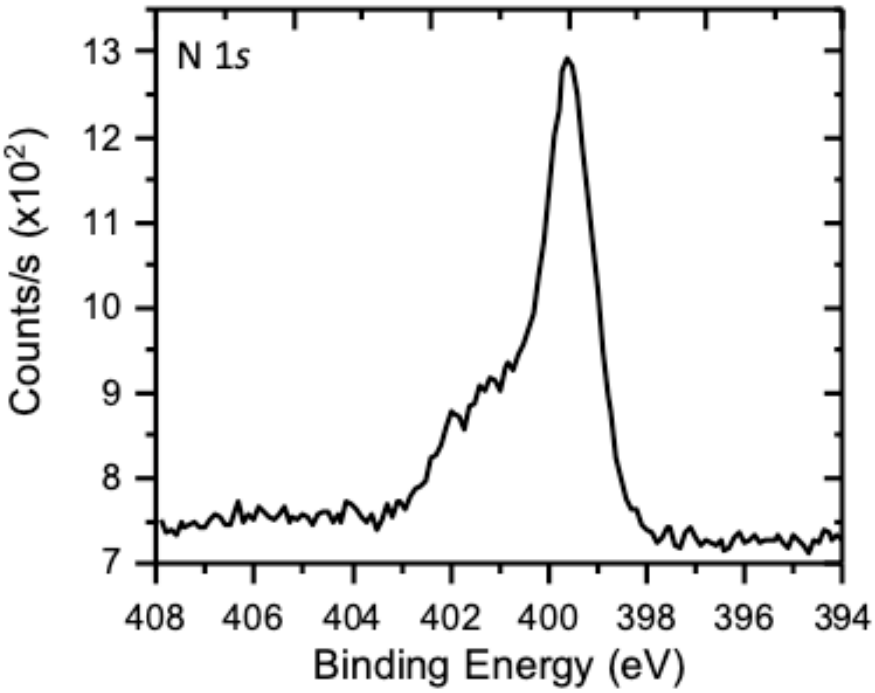
N 1s
Counts/s (x10²)
13
12
11
10
9
8
7
408
406
404
402
400
398
396
394
Binding Energy (eV)

d)

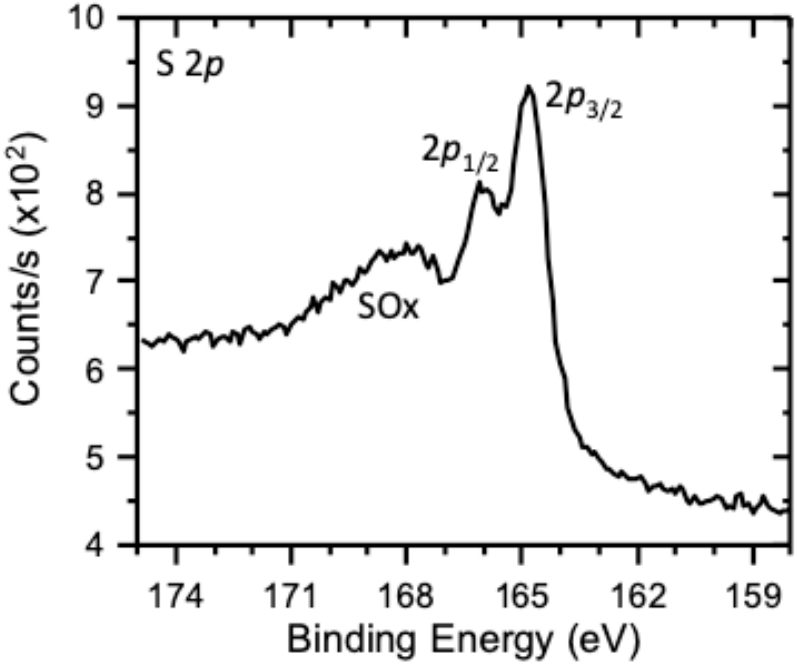
S 2p
2p3/2
2p1/2
SOx
Counts/s (x10²)
10
9
8
7
6
5
4
174
171
168
165
162
159
Binding Energy (eV)

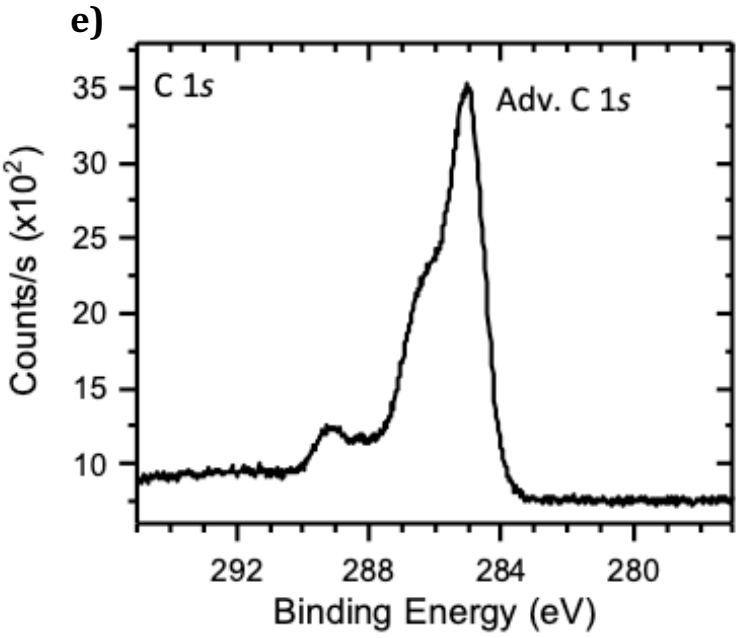

Figure 40. $(Allyl_2TTz)^{2+}$ $(Br^-)_2$ Modified Silicon (111) surface. a) Si electrons and SiOx formation. b) Bromine 3d electrons. c) Nitrogen 1s Electrons. d) Sulfur 2p electrons. e) Carbon 1s electrons.

5.3.2 CV of Si-TTz Electrodes

The TTz functionalized surface showed a significant increase in current over a methylated surface, even without TTz present in the solution. This is likely the reduction of the TTzs that are present on the surface, as the actual interaction of the two electrodes with the aqueous 1M H_2SO_4 shows an onset at approximately the same voltage. The onset voltage of this reduction of the surface bound TTz molecules is approximately -500 mV vs. SCE, which tracks with the reduction of TTz in solution by a silicon electrode (**Figure 41**).

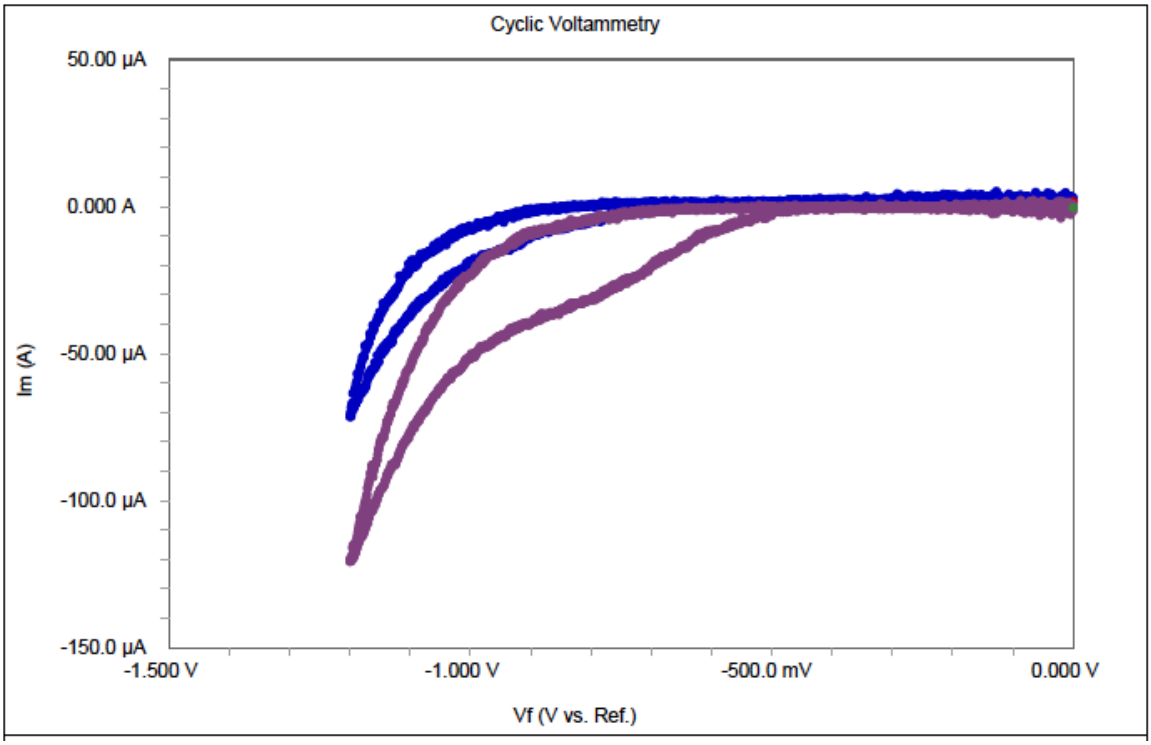

Figure 41. CV of Me-Si(111) electrode (Blue) vs. $(Allyl_2TTz)^{2+}$ $(Br^-)_2$-Si(111) electrode (Purple) in 1M H_2SO_4 in H_2O with H_2 bubbling.

Attempts to repeat the test in Figure 44 using the same electrode showed no additional electrochemical activity, so a fresh TTz-Si (111) electrode was tested with a 0.1M $TBAPF_6$ in DMSO solution and multiple cycles in order to see the effects of cycling on only the surface bound TTz molecules (**Figure 42**).

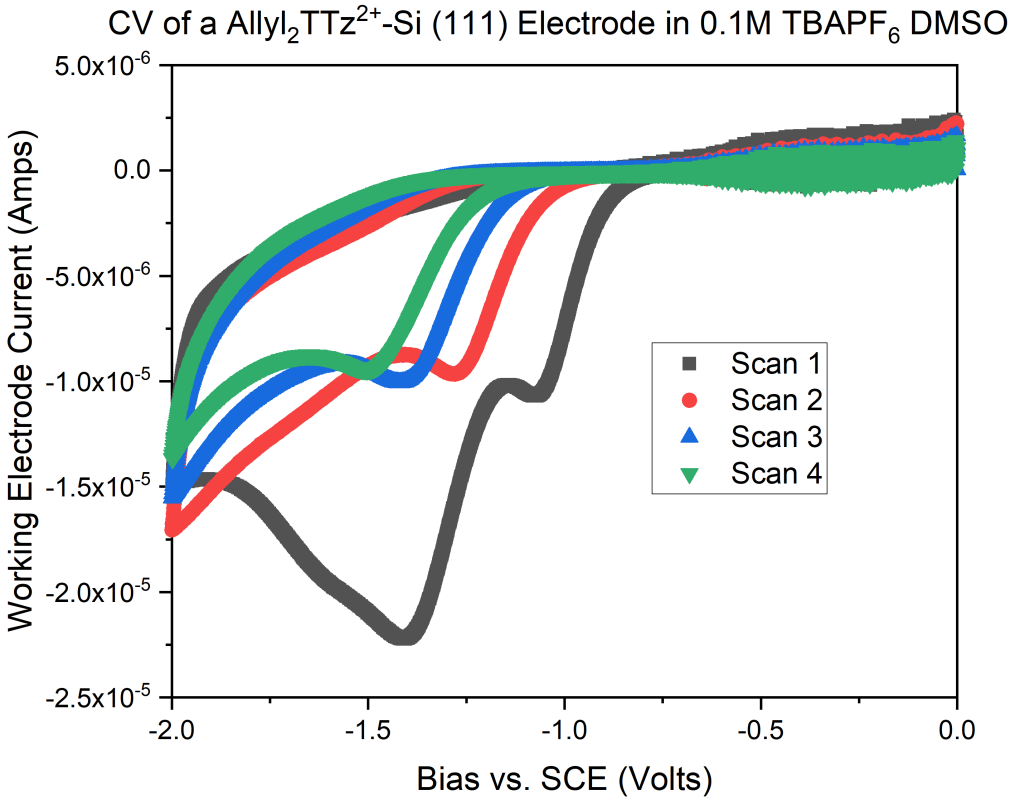

Figure 42. CV of $(Allyl_2TTz)^{2+}$ $(Br^-)_2$-Si(111) electrode in 0.1M $TBAPF_6$ in DMSO with 13 mM TFA.

From this figure it is apparent that the surface bound $Allyl_2TTz^{2+}$ is being reduced, but it is being reduced irreversibly. Thus, any electrochemical activity observed with the trifluoroacetic acid was likely from the reduction of $Allyl_2TTz^{2+}$ molecules on the freshly made electrode, and not proton reduction. For solutions of $Allyl_2TTz^{2+}$ it is not noticeable because the reduced molecules are quickly replaced by those from the solution. By limiting the experiment to a small number of surface bound molecules, it becomes apparent that these are being reduced and then ceasing to have any further interaction.

5.4 Conclusions

We demonstrated that the novel TTz compound synthesized in Chapter 4 did attach to the silicon surface through its alkene moiety. We have also demonstrated its usefulness as an easily reduced species attached to a silicon surface. It was directly attached to the silicon surface through a hydrosilylation reaction demonstrated by XPS data from that surface. A clear increase in electrochemical current indicates that the surface-bound TTz is electrochemically active. Unfortunately, its long-term stability is poor, due to the electrochemical irreversibility of the TTzs compounds when bound to the silicon surface.

Chapter 6 - Conclusions and Future Work

6.1 Conclusions

The interactions of crystalline silicon surfaces with organic conductors and organic redox active groups were investigated. In both cases, it was useful to form covalent bonds between the silicon surface atoms and passivating or redox-active molecules studied. Ohmic and rectifying junctions between p-type and n-type silicon and an organic conductor were produced, and the chemical interaction with the surface was critical in determining the behavior of the rectifying contacts. Thiazolo[4,5-d]thiazole redox active groups were synthesized, characterized, and investigated as electron shuttles for reduction reactions both in solution and bound to a silicon surface.

Crystalline silicon:s-PEDOT:PSS solar cell devices can be easily fabricated, however, silicon-surface passivation is required for engineering efficient devices. Without surface passivation, photogenerated charge was not extracted, fill factors were low, and turn on voltage was high. By simply preventing the silicon surface atoms from reacting with the d-sorbitol in the s-PEDOT:PSS, the diode looks like a standard metal-semiconductor Schottky diode, and can function as a solar cell. This was accomplished through silicon (111) surface methylation using a two-step chlorination/methylation procedure.

Diallylpyridinium-thiazolo[4,5-d]thiazole dibromide was synthesized as well as the hexafluorophosphate salt. This compound had interesting redox properties, and showed two electrochemical reductions using either a platinum or a silicon working electrode. The diallyl TTz compound was successfully attached to the silicon surface as confirmed with XPS and electrochemical studies. However, it did not perform well as a catalyst on a silicon

surface, and in solution the interactions with reducible acids were more complex than simple reduction or electron shuttle behavior. For silicon electrodes, it greatly increased the current flow to an acidic solution over an acidic solution with no TTz. However, no definitive statement can be made as to whether protons were being reduced. The increase in current through a silicon electrode to acidic solutions was also investigated by attaching the TTz directly to the silicon through hydrosilylation of the terminal alkenes. It was demonstrated that binding the TTz groups to the silicon did increase the current initially, but multiple voltage sweeps saw this reduction disappear. Additionally, there was no oxidative peak when the voltage scan was reversed, showing that this reaction was irreversible.

6.2 Future Work

It would be useful to investigate how this TTz compares with conventional diallyl-viologen in its catalytic ability, because there is no easy way for the viologen without the TTz core to bind protons, even in a strongly acidic solution. It might also be interesting to see if attachment of a different TTz by a chlorination/Grignard route is possible. In this way, the number of carbons between the TTz and the silicon would be reduced. Additionally, the TTz could be modified with various electron donating or withdrawing groups on the pyridine ring to change its redox potential or protect it from irreversible reactions when exposed to acid and used as an electron shuttle.

For devices, most significant next step would be to use p-type silicon rather than n-type silicon in this experiment. In this way, photons would generate minority carriers, electrons, boosting the effective voltage of the system. P-type silicon might also be usable

to reoxidize the TTz where n-type silicon could not due to the majority carriers being holes which could oxidize the neutral TTz back to the $^{2+}$ state. This would lead to a system where the potential needed for reduction reactions was significantly reduced. This would constitute part of a solar water splitting system for fuel generation. The oxygen evolution reaction side would have to be provided by a separate catalyst and system for generating potential. The hydrogen evolution side could be evaluated by cyclic voltammetry with a potentiostat responsible for the extra voltage needed. The difference in light and dark voltage needed for catalysis would constitute the effectiveness of the hydrogen evolution system.

The $(Allyl_2TTz)^{2+}$ also lends itself well to polymerization reactions through the alkene moieties on either side, so a possible thin film of TTz polymers could be coated onto silicon in order to study whether this method would work well at a catalyst. Just as with the PEDOT:PSS work, this would likely require methylation of the silicon surface.

A significant synthetic undertaking would also be to make an alkynyl-pyridinium linkage. Published articles have recently shown how that this is possible through trivalent iodine intermediates,[65] but fell beyond the synthetic scope of this work. This would result in a straight rod-like molecule that might achieve a higher surface coverage of the silicon without so much stearic hindrance. It would also be possible to create conjugated polymers or oligomers using this method. Such a compound might also be interesting as a conductive polymer.

References

1. Yoshikawa, K.; Kawasaki, H.; Yoshida, W.; Irie, T.; Konishi, K.; Nakano, K.; Uto, T.; Adachi, D.; Kanematsu, M.; Uzu, H.; Yamamoto, K., Silicon heterojunction solar cell with interdigitated back contacts for a photoconversion efficiency over 26%. *Nat Energy* **2017,** *2* (5), 8.
2. Battaglia, C.; Cuevas, A.; De Wolf, S., High-efficiency crystalline silicon solar cells: status and perspectives. *Energy Environ. Sci.* **2016,** *9* (5), 1552-1576.
3. Bardeen, J., Surface States and Rectification at a Metal Semi-Conductor Contact. *Phys Rev* **1947,** *71* (10), 717-727.
4. Hunger, R.; Fritsche, R.; Jaeckel, B.; Webb, L. J.; Jaegermann, W.; Lewis, N. S., High-resolution photoemission studies of the interfacial reactivity and interfacial energetics of Au and Cu Schottky barriers on methyl-terminated Si(111) surfaces. *Surf Sci* **2007,** *601* (14), 2896-2907.
5. Walter, M. G.; Liu, X.; O'Leary, L. E.; Brunschwig, B. S.; Lewis, N. S., Electrical Junction Behavior of Poly(3,4-ethylenedioxythiophene) (PEDOT) Contacts to H-Terminated and CH3-Terminated p-, n-, and n+-Si(111) Surfaces. *J. Phys. Chem. C* **2013,** *117* (28), 14485-14492.
6. Pulfrey, D. L.; Mcouat, R. F., Schottky-Barrier Solar-Cell Calculations. *Applied Physics Letters* **1974,** *24* (4), 167-169.
7. Zhang, J.; Zhang, Y. F.; Zhang, F. T.; Sun, B. Q., Electrical characterization of inorganic-organic hybrid photovoltaic devices based on silicon-poly(3,4-ethylenedioxythiophene):poly(styrenesulfonate). *Applied Physics Letters* **2013,** *102* (1).
8. Nagamatsu, K. A.; Avasthi, S.; Jhaveri, J.; Sturm, J. C., A 12% Efficient Silicon/PEDOT:PSS Heterojunction Solar Cell Fabricated at < 100 degrees C. *Ieee J Photovolt* **2014,** *4* (1), 260-264.
9. Wilson, G. M.; Al-Jassim, M.; Metzger, W. K.; Glunz, S. W.; Verlinden, P.; Xiong, G.; Mansfield, L. M.; Stanbery, B. J.; Zhu, K.; Yan, Y. F.; Berry, J. J.; Ptak, A. J.; Dimroth, F.; Kayes, B. M.; Tamboli, A. C.; Peibst, R.; Catchpole, K.; Reese, M. O.; Klinga, C. S.; Denholm, P.; Morjaria, M.; Deceglie, M. G.; Freeman, J. M.; Mikofski, M. A.; Jordan, D. C.; TamizhMani, G.; Sulas-Kern, D. B., The 2020 photovoltaic technologies roadmap. *J Phys D Appl Phys* **2020,** *53* (49), 47.
10. Sharma, M.; Pudasaini, P. R.; Ruiz-Zepeda, F.; Elam, D.; Ayon, A. A., Ultrathin, Flexible Organic-Inorganic Hybrid Solar Cells Based on Silicon Nanowires and PEDOT:PSS. *Acs Applied Materials & Interfaces* **2014,** *6* (6), 4356-4363.
11. Ouyang, H. Y.; Yang, Y., Conducting polymer as transparent electric glue. *Advanced Materials* **2006,** *18* (16), 2141-+.
12. Shimada, C.; Shiratori, S., Viscous Conductive Glue Layer in Semitransparent Polymer-Based Solar Cells Fabricated by a Lamination Process. *Acs Applied Materials & Interfaces* **2013,** *5* (21), 11087-11092.
13. Cohen, D.; Bostian, M. E.; Nguyen, L.; Walter, M. G., Conductive poly(3,4-ethylenedioxythiophene): poly(styrene sulfonate) polymer glue as an ohmic and rectifying electrical contact for H-terminated n-Si and p-Si wafers. *Polymer International* **2018,** *67* (7), 853-858.

14. Yu, H. B.; Webb, L. J.; Heath, J. R.; Lewis, N. S., Scanning tunneling spectroscopy of methyl- and ethyl-terminated Si(111) surfaces. *Applied Physics Letters* **2006,** *88* (25).
15. Shockley, W.; Queisser, H. J., Detailed Balance Limit of Efficiency of P-N Junction Solar Cells. *Journal of Applied Physics* **1961,** *32* (3), 510-&.
16. Swanson, R. M., Approaching the 29% limit efficiency of silicon solar cells. *Conference Record of the Thirty-First IEEE Photovoltaic Specialists Conference - 2005* **2005**, 889-894.
17. Powell, D. M.; Winkler, M. T.; Choi, H. J.; Simmons, C. B.; Needleman, D. B.; Buonassisi, T., Crystalline silicon photovoltaics: a cost analysis framework for determining technology pathways to reach baseload electricity costs. *Energy Environ. Sci.* **2012,** *5* (3), 5874-5883.
18. Saga, T., Advances in crystalline silicon solar cell technology for industrial mass production. *Npg Asia Mater* **2010,** *2* (3), 96-102.
19. Morita, M.; Ohmi, T.; Hasegawa, E.; Kawakami, M.; Ohwada, M., Growth of Native Oxide on a Silicon Surface. *Journal of Applied Physics* **1990,** *68* (3), 1272-1281.
20. Atalla, M. M.; Tannenbaum, E.; Scheibner, E. J., Stabilization of Silicon Surfaces by Thermally Grown Oxides. *At&T Tech J* **1959,** *38* (3), 749-783.
21. O'Leary, L. E.; Johansson, E.; Brunschwig, B. S.; Lewis, N. S., Synthesis and Characterization of Mixed Methyl/Allyl Monolayers on Si(111). *Journal of Physical Chemistry B* **2010,** *114* (45), 14298-14302.
22. Johansson, E.; Boettcher, S. W.; O'Leary, L. E.; Poletayev, A. D.; Maldonado, S.; Brunschwig, B. S.; Lewis, N. S., Control of the pH-Dependence of the Band Edges of Si(111) Surfaces Using Mixed Methyl/Allyl Monolayers. *J. Phys. Chem. C* **2011,** *115* (17), 8594-8601.
23. Plymale, N. T.; Kim, Y. G.; Soriaga, M. P.; Brunschwig, B. S.; Lewis, N. S., Synthesis, Characterization, and Reactivity of Ethynyl- and Propynyl-Terminated Si(111) Surfaces. *Journal of Physical Chemistry C* **2015,** *119* (34), 19847-19862.
24. Linford, M. R.; Fenter, P.; Eisenberger, P. M.; Chidsey, C. E. D., Alkyl Monolayers on Silicon Prepared from 1-Alkenes and Hydrogen-Terminated Silicon. *Journal of the American Chemical Society* **1995,** *117* (11), 3145-3155.
25. Lattimer, J. R. C.; Brunschwig, B. S.; Lewis, N. S.; Gray, H. B., Redox Properties of Mixed Methyl/Vinylferrocenyl Monolayers on Si(111) Surfaces. *Journal of Physical Chemistry C* **2013,** *117* (51), 27012-27022.
26. Luo, J.; Hu, B.; Debruler, C.; Liu, T. L., A pi-Conjugation Extended Viologen as a Two-Electron Storage Anolyte for Total Organic Aqueous Redox Flow Batteries. *Angew Chem Int Edit* **2018,** *57* (1), 231-235.
27. Woodward, A. N.; Kolesar, J. M.; Hall, S. R.; Saleh, N. A.; Jones, D. S.; Walter, M. G., Thiazolothiazole Fluorophores Exhibiting Strong Fluorescence and Viologen-Like Reversible Electrochromism. *Journal of the American Chemical Society* **2017,** *139* (25), 8467-8473.
28. Abruna, H. D.; Bard, A. J., SEMICONDUCTOR ELECTRODES .40. PHOTOASSISTED HYDROGEN EVOLUTION AT POLY(BENZYL VIOLOGEN)-COATED P-TYPE SILICON ELECTRODES. *Journal of the American Chemical Society* **1981,** *103* (23), 6898-6901.

29. Esswein, A. J.; Nocera, D. G., Hydrogen production by molecular photocatalysis. *Chemical Reviews* **2007,** *107* (10), 4022-4047.
30. Huang, J. S.; Miller, P. F.; Wilson, J. S.; de Mello, A. J.; de Mello, J. C.; Bradley, D. D. C., Investigation of the effects of doping and post-deposition treatments on the conductivity, morphology, and work function of poly (3,4-ethylenedioxythiophene)/poly (styrene sulfonate) films. *Advanced Functional Materials* **2005,** *15* (2), 290-296.
31. Dimitriev, O. P.; Grinko, D. A.; Noskov, Y. V.; Ogurtsov, N. A.; Pud, A. A., PEDOT:PSS films-Effect of organic solvent additives and annealing on the film conductivity. *Synthetic Metals* **2009,** *159* (21-22), 2237-2239.
32. Nardes, A. M.; Kemerink, M.; de Kok, M. M.; Vinken, E.; Maturova, K.; Janssen, R. A. J., Conductivity, work function, and environmental stability of PEDOT : PSS thin films treated with sorbitol. *Organic Electronics* **2008,** *9* (5), 727-734.
33. Crispin, X.; Jakobsson, F. L. E.; Crispin, A.; Grim, P. C. M.; Andersson, P.; Volodin, A.; van Haesendonck, C.; Van der Auweraer, M.; Salaneck, W. R.; Berggren, M., The origin of the high conductivity of poly(3,4-ethylenedioxythiophene)-poly(styrenesulfonate) (PEDOT- PSS) plastic electrodes. *Chemistry of Materials* **2006,** *18* (18), 4354-4360.
34. Jäckle, S.; Liebhaber, M.; Niederhausen, J.; Büchele, M.; Félix, R.; Wilks, R. G.; Bär, M.; Lips, K.; Christiansen, S., Unveiling the Hybrid n-Si/PEDOT:PSS Interface. *ACS Applied Materials & Interfaces* **2016,** *8* (13), 8841-8848.
35. Brabec, C. J., Organic photovoltaics: technology and market. *Solar Energy Materials and Solar Cells* **2004,** *83* (2-3), 273-292.
36. Lee, M. M.; Teuscher, J.; Miyasaka, T.; Murakami, T. N.; Snaith, H. J., Efficient Hybrid Solar Cells Based on Meso-Superstructured Organometal Halide Perovskites. *Science* **2012,** *338* (6107), 643-647.
37. Gogolin, R.; Zielke, D.; Lovenich, W.; Sauer, R.; Schmidt, J., Silicon heterojunction solar cells combining an a-Si:H(n) electron-collector with a PEDOT:PSS hole-collector. *Proceedings of the 6th International Conference on Crystalline Silicon Photovoltaics (Siliconpv 2016)* **2016,** *92*, 638-643.
38. Jackle, S.; Mattiza, M.; Liebhaber, M.; Bronstrup, G.; Rommel, M.; Lips, K.; Christiansen, S., Junction formation and current transport mechanisms in hybrid n-Si/PEDOT:PSS solar cells. *Scientific Reports* **2015,** *5*.
39. Price, M. J.; Foley, J. M.; May, R. A.; Maldonado, S., Comparison of majority carrier charge transfer velocities at Si/polymer and Si/metal photovoltaic heterojunctions. *Applied Physics Letters* **2010,** *97* (8).
40. Yang, Z. H.; Gao, P. Q.; He, J.; Chen, W. C.; Yin, W. Y.; Zeng, Y. H.; Guo, W.; Ye, J. C.; Cui, Y., Tuning of the Contact Properties for High Efficiency Si/PEDOT:PSS Heterojunction Solar Cells. *Acs Energy Letters* **2017,** *2* (3), 556-562.
41. Srivastava, S. K.; Kumar, D.; Singh, P. K.; Kar, M.; Kumar, V.; Husain, M., Excellent antireflection properties of vertical silicon nanowire arrays. *Solar Energy Materials and Solar Cells* **2010,** *94* (9), 1506-1511.
42. Hiremath, R. K.; Rabinal, M. K.; Mulimani, B. G.; Khazi, I. M., Molecularly controlled metal-semiconductor junctions on silicon surface: A dipole effect. *Langmuir* **2008,** *24* (19), 11300-11306.

43. Wayner, D. D. M.; Wolkow, R. A., Organic modification of hydrogen terminated silicon surfaces. *J Chem Soc Perk T 2* **2002,** (1), 23-34.
44. Janardhanam, V.; Yun, H. J.; Jyothi, I.; Lee, J.; Hong, H.; Reddy, V. R.; Choi, C. J., Energy-level alignment and electrical properties of Al/p-type Si Schottky diodes with sorbitol-doped PEDOT:PSS as an organic interlayer. *J Alloy Compd* **2015,** *637*, 84-89.
45. Sah, C. T.; Noyce, R. N.; Shockley, W., Carrier Generation and Recombination in P-N Junctions and P-N Junction Characteristics. *P Ire* **1957,** *45* (9), 1228-1243.
46. Wong, K. T.; Lewis, N. S., What a Difference a Bond Makes: The Structural, Chemical, and Physical Properties of Methyl-Terminated Si(111) Surfaces. *Accounts of Chemical Research* **2014,** *47* (10), 3037-3044.
47. Webb, L. J.; Lewis, N. S., Comparison of the electrical properties and chemical stability of crystalline silicon(111) surfaces alkylated using grignard reagents or olefins with Lewis acid catalysts. *Journal of Physical Chemistry B* **2003,** *107* (23), 5404-5412.
48. O'Leary, L. E.; Rose, M. J.; Ding, T. X.; Johansson, E.; Brunschwig, B. S.; Lewis, N. S., Heck Coupling of Olefins to Mixed Methyl/Thienyl Monolayers on Si(111) Surfaces. *Journal of the American Chemical Society* **2013,** *135* (27), 10081-10090.
49. Dumas, P.; Chabal, Y. J., Electron-Energy-Loss Characterization of the H-Terminated Si(111) and Si(100) Surfaces Obtained by Etching in Nh4f. *Chemical Physics Letters* **1991,** *181* (6), 537-543.
50. Plymale, N. T.; Ramachandran, A. A.; Lim, A.; Brunschwig, B. S.; Lewis, N. S., Control of the Band-Edge Positions of Crystalline Si(111) by Surface Functionalization with 3,4,5-Trifluorophenylacetylenyl Moieties. *Journal of Physical Chemistry C* **2016,** *120* (26), 14157-14169.
51. Bansal, A.; Li, X. L.; Lauermann, I.; Lewis, N. S.; Yi, S. I.; Weinberg, W. H., Alkylation of Si surfaces using a two-step halogenation Grignard route. *Journal of the American Chemical Society* **1996,** *118* (30), 7225-7226.
52. Chen, M. X.; Hack, J. H.; Iyer, A.; Jones, K. J.; Opila, R. L., Radical-Driven Silicon Surface Passivation by Benzoquinone- and Hydroquinone-Methanol and Photoinitiators. *Journal of Physical Chemistry C* **2017,** *121* (39), 21364-21373.
53. Michaelis, L.; Hill, E. S., The viologen indicators. *J Gen Physiol* **1933,** *16* (6), 859-873.
54. Bus, J. S.; Gibson, J. E.; Aust, S. D., Superoxide-Catalyzed and Singlet Oxygen-Catalyzed Lipid Peroxidation as a Possible Mechanism for Paraquat (Methyl Viologen) Toxicity. *Biochem Bioph Res Co* **1974,** *58* (3), 749-755.
55. Durben, S.; Baumgartner, T., 3,7-Diazadibenzophosphole Oxide: A Phosphorus-Bridged Viologen Analogue with Significantly Lowered Reduction Threshold. *Angew Chem Int Edit* **2011,** *50* (34), 7948-7952.
56. Hwang, E.; Seo, S.; Bak, S.; Lee, H.; Min, M.; Lee, H., An Electrolyte-Free Flexible Electrochromic Device Using Electrostatically Strong Graphene Quantum Dot–Viologen Nanocomposites. *Adv. Mater.* **2014,** *26* (30), 5129-5136.
57. Kolesar, J. M.; Hall, S. J.; Woodward, A. N.; Walter, M. G., Highly Fluorescent Thiazolothiazole Viologens with Acttive Electrochromism. *J. Am. Chem. Soc.* **2016**, in prep.

58. Walter, M. G.; Warren, E. L.; McKone, J.; Boettcher, S. W.; Mi, Q.; Santori, E. A.; Lewis, N. S., Solar Water Splitting Cells. *Chem. Rev.* **2010,** *110*, 6446-6473.
59. Brandeis, M.; Nahor, G. S.; Rabani, J., Reactions of Colloidal Platinum in Aqueous-Solutions Containing Methyl Viologen, Its Cation Radical, and Hydrogen, Studied by Pulse-Radiolysis. *Journal of Physical Chemistry* **1984,** *88* (8), 1615-1623.
60. Kim, J. Y.; Lee, C. M.; Park, J. W., The kinetics of neutral methyl viologen in acidic H2O+DMF mixed solutions studied by cyclic voltammetry. *Journal of Electroanalytical Chemistry* **2001,** *504* (1), 104-110.
61. Fan, L.; Jia, C. K.; Zhu, Y. G.; Wang, Q., Redox Targeting of Prussian Blue: Toward Low-Cost and High Energy Density Redox Flow Battery and Solar Rechargeable Battery. *Acs Energy Letters* **2017,** *2* (3), 615-621.
62. Boettcher, S. W.; Warren, E. L.; Walter, M. G.; McKone, J.; Lewis, N. S.; Atwater, H. A., Photoelectrochemical hydrogen evolution using Si microwire arrays. *J. Am. Chem. Soc.* **2010,** *133*, 1216-1219.
63. Fabre, B., Functionalization of Oxide-Free Silicon Surfaces with Redox-Active Assemblies. *Chemical Reviews* **2016,** *116* (8), 4808-4849.
64. Ciampi, S.; Harper, J. B.; Gooding, J. J., Wet chemical routes to the assembly of organic monolayers on silicon surfaces via the formation of Si-C bonds: surface preparation, passivation and functionalization. *Chemical Society Reviews* **2010,** *39* (6), 2158-2183.
65. Toriumi, N.; Asano, N.; Miyamoto, K.; Muranaka, A.; Uchiyama, M., N-Alkynylpyridinium Salts: Highly Electrophilic Alkyne-Pyridine Conjugates as Precursors of Cationic Nitrogen-Embedded Polycyclic Aromatic Hydrocarbons. *Journal of the American Chemical Society* **2018,** *140* (11), 3858-3862.

Appendix A – MALDI-TOF

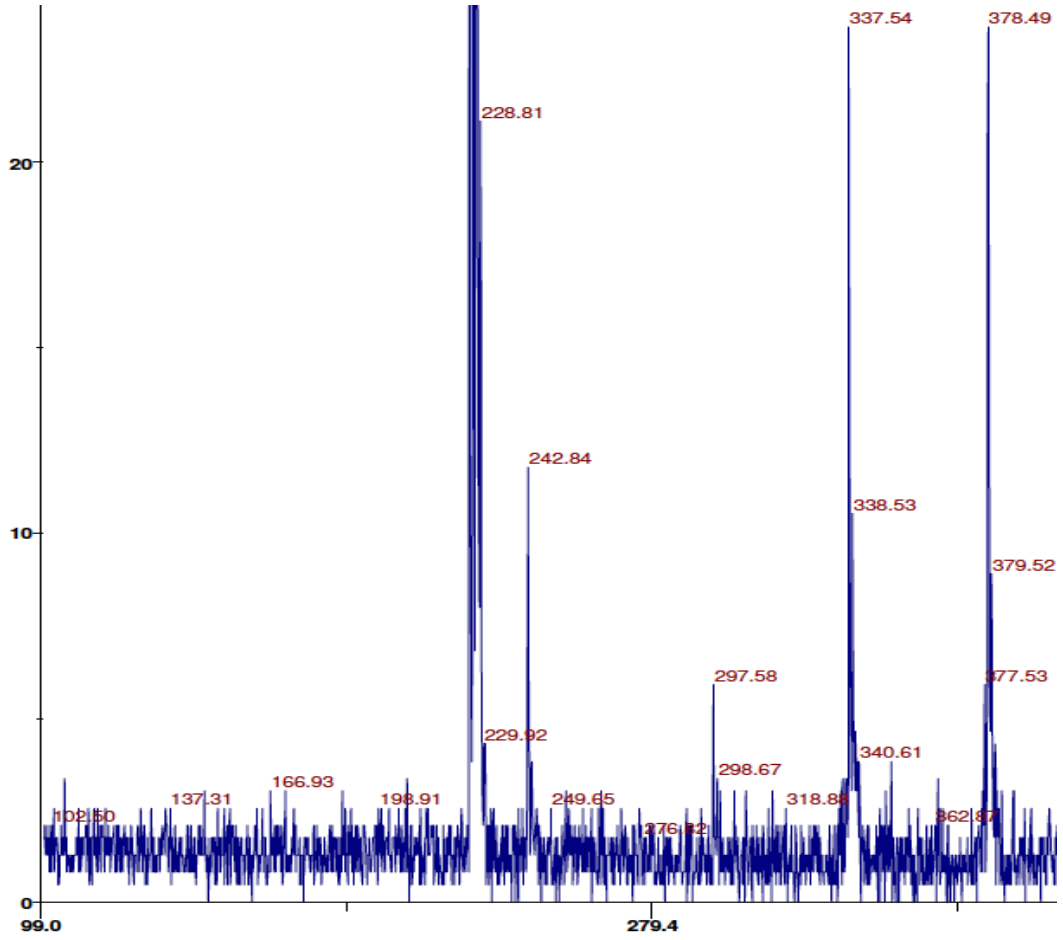

Figure A1. MALDI-TOF spectrum with relative abundance of species vs molecular mass.

Appendix B – NMR

NMR Spectra of Allyl$_2$TTz-VG^{2+}(Br$^-$)$_2$ in D_2O With Integrations and Coupling Constants

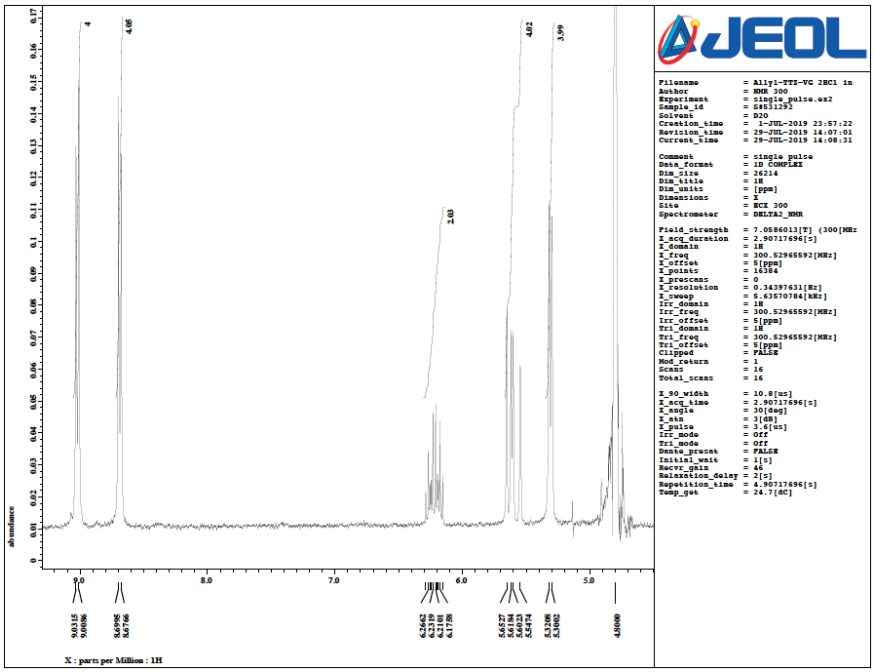

Figure B1. Full scale ^{1}H NMR spectrum.

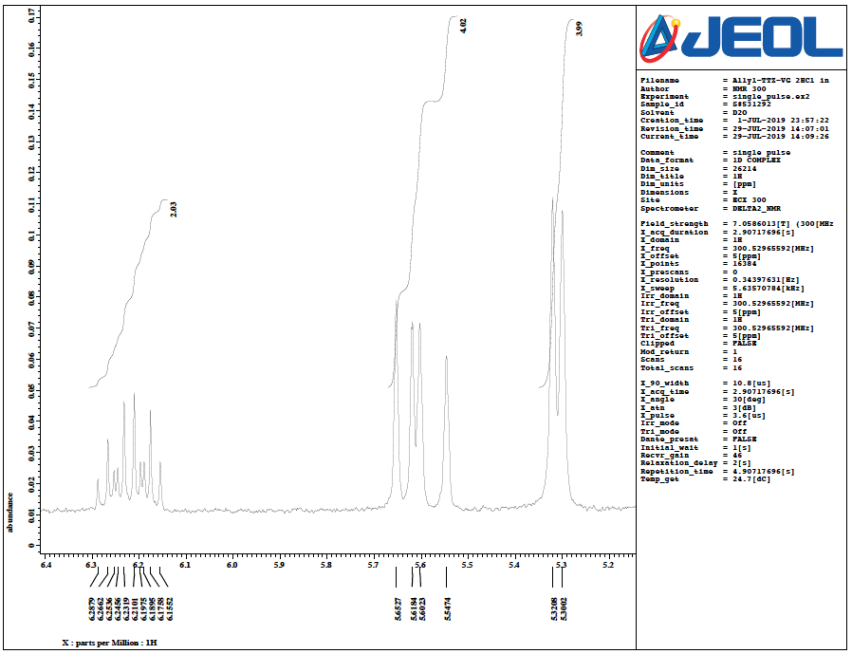

Figure B2. Detailed ^{1}H NMR spectrum from 5-7ppm.

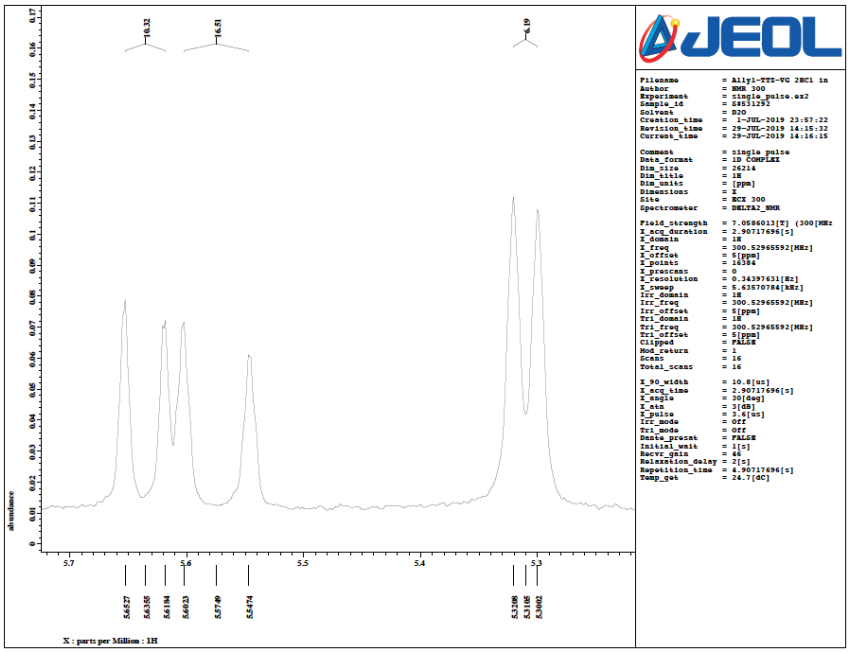

Figure B3. ^{1}H NMR Spectrum at 5.5ppm showing coupling constants.

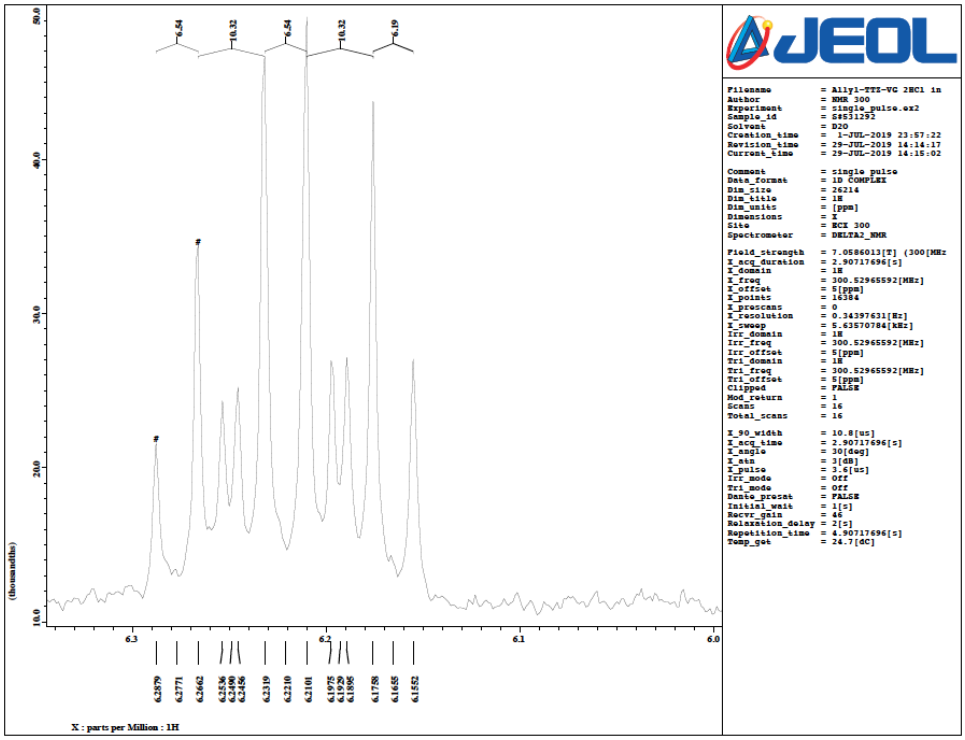

Figure B4. ^{1}H NMR spectrum at 6ppm showing coupling constants.

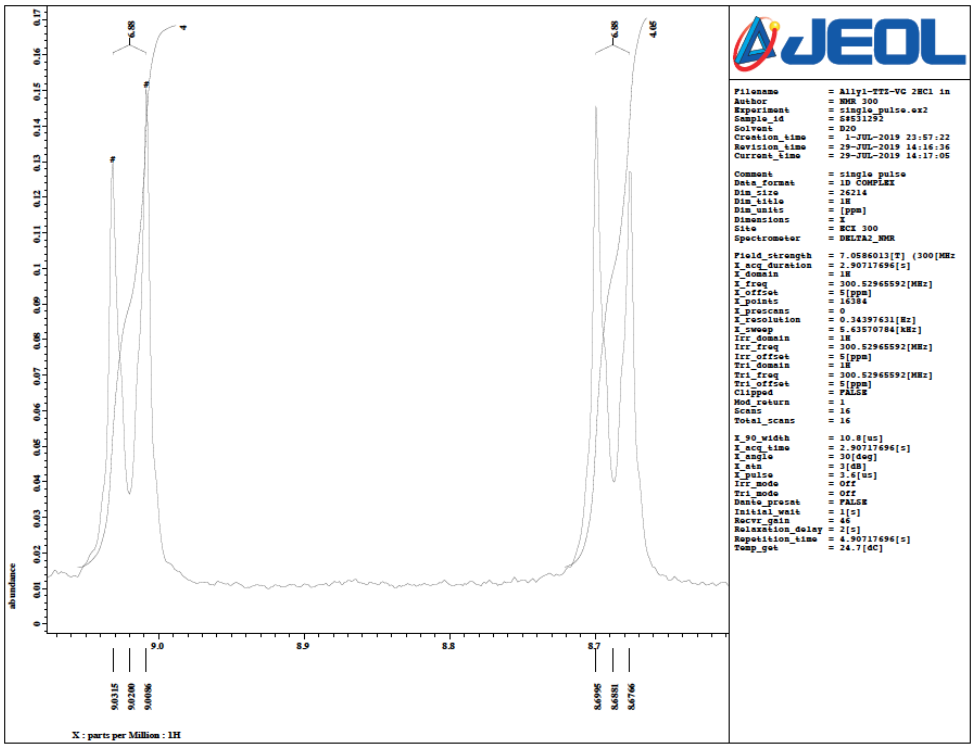

Figure B5. ^{1}H NMR spectrum at 9ppm showing coupling constants.

Appendix C – Cyclic Voltammetry of Different Acids

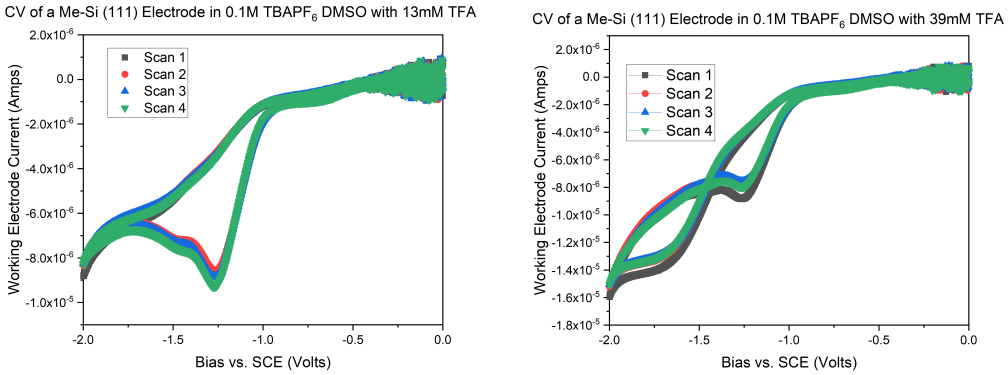

Figure C1. CV of Me-Si(111) working electrode with 0.1M $TBAPF_6$ in DMSO, with 13mM TFA or 39mM TFA and no $(Allyl_2TTz)^{2+}(Br^-)_2$.

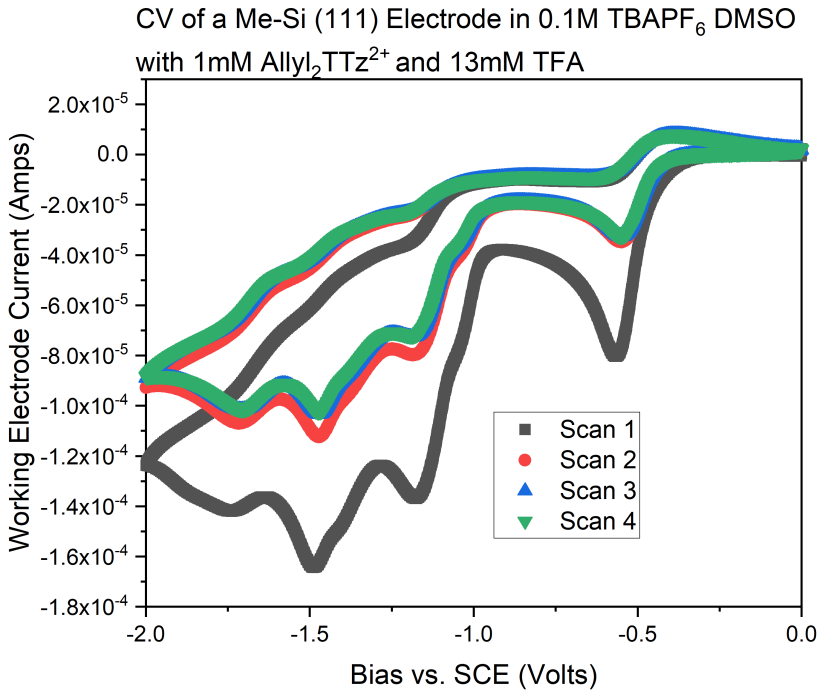

Figure C2. CV of Me-Si(111) working electrode with 0.1M $TBAPF_6$ in DMSO and 13mM TFA and 1mM $(Allyl_2TTz)^{2+}(Br^-)_2$.

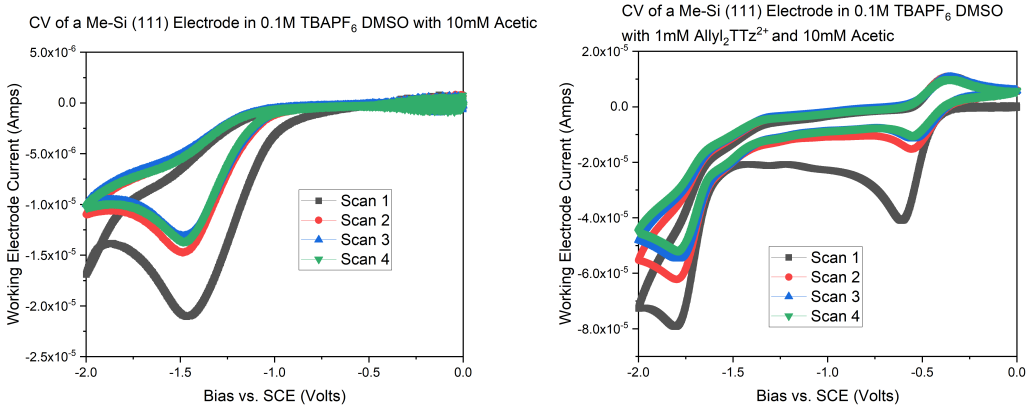

Figure C3. CV of Me-Si working electrode with 0.1M $TBAPF_6$ in DMSO and 10mM Acetic acid, and 0mM or 1mM $(Allyl_2TTz)^{2+}(Br^-)_2$.

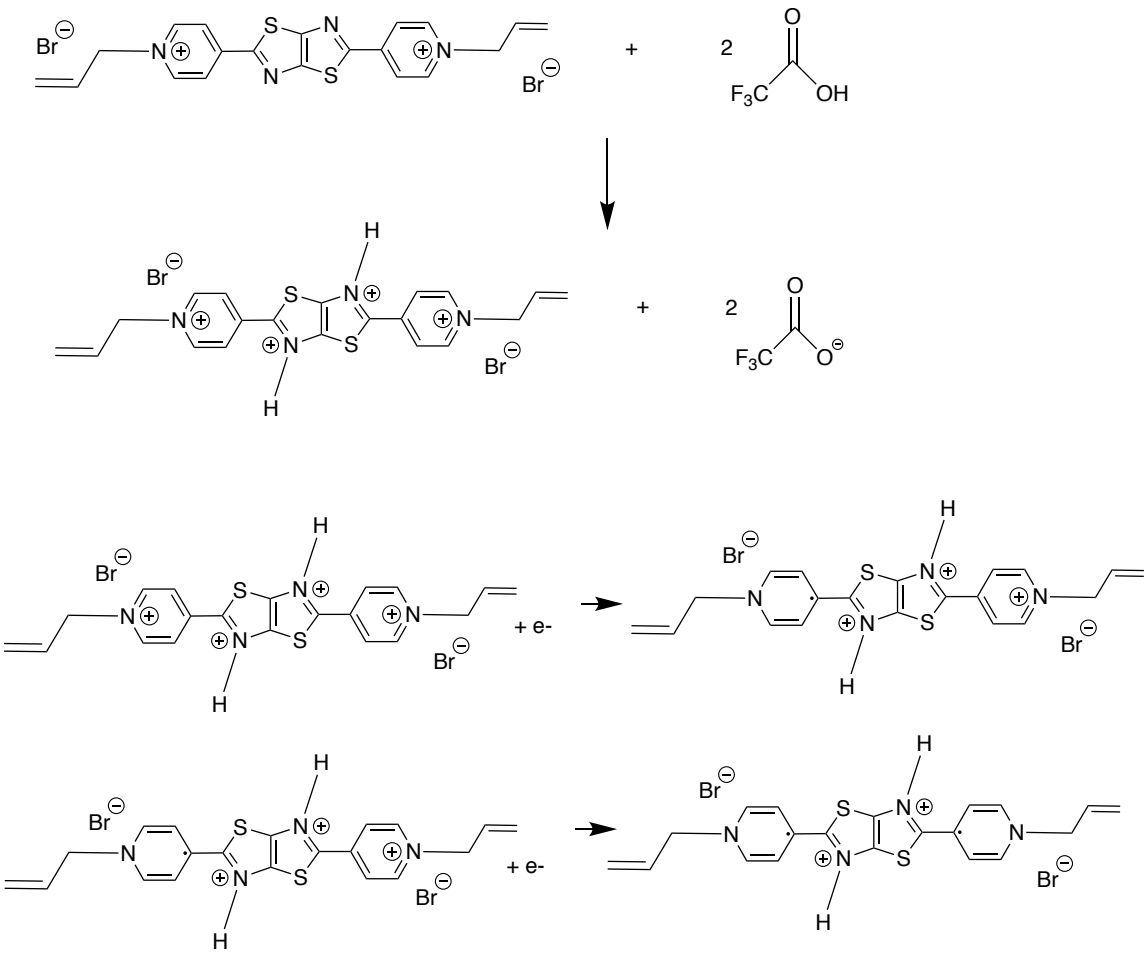

Figure C4. Protonation of TTZ core nitrogen atoms by TFA followed by reductions of the protonated species. One or two protonations are possible.